Mechanisms of gemcitabine resistance in pancreatic cancer

Thesis submitted in accordance with the requirements of the University of Liverpool for the degree of Doctor of Medicine by:

James Melling
Student number: 980351312
November 2017

ACKNOWLEDGEMENTS

I would like to take the opportunity to thank all of my colleagues at the University of Liverpool. In particular, special mention should go to my supervisors, Professor Paula Ghaneh and Dr Bill Greenhalf, as well as Liz Garner who was instrumental in helping develop my laboratory techniques. I would also like to thank the various other scientists and clinicians present in the department during my time in research for their patience and camaraderie. They include Miss Amy Thomas, Robert Ferguson, Mr Paul Sykes and Mr Owain Jones.

This thesis would not have been possible without the constant support of my wife Charlotte, to whom I am eternally grateful.

DECLARATION

I declare that this thesis, along with the laboratory work and research on which it is based were the result of my own work. Where I have incorporated the work of others, this is clearly marked in the text.

It has not been otherwise submitted for degree purposes, and I have no plans to do so.

Parts of the work have been submitted and presented at the following scientific conferences, with accompanying abstracts published as shown below:

Presentations:
Melling J. Ribonucleotide reductase subunit M2 levels affect resistance to gemcitabine *in vitro*. *Oral presentation at the Liverpool and North West Society of Surgeons Meeting, Victoria building, Liverpool University, 4th December 2015.*

Melling J. Acquired gemcitabine resistance is associated with expression of Ribonucleotide reductase subunit M2. *Poster presentation at the Pancreatic society of Great Britain and Ireland, Loch Lomond, 15th November 2012.*

Melling J. Ribonucleotide reductase subunit M2 levels affect resistance to gemcitabine *in vitro*. Poster presentation at the *American Pancreatic Association annual meeting, Miami, 1st November 2012.*

Abstract:
Melling J, Shaw E, Dajani K, Lane B, Bauer A, Hoheisel J, Neoptolemos J, Greenhalf W, Ghaneh P. Ribonucleotide reductase subunit M2 levels affect resistance to gemcitabine *in vitro*. *Pancreas. 41(8):1344-1416, November 2012.*

Parts of the introduction are based on the following publication, of which I was a lead author:

Jones O, Melling J, Ghaneh P. Adjuvant therapy in pancreatic cancer. *World Journal of Gastroenterology*, *2014 Oct 28;20(40):14733-46*

ABSTRACT

Mechanisms of gemcitabine resistance in pancreatic cancer

James Melling

Introduction: Gemcitabine is the chemotherapy of choice for pancreatic cancer in palliative and adjuvant settings but prognosis remains poor as patients may not respond or develop resistance.

Aims: To investigate the mechanisms of gemcitabine resistance developed *in vitro*.

Methods: Previously, cell lines shown to be relatively resistant and sensitive to gemcitabine were produced and subjected to microarray analysis (Dajani, unpublished). Following these results, suggested differential RNA and protein expression was confirmed using qRT-PCR or western blot. Candidate genes were then inhibited using siRNA knockdown and any effect on resistance to gemcitabine measured. Immunocytochemistry (ICC) and immunohistochemistry (IHC) were then optimised to allow human tissue to be probed for the presence of candidate proteins of interest in the future.

Results: The *Illumina Human RNA v3Bead* and *810 Protein Antibody* microarrays indicated differential expression of 4 genes at RNA level and 5 proteins. The most significant transcript was SERPINA1 ($p=0.002$). This was confirmed with qRT-PCR (75% decreased expression in resistant Suit-2 cell line). Knockdown of SERPINA1 did not affect resistance. The most significant protein was RRM2. Western blot confirmed differential expression in the resistant cell line and knockdown of RRM2 decreased resistance in both parental Suit-2 cells (IC50 value of 0.1nM vs 0.004nM of gemcitabine) and the resistant cells (IC50 value of >300,000nM vs 29,500nM of gemcitabine). Conditions for ICC and IHC were then optimised for RRM2 expression.

Conclusion: Investigation by microarray identified RRM2 as a candidate protein involved in gemcitabine resistance. RRM2 was confirmed by protein levels and knockdown in vitro to affect resistance. RRM2 should be further investigated as a potential prognostic marker and therapeutic target in adjuvant therapy of pancreatic cancer.

ABBREVIATIONS

αSMA	α-smooth muscle actin
A1AT	α-1-antitrypsin
APS	Ammonium persulfate
AS	Original 'sensitive' Suit-2 cell line
BEX4	Brain expressed X-linked 4
BMP	Bone morphogenic proteins
BSA	Bovine serum albumin
Bx	BxPC3 cell line
^{0}C	Degrees centigrade
CA19-9	Carbohydrate antigen 19-9
CDK	Cyclin dependent kinases
cDNA	Copy DNA
CDP	Cytidine diphosphate
CEA	Carcinoembryonic antigen
CNT	Concentrative nucleoside transporter
CO_2	Carbon dioxide
CP	Crossing point (qRT-PCR)
CT	Computed tomography
dCDP	Deoxycytidine diphosphate
dCK	Deoxycitidine kinase
dCTD	Deoxycytidylate triphosphate
dFdC	Difluorodeoxycytidine (Gemcitabine)
dFdCDP	Difluorodeoxycitidine diphosphate
dFdCMP	Difluorodeoxycitidine monophosphate
dFdCTP	Difluorodeoxycitidine triphosphate
dFdU	Diflurodeoxyuridine
dFdUMP	Difluorodeoxyuridine monophosphate
dH_2O	Distilled water
DHH	Desert hedgehog
DMSO	Dimethyl Sulfoxide
DNA	Deoxyribonucleic acid
DPC4	Deleted in pancreatic cancer gene 4
dNTP	Deoxy-nucleotide-triphosphate
DTT	DL-Dithiothreitol
ECL	Enhanced chemiluminescence
ECM	Extracellular matrix
EGFR	Epidermal growth factor receptor
EMT	Epithelial to mesenchymal transition
ERCC	Excision repair cross-complementation 1
ERCP	Endoscopic retrograde cholangiopancreatography
EUS	Endoscopic ultrasound
ESA	Epithelial-specific antigen
ESPAC	European Study group for Pancreas Cancer
FAMM	Familial Atypical Multiple Mole Melanoma Syndrome
FAP	Familial adenomatous polyposis coli
FBS	Foetal bovine serum
FNA	Fine needle aspiration

FOLFIRINOX	Folinic acid, 5FU, Irinotecan, Oxaliplatin
FOLR	Folate receptor α
5FU	5-fluorouracil
GEMM	Genetically engineered mouse models
GTP	Guanine triphosphate
GR	Clonally resistant Suit-2 cell line
GSTP	Glutathione-S-transferase-P
HA	Hyaluronic acid
HCl	Hydrochloric acid
hENT	Human equilibrative nucleoside transporter
HGF	Hepatocyte growth factor
HR	Hazard ratio
IHH	Indian hedgehog
IFP	Interstitial fluid pressure
IL1β	Interleukin 1-β
ICC	Immunocytochemistry
IHC	Immunohistochemistry
IPMN	intraductal papillary mucinous neoplasm
ISGPS	International study group of pancreatic surgery
IV	Intravenous
JASPAC	Japanese adjuvant study group for pancreatic cancer
JSAP	Japanese study group of adjuvant therapy for pancreatic cancer
KD	Knockdown
kDa	Kilo-Dalton
K-ras	Kirsten rat sarcoma
M	Mole(s)
MAPK	Mitogen-activated kinase
MCN	Mucinous cystic neoplasm
MDM2	Murine double minute protein
MgCl	Magnesium chloride
mls	Mililitres
MP	MiaPaCa cell line
mRNA	Messenger RNA
MTS	3-(4,5-dimethylthiazol-2-yl)-5-(3-carboxymethoxyphenyl)-2-(4-sulfophenyl)-2H-tetrazolium
NaCl	Sodium chloride
nm	Nano-metre
nM	Nano-moles
OT	Off target control
OR	Odds ratio
P1	Panc-1 cell line
PanIN	Pancreatic intraepithelial neoplasia
PBS	Phosphate buffered saline
PCR	Polymerase chain reaction
PDAC	Pancreatic ductal adenocarcinoma
PDGF	platelet derived growth factor
Plk1	Polo-like kinase 1
pRb	Retinoblastoma protein
PTCH	Patched receptor

PV	Portal vein
qRT-PCR	Quantitative reverse transcription PCR
RISC	RNA-induced silencing complex
RNA	Ribonucleic acid
RNR	Ribonucleotide reductase
Rpm	Revolutions per minute
RRM1	Ribonucleotide reductase molecule subunit 1
RRM2	Ribonucleotide reductase molecule subunit 2
RTOG	Radiation Therapy Oncology Group
siRNA	Short interfering RNA
SDS	Sodium dodecyl sulfate
SHH	Sonic hedgehog
SMA	Superior mesenteric artery
SMO	Smoothened receptor
SMV	Superior mesenteric vein
SNAR-A1	small ILF3/NF90-associated RNA A1
TBS	Tris-buffered solution
TBST	Tris-buffered solution with tween
TEMED	N, N, N', N'-tetramethylethylenediamine
TGFβ	Transforming growth factor beta
TNM	Tumour, node, metastases staging system
UV	Ultraviolet
V	Volts
VEGF	Vascular endothelial growth factor

CONTENTS

Acknowledgements 2
Declaration 3
Abstract 4
Abbreviations 5
Contents 8
List of figures 10
List of tables 12

1 INTRODUCTION 13

1.1 PANCREATIC DUCTAL ADENOCARCINOMA (PDAC) 13
1.1.1 EPIDEMIOLOGY 13
1.1.2 AETIOLOGY 15
1.1.3 MOLECULAR BIOLOGY 17
1.1.4 CLINICAL PRESENTATION 30
1.1.5 INVESTIGATIONS 31
1.1.6 STAGING 33
1.1.7 SURGERY 34
1.1.8 ADJUVANT THERAPY 36
1.1.9 PALLIATIVE THERAPY 41
1.2 GEMCITABINE 44
1.2.1 INDICATIONS, ADMINISTRATION AND SIDE EFFECTS 44
1.2.2 MODE OF ACTION 45
1.2.3 MECHANISMS OF RESISTANCE 49
1.3 PDAC IMMORTAL CELL LINES 59
1.3.1 SUIT-2 59
1.3.2 BXPC3 60
1.3.3 PANC1 60
1.3.4 MIAPACA 60
1.4 PREVIOUS WORK 61
1.4.1 DEVELOPMENT OF RESISTANT CELL LINES 61
1.4.2 DETERMINATION OF GEMCITABINE SENSITIVITY 63
1.4.3 MICROARRAY 65
1.4.4 BIOINFORMATICS 65
1.5 GENES AND PROTEINS OF INTEREST 66
1.5.1 GENES OF INTEREST 66
1.5.2 PROTEINS OF INTEREST 68
1.6 SUMMARY 74

2 AIMS AND OBJECTIVES 75

3 MATERIALS AND METHODS 76

3.1 MATERIALS 76
3.1.1 CHEMICAL OR REAGENT 76
3.1.2 EQUIPMENT 79
3.1.3 PREPARATION OF SOLUTIONS 80

3.2 METHODS **82**
3.2.1 CELL CULTURE METHODS 82
3.2.2 CYTOTOXICITY STUDIES USING MTS ASSAY METHODS 85
3.2.3 WESTERN BLOT METHODS 88
3.2.4 POLYMERASE CHAIN REACTION 97
3.2.5 GENE KNOCKDOWN 104
3.2.6 IMMUNOCYTOCHEMISTRY 106
3.2.7 IMMUNOHISTOCHEMISTRY 107

4 RESULTS **110**

4.1 CONFIRMATION OF RESISTANCE AND ESTABLISHMENT OF LEVELS OF PROTEINS PREVIOUSLY ASSOCIATED WITH GEMCITABINE METABOLISM AND RESISTANCE **110**
4.1.1 OVERVIEW 110
4.1.2 GEMCITABINE RESISTANCE IN CELL LINES 110
4.1.3 PROTEINS PREVIOUSLY ASSOCIATED WITH GEMCITABINE METABOLISM AND RESISTANCE 117
4.1.4 CONCLUSIONS 123
4.2 VALIDATION OF MICROARRAY RESULTS **125**
4.2.1 OVERVIEW 125
4.2.2 SERPINA1/A-1-ANTITRYPSIN (A1AT) 126
4.2.3 GLUTATHIONE S-TRANSFERASE P (GSTP) 137
4.2.4 OCCLUDIN 139
4.2.5 FOLATE RECEPTOR ALPHA (FOLR) 141
4.2.6 RIBONUCLEOTIDE REDUCTASE SUBUNIT 2 (RRM2) 142
4.2.7 INTERLEUKIN-1B 145
4.2.8 CONCLUSIONS 147
4.3 KNOCKDOWN OF DIFFERENTIALLY EXPRESSED GENES AND PROTEINS OF INTEREST **148**
4.3.1 OVERVIEW 148
4.3.2 SERPINA1 149
4.3.3 GSTP 156
4.3.4 RRM2 159
4.3.5 TREATING WITH EXOGENOUS A1AT 165
4.3.6 CONCLUSIONS 168
4.4 ICC AND IHC FOR RRM2 **169**
4.4.1 OVERVIEW 169
4.4.2 IMMUNOCYTOCHEMISTRY (ICC) FOR RRM2 169
4.4.3 IMMUNOCYTOCHEMISTRY (IHC) FOR RRM2 171
4.4.4 CONCLUSION 172

5 DISCUSSION **173**

5.1 SUMMARY **173**
5.2 CLINICAL RELEVANCE AND FURTHER WORK **174**
5.3 CONCLUSION **177**

6 REFERENCES **178**

LIST OF FIGURES

FIGURE 1:*PANCREATIC CANCER, AVERAGE NUMBER OF NEW CASES PER YEAR AND AGE-SPECIFIC INCIDENCE RATES* 14
FIGURE 2:*PANCREATIC CANCER, WORLD AGE-STANDARDISED INCIDENCE RATES* 15
FIGURE 3:*MODEL OF STEPWISE PANCREATIC CARCINOGENESIS* 18
FIGURE 4:*THE CORE SIGNALLING PATHWAYS IN PANCREATIC CANCER DEVELOPMENT* 19
FIGURE 5:*MOLECULAR STRUCTURE OF GEMCITABINE* 44
FIGURE 6:*UPTAKE AND METABOLISM OF GEMCITABINE* 46
FIGURE 7:*MAIN MECHANISMS OF ACTION OF GEMCITABINE* 48
FIGURE 8:*CYTOTOXICITY CURVES FOR AS AND GR CELL LINES TREATED WITH GEMCITABINE* 63
FIGURE 9:*CYTOTOXICITY CURVES FOR AS AND KR CELL LINES TREATED WITH GEMCITABINE* 64
FIGURE 10:*AN EXAMPLE OF A 96-WELL PLATE FOLLOWING MTS ASSAY* 87
FIGURE 11:*IC50 CURVE FOR SUIT2 CELLS TREATED WITH GEMCITABINE* 111
FIGURE 12:*IC50 CURVE FOR BXPC3 CELLS TREATED WITH GEMCITABINE*111
FIGURE 13: *IC50 CURVE FOR PANC1 CELLS TREATED WITH GEMCITABINE* 112
FIGURE 14: *IC50 CURVE FOR MIAPACA CELLS TREATED WITH GEMCITABINE* 112
FIGURE 15:*CYTOTOXICITY CURVES FOR AS AND KR CELL LINES TREATED WITH GEMCITABINE* 113
FIGURE 16: *IC50 CURVE FOR CLONAL RESISTANT SUIT2 CELLS (GR) TREATED WITH GEMCITABINE* 114
FIGURE 17:*IC50 CURVES FOR ALL THE CELL LINES COMBINED WHEN TREATED WITH GEMCITABINE* 115
FIGURE 18:*WESTERN BLOT FOR HENT1* 118
FIGURE 19:*WESTERN BLOT FOR CNT-1* 119
FIGURE 20:*WESTERN BLOT FOR DCK* 120
F**IGURE 21:***WESTERN BLOT FOR DCTD* 121
FIGURE 22:*WESTERN BLOT FOR RRM1* 122
FIGURE 23:*WESTERN BLOT FOR A1AT* 126
FIGURE 24:*REPEAT WESTERN BLOT FOR A1AT* 127
FIGURE 25:*WESTERN BLOT FOR A1AT USING SUPERNATANT COLLECTED FROM CULTURED CELLS* 128
FIGURE 26:*RT-PCR FOR GAPDH* 131
FIGURE 27:*RT-PCR FOR SERPIN A1* 132
FIGURE 28:*QRT-PCR FOR GAPDH* 134
FIGURE 29:*QRT-PCR FOR SERPIN A1 IN AS,GR AND KR CELL LINES* 135
FIGURE 30:*EXAMPLE WESTERN BLOT FOR GLUTATHIONE S TRANSFERASE P (GSTP)* 137
FIGURE 31:*BAR CHART REPRESENTING THE RESULTS OF WESTERN BLOTS FOR GSTP* 138
FIGURE 32:*EXAMPLE WESTERN BLOT FOR OCCLUDIN* 139

FIGURE 33:*EXAMPLE WESTERN BLOT FOR FOLATE RECEPTOR ALPHA (FOLR)* 141
FIGURE 34:*EXAMPLE WESTERN BLOT FOR RRM2* 142
FIGURE 35:*REPEAT WESTERN BLOT FOR RRM2* 143
FIGURE 36:*EXAMPLE WESTERN BLOT FOR IL-1B* 145
FIGURE 37:*WESTERN BLOT PROBING FOR IL-1B IN SUPERNATANT* 146
FIGURE 38:*QRT-PCR FOR GAPDH IN SERPINA1 KD* 149
FIGURE 39: *QRT-PCR AMPLIFICATION CURVES FOR SERPIN A1 KNOCKDOWN* 150
FIGURE 40:*QRT-PCR FOR GAPDH IN REPEAT SERPIN A1 KNOCKDOWN* 152
FIGURE 41:*QRT-PCR FOR SERPIN A1 IN REPEAT SERPIN A1 KNOCKDOWN* 153
FIGURE 42:*MTS ASSAY FOLLOWING SERPIN A1 KNOCKDOWN* 155
FIGURE 43:*KNOCKDOWN OF GSTP IN AS AND GR CELL LINES* 156
FIGURE 44: *IC50 CURVES FOLLOWING KNOCKDOWN OF GSTP IN AS AND GR* 158
FIGURE 45:*WESTERN BLOT SHOWING RRM2 KNOCKDOWN IN AS CELLS* 159
FIGURE 46:*RRM2 KNOCKDOWN IN GR CELLS* 160
FIGURE 47: *MTS 96-WELL PLATES FOR KNOCKDOWN OF RRM2 IN GR CELLS* 161
FIGURE 48:*IC50 CURVES FOLLOWING KNOCKDOWN OF RRM2* 163
FIGURE 49:*MTS ASSAY FOLLOWING EXOGENOUS A1AT TREATMENT* 166
FIGURE 50:*CYTOTOXICITY CURVES CREATED FROM THE VALUES IN THE ABOVE TABLE* 167
FIGURE 51:*EXAMPLE ICC FOR RRM2* 170
FIGURE 52:*EXAMPLE OF IHC STAINING FOR RRM2 USING HUMAN TISSUE* 171

LIST OF TABLES

TABLE 1:*UICC TNM STAGING CLASSIFICATION FOR PANCREATIC CANCER* 33
T**ABLE 2:***UICC TNM STAGING CLASSIFICATION FOR PANCREATIC CANCER* 34
TABLE 3:*MAJOR ADJUVANT CHEMOTHERAPY TRIALS IN PANCREATIC CANCER* 40
TABLE 4:*MUTATIONS IN SUIT-2 CELL LINE* 59
TABLE 5:*MUTATIONS IN BXPC3 CELL LINE* 60
TABLE 6:*MUTATIONS IN THE PANC1 CELL LINE* 60
TABLE 7:*MUTATIONS IN THE MIAPACA CELL LINE* 60
TABLE 8:*DIFFERENTIALLY EXPRESSED GENES AND PROTEINS IN MICROARRAYS* 65
TABLE 9:*ANTIBODIES, CONTROLS AND CONDITIONS USED FOR WESTERN BLOT* 88
TABLE 10:*MAKING UP STANDARDS FOR COOMASSIE BLUE STAINING* 91
TABLE 11:*PERCENTAGE GELS USED FOR WESTERN BLOT DEPENDING ON MOLECULAR WEIGHT OF PROTEIN* 91
TABLE 12:*INGREDIENTS (IN MLS) PER PERCENTAGE FOR ONE RESOLVING GEL (5MLS TOTAL)* 92
TABLE 13:*INGREDIENTS (IN MLS) FOR ONE STACKING GEL (2MLS TOTAL)* 92
TABLE 14:*SUMMARY OF IC50 VALUES FOR ALL CELL LINES USED, TREATED WITH GEMCITABINE* 115
TABLE 15:*RELATIVE LEVELS OF PROTEINS PREVIOUSLY ASSOCIATED WITH GEMCITABINE METABOLISM AND RESISTANCE IN A VARIETY OF DIFFERENT IMMORTAL PANCREATIC CANCER CELL LINES.* 123
TABLE 16:*CROSSING POINTS FOR QRT-PCR FOR GAPDH* 134
TABLE 17:*CROSSING POINTS FOR QRT-PCR FOR SERPIN A1* 136
TABLE 18:*RELATIVE DENSITY OF GSTP WESTERN BLOT BANDS* 138
TABLE 19:*RELATIVE LEVELS OF THE PROTEINS AND GENES OF INTEREST IN THE DIFFERENT SUIT-2 CELL LINES* 147
TABLE 20:*CROSSING POINTS FOR SERPIN A1 KNOCKDOWN* 151
TABLE 21:*CROSSING POINTS FOR REPEAT SERPINA1 KNOCKDOWN* 153
TABLE 22:*SPECTROPHOTOMETRY OF MTS 96-WELL PLATES FOR KNOCKDOWN OF RRM2 IN GR CELLS* 162
TABLE 23:*SPECTROPHOTOMETRY OF MTS 96-WELL PLATES USING AS CELLS FOLLOWING EXOGENOUS A1AT TREATMENT* 167

1 INTRODUCTION

1.1 Pancreatic Ductal Adenocarcinoma (PDAC)

1.1.1 Epidemiology

Pancreatic cancer is the 11th most common cancer in the UK with 9618 new cases diagnosed in 2014. This represents 2.7% of the 356,860 people diagnosed with any form of cancer for the same year[1]. Worldwide, around 278,684 people were diagnosed with pancreatic cancer in 2008[2]. The overall 5-year survival rate is dismal with only 4% of adults with pancreatic cancer in England surviving 5 years for the period 2005-2009. Due to this poor survival rate, pancreatic cancer represented the 5th most common cause of all cancer deaths in the UK in 2014 with 8,817 deaths.

The incidence increases with age and approximately 75% of cases occur in those over the age of 65 years (figure 1). The age standardised rates show a higher incidence in men of 10.5 per 100,000 vs 8.2 per 100,000 in women. This reverses over the age of 85 due to the higher life expectancy of women. The lifetime risk of developing pancreatic cancer in the UK is estimated at 1 in 77 for men and 1 in 79 for women. The incidence of pancreatic cancer remained stable between 1993 and 2008[1].

Worldwide, Europe and North America have the highest incidence rates, with Asia and Africa having the lowest incidences(figure 2)[1,3].

More than 95% of cancers are Pancreatic Ductal Adenocarcinomas (PDAC), arising from the exocrine part of the pancreas. Other histological types of pancreatic cancer include sarcomas and neuroendocrine tumours but these are rare and the work in this thesis relates specifically to PDAC.

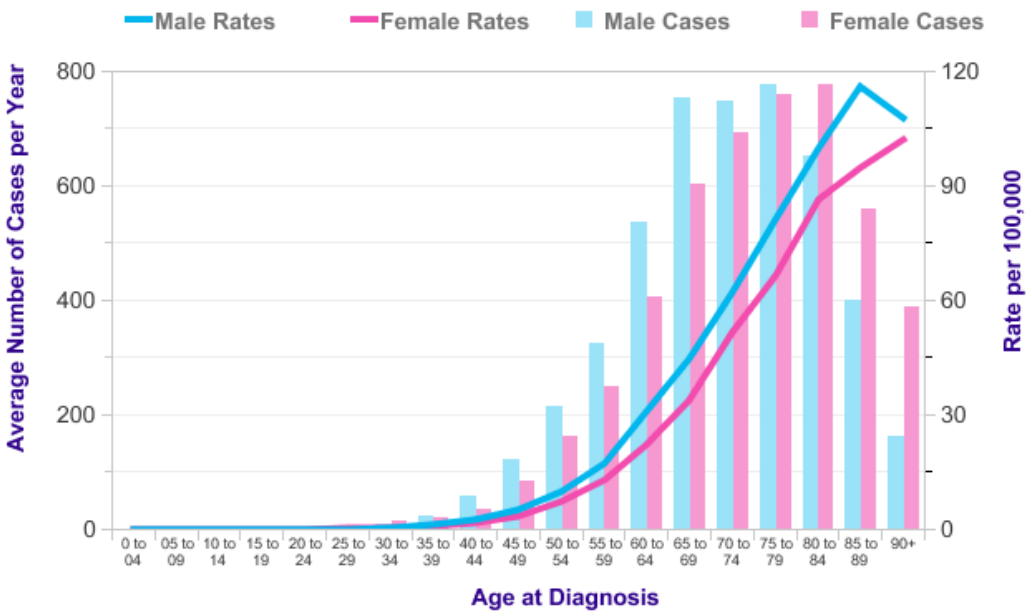

Figure 1: Pancreatic Cancer, Average Number of New Cases per Year and Age-Specific Incidence Rates per 100,000 population in the UK, 2012-2014 (www.cancerresearchuk.org)[1]

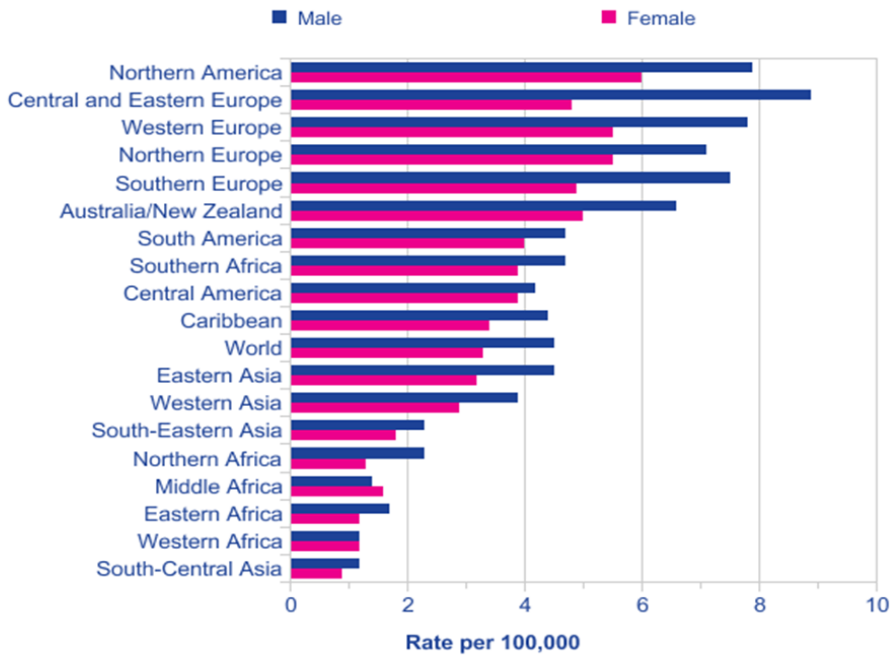

Figure 2: Pancreatic cancer (C25), World Age-Standardised Incidence Rates, World Regions, 2008 Estimates (taken from the cancer research UK website)[1]

1.1.2 **Aetiology**

There are a number of familial factors which have been associated with PDAC. Certain familial pancreatic cancer families have been identified where despite the absence of an identifiable germline mutation, there remains an apparent inherited predisposition to the disease[3]. In these families, it has been shown that individuals with two first degree relatives affected with pancreatic cancer have a risk of developing the disease themselves 18 times that of those individuals with only one affected relative. This risk increases to 57-fold when 3 or more relatives are affected[4]. This is compared to first

degree relatives of sporadic cases of pancreatic cancer who carry no significantly increased risk compared to the general population.

As well as these families, there are a number of well-defined cancer susceptibility syndromes where a certain germline mutation has been identified. These include Familial Atypical Multiple Mole Melanoma Syndrome (FAMMM, a mutation of tumour suppressor CDKN2A), Peutz-Jeghers Syndrome (mutation of STK11 gene), familial hereditary pancreatitis (mutation of cationic trypsinogen gene PRSS1), cystic fibrosis, Lynch syndrome (mismatch repair pathway deficiency), Familial Adenomatous Polyposis (mutation of adenomatous polyposis coli gene), Li-Fraumeni syndrome (mutation of TP53 tumour suppressor gene), and familial breast-ovarian cancer (mutations of tumour suppressor genes BRCA1 + 2). The risk conferred by these mutations varies but can be as high as high as a lifetime risk of developing pancreatic cancer of 17%, such as in FAMM mutations[3,5].

Various factors have also been implicated in the development of pancreatic cancer. These include chronic pancreatitis, obesity, diabetes mellitus, non-O blood group, alcohol and smoking. These factors are all relatively low risk factors when compared with the familial factors[3,5–7].

These familial and specific predisposing factors account for only a small number of cases of pancreatic cancer[8]. The majority of cases are related to acquired molecular changes as discussed below.

1.1.3 **Molecular biology**

1.1.3.1 Precursor lesions

The development of pancreatic cancer is now thought to result from the successive accumulation of genetic mutations, initially producing pre-malignant lesions which evolve into fully invasive cancer. There are 3 such pre-malignant lesions; pancreatic intraepithelial neoplasia (PanIN), intraductal papillary mucinous neoplasm (IPMN) and mucinous cystic neoplasm (MCN)[8]. The most well studied of these are PanINs from which most PDAC develops. These are classified histologically in a stepwise manner according to the degree of cellular atypia within pancreatic ducts characterised by loss of polarity, nuclear crowding, enlarged nuclei, pseudo-stratification and hyperchromatism[9]. PanIN 1A and 1B representing hyperplasia through to PanIN3 being carcinoma in situ[10]. These histological changes are also associated with defined stepwise genetic alterations starting with activating KRAS mutations and telomere shortening in PanIN 1, moving through inactivation of CDKN2A in PanIN 2 and finally TP53 and DPC4 mutations in PanIN 3[11,12] (Figure 3). This stepwise progression suggests that single gene alterations are not enough to cause development of PDAC in isolation.

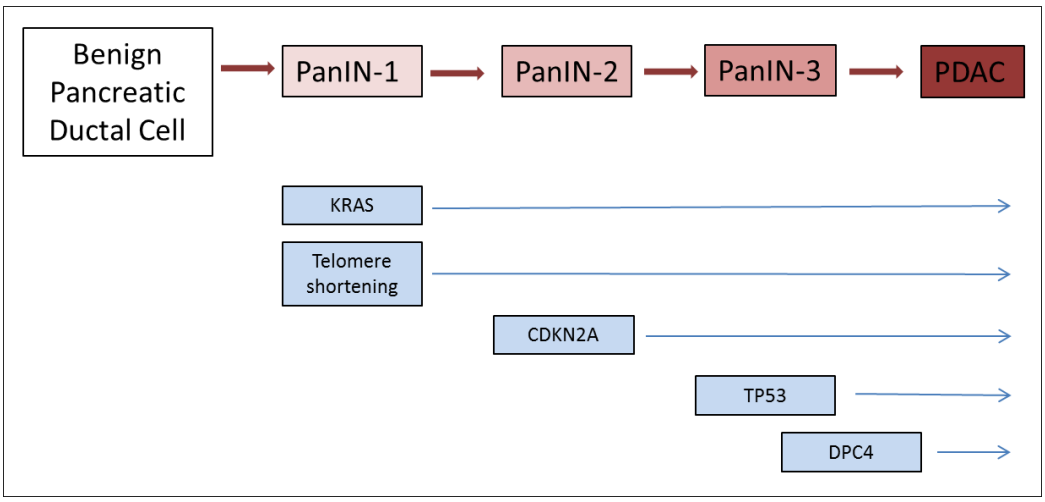

Figure 3: ***Model of stepwise pancreatic carcinogenesis. There is a progressive accumulation of genetic mutations through progressive grades of PanIN culminating in invasive PDAC. These are the most common mutations and other genetic abnormalities may occur alongside these[11,12].***

In fact, comprehensive genetic analysis of 24 different pancreatic cancers found an average of 63 genetic alterations per cancer which were likely to be relevant. These were mostly point mutations and suggest that the genetic basis of pancreatic cancer is extremely complex and heterogeneous. These genetic abnormalities can be organised into 13 relevant pathways (Figure 4) but the key mutations in each pathway differ from one tumour to another which is not surprising given a total of 1562 mutations were found in total in the 24 cancers[13].

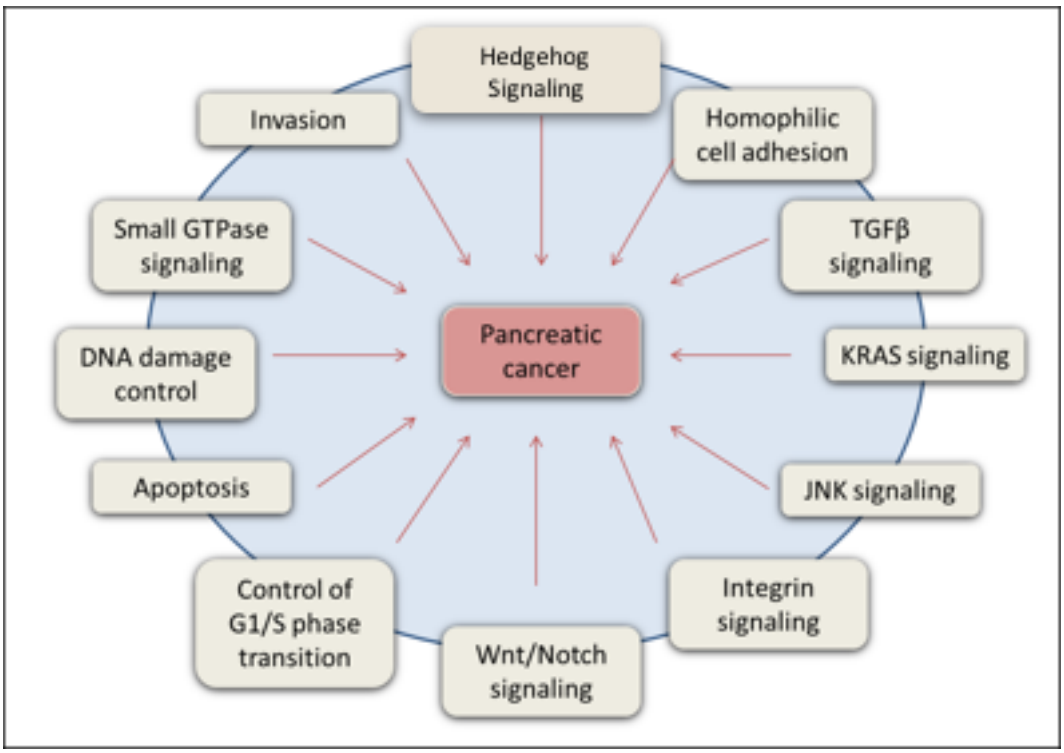

Figure 4: The core signalling pathways in pancreatic cancer development (GTP = guanosine triphosphate, TGFβ = transforming growth factor β)[12]

Of these 13 pathways, chromatin regulation is the more recently identified in pancreatic cancer. This has been identified through alterations in both the ARIDIA gene which encodes for a protein involved in SWI/SNF ATP-dependent chromatin remodelling complex, and mutations in MLL3 (mixed-lineage leukaemia 3) which encodes a histone methyltransferase.

Some of the other common genetic mutations, pathways and events involved in the development of pancreatic cancer shall be described in the following sections.

1.1.3.2 KRAS

The KRAS oncogene codes for the 21kDa membrane bound Kirsten rat sarcoma protein (K-ras) and is located on chromosome 12. Mutations are usually point mutations and occur at codon 12, 13 or 61. Mutations are found in 80-90% of pancreatic cancers[15] and are also commonly found in PanIN1A and 1B lesions suggesting this is an important initiating step in carcinogenesis[12]. The K-ras protein is a key mediator of a variety of signalling pathways. In its inactive form, it is bound to GDP but on activation by growth factor receptors such as epidermal growth factor receptor (eGFR), GDP is released in exchange for GTP. This converts the K-ras protein to the 'on' state in which it activates a number of downstream signalling pathways.

Mutations of the KRAS gene lead to impaired GTPase function which causes the K-ras protein to be locked in the 'on' state leading to various downstream actions. Activation of the Raf/MEK/ERK pathway leads to phosphorylation of the tumour suppressing retinoblastoma protein (pRb) which in turn controls transition from G1 into S phase and cell cycle progression. Initiation of the phosphoinositide-3-kinase (P13K)/AKT signalling pathway leads to cellular proliferation, whereas p53 inhibition is achieved by activation of the murine double minute protein (MDM2) leading to evasion of apoptosis and enhanced cell survival[9,11,15–17].

1.1.3.3 CDKN2A

The tumour suppressor gene CDKN2A is located on chromosome 9 and through alternative splicing sites, codes for both the $p16^{INK4A}$ and $P14^{ARF}$

proteins. The $p16^{INK4A}$ protein inhibits the formation of complexes between cyclin and cyclin dependent kinases (CDKs) which affects phosphorylation of pRb and subsequently, the G1 checkpoint and entry into S phase and progression through the cell cycle. The $p14^{ARF}$ protein sequesters MDM2 which stabilises p53.

Therefore, silencing of the CDKN2A gene which occurs in over 90% of PDACs leads to increased cellular proliferation, reduced apoptosis and survival of the mutated cell. The mutation can occur via a homozygous deletion or methylation of the promoter region among other methods[18,19].

1.1.3.4 TP53

The TP53 gene is found on chromosome 17 and codes for the tumour suppressing transcription factor p53. p53 produces a transcription response including pro-apoptotic factors and p21, which is a CDK inhibitor that leads to cell cycle arrest, usually in the G1 phase. Levels of p53 are usually maintained at a very low level by MDM2 which both transports p53 out of the nucleus and marks it for proteasomal degradation.

In conditions of cellular stress such as DNA damage or oncogene activation, MDM2 is inhibited and p53 therefore stabilised, leading to increased levels within the nucleus with subsequent apoptosis or cell senescence[10,12].

1.1.3.5 DPC4

The Deleted in Pancreatic Cancer 4 gene (DPC4) codes for the SMAD4 protein which plays a key role in the transforming growth factor β (TGFβ) signalling

pathway. TGFβ is a cytokine secreted by epithelial, endothelial, haematopoietic and mesenchymal cells which when binding to TGFβ receptor causes phosphorylation of the receptor regulated cytoplasmic proteins SMAD2 and SMAD3. These form a complex with SMAD4 which accumulates in the nucleus. There it stimulates transcription of genes which cause cell cycle arrest. Thus, SMAD4 has a pivotal role in the tumour suppressive effects of TGFβ.

The DPC4 gene is located on chromosome 18 and is so called because it was originally isolated as a tumour suppressor gene for cancer. Mutations are not particularly common in cancer in general, but approximately 90% of pancreatic cancers show mutations to at least one allele. Due to its recessive nature, the complete loss of SMAD4 function only happens following homozygous deletion or intragenic mutation with the loss of the second allele, and this situation occurs in about 55% of pancreatic cancers. As is seen with TP53, DPC4 mutations are observed in high grade PanIN lesions.

Interestingly, DPC4 mutation and loss of SMAD4, while abolishing the tumour suppressive effects of TGFβ, does not seem to affect TGFβ mediated tumour promoting functions such as epithelial to mesenchymal transition (EMT)[9,10,12,15,16,20,21].

1.1.3.6 Epithelial to mesenchymal transition and pancreatic cancer stem cells

EMT represents a number of events leading to an epithelial cell, adherent within an organised tissue, to convert to an independent cell, capable of migration and invasion. During this process, the polarised, basal membrane anchored cell acquires a mesenchymal fibroblastic phenotype via a number of molecular changes. These include the loss of normal epithelial surface markers involved in cell to cell interaction including E-cadherin, claudins and occludin, as well as gaining mesenchymal markers such as S100A4, N-cadherin, vimentin and α-smooth muscle actin.

This change is stimulated by a number of factors already present in the tumour micro-environment including TGFβ, hepatocyte growth factor (HGF), bone morphogenic proteins (BMPs) and vascular endothelial growth factor (VEGF) as well as cellular stress[22,23].

EMT has been shown to represent an important step in metastasis and until recently was felt to be a late event in the evolution of a pancreatic cancer. However, recent evidence in mouse models has shown that both EMT and the presence of pancreatic epithelial cells in the bloodstream occur early in the disease process, before histological evidence of cancer is demonstrable. This suggests a paradigm shift to considering pancreatic cancer a disease which metastasises early, even at the level of PanIN development[24–26].

Cancer stem cells were first identified when different cancer cells within the same tumours were assayed for their proliferative potential and this showed only a small minority demonstrating extensive proliferation. Further investigation showed this small subset to demonstrate distinct cell surface marker expression. In pancreatic cancer, these stem cells have been found to express the surface markers CD133, CD44, CD24 and epithelial-specific antigen (ESA) and are capable of unlimited self-renewal (immortality) and to reproduce all derived cell phenotypes within the cancer. This subset of pancreatic cancer stem cells represents only 0.2-0.8% of pancreatic cancer cells and they have a tumorigenic potential 100 times that of the other cells, demonstrated by the ability to induce tumours in 50% of animals injected with as few as 100 cells.

Pancreatic cancer stem cells are resistant to chemo and radiotherapy and may explain disease which relapses following a good initial response to such treatments. It is also thought that the stem cell and EMT phenotypes may overlap through shared molecular features. Dysregulation of various embryonic pathways including Notch, Wnt and Hedgehog signalling have also been linked to EMT and cancer stem cells.[8,16,23,27].

1.1.3.7 Notch/Hedgehog/Wnt signalling

These pathways are all important in normal embryonic development of tissues but may be reactivated in the development of cancer.

The Notch pathway has a role in the developing pancreas and is activated by ligands of the delta and jagged families expressed on the cell surface binding

to heterodimeric transmembrane Notch receptors of adjacent cells. This leads to cleavage of the notch receptors within the membrane, releasing their active intracellular domain which is then transferred to the nucleus and bound to the transcription factor CSL, leading to the expression of a variety of genes involved in tissue proliferation, differentiation and apoptosis.

In the normal adult pancreas, Notch and its ligands are expressed only at very low levels but aberrant expression of ligands, receptors and Notch transcription targets can be observed in pancreatic cancer and its precursor lesions. Also genetic downregulation of Notch can inhibit cell growth and induce apoptosis in pancreatic cancer cell lines in vitro[28,29].

The Hedgehog signalling pathway is vital in the normal development of the embryonic gut amongst other tissues and involves 3 different ligands (sonic hedgehog (SHH), Indian hedgehog (IHH) and desert hedgehog (DHH). In the absence of these ligands, the membrane receptor patched (PTCH) blocks the smoothened receptor (SMO), inhibiting its activity. However, binding of hedgehog ligands to PTCH, reduces the inhibitory effect on SMO, allowing signal transduction which ends with activation of transcriptional factors.

There are a number of findings suggesting hedgehog signalling is important in the development of pancreatic cancer. Firstly, SHH is expressed in 70% of human pancreatic cancers and there is 35 times increased expression of IHH in cancer compared to normal cells. Elements of the hedgehog pathway are found not just secreted from the cells comprising most of the tumour (so-called 'bulk' cancer cells) but also appear to be integral to the maintenance of

pancreatic cancer stem cells as well as the ligand responsive stroma. Inhibition of the hedgehog pathway by cyclopamine which binds to SMO has been shown to enhance response to chemotherapy and reduce metastatic spread experimentally. Furthermore, the hedgehog pathway was one of the 12 core pathways previously identified[10,16,30].

Wnt signalling is important in the development of the endocrine pancreas and can be activated as part of pancreatic carcinogenesis. Wnt ligands interact with a family of membrane bound receptors known as Frizzled. Following this a number of different pathways can be followed, of which the canonical is the most investigated and understood. In this pathway, a cascade leads to inhibition of β-Catenin phosphorylation, causing accumulation of β-Catenin and translocation from the cytoplasm to the nucleus. Here it binds to the TCF-LEF family of transcription factors which activate transcription of Wnt target genes. Upregulation of Wnt signalling is thought to result in carcinogenesis and progression of various cancers including pancreatic cancer. Wnt signalling is also thought to be activated downstream of the hedgehog pathway, which as discussed above is relevant to pancreatic cancer development.

Although the relevance of upregulated Wnt signalling in pancreatic cancer is controversial, the evidence is growing. Aberrant activation in the pathway has been found in 65% of pancreatic cancers, and high levels of β-catenin in the nucleus has been confirmed in both high grade PanINs and advanced

cancers. Furthermore, Wnt inhibition has been shown to both block proliferation and induce apoptosis in cultured adenocarcinoma cells[9,11,15,16,31].

1.1.3.8 Telomere shortening

Telomeres are located at the end of chromosomes and are repetitive nucleotide sequences which normally shorten with each cell division, thereby causing a cell to have a finite lifespan. To avoid entering senescence, telomeres can be lengthened via activation of telomerase (a reverse transcriptase containing an RNA template which elongates telomeres) or alternative lengthening of telomeres (ALT), potentially bypassing the cells natural finite lifespan. Telomerase is expressed in 85-90% of pancreatic cancers[16,32,33].

1.1.3.9 Stroma and pancreatic stellate cells

One of the hallmarks of pancreatic cancer is a dynamic fibro-inflammatory or desmoplastic response which surrounds the tumour and is known as stroma. Although a desmoplastic reaction has been noted in other cancers such as breast, prostate and ovarian cancer, pancreatic cancer shows the most extensive reaction with stroma estimated to account for up to 90% of the whole tumour volume. The stroma is composed of activated fibroblasts and myofibroblasts including pancreatic stellate cells, inflammatory cells, extracellular matrix (ECM) and blood and lymphatic vessels[34].

Previously, it was hypothesised that the stroma represented a host immune response to the tumour, attempting to wall off the threat, but evidence in

recent years has emerged showing a highly complex and dynamic set of interactions between tumour and stroma cells which is critically involved in tumour formation, proliferation, invasion and metastasis[8,34].

Pancreatic stellate cells, first isolated in 1998[35], are pancreas specific mesenchymal cells which are important mediators of the desmoplastic reaction. Functionally and morphologically they are similar to hepatic stellate cells which had previously been implicated in liver fibrosis. They exist in 2 distinct states; the quiescent state and the activated or myofibroblastic state. They are characterised when quiescent by lipid droplets containing vitamin A and expression of desmin and glial fibrillar acidic protein. They are activated in the presence of growth factors such as TGFβ, platelet derived growth factor (PDGF) and VEGF secreted by tumour cells, and secrete excessive amounts of the components of ECM (leading to the characteristic stroma) express α-smooth muscle actin (α-SMA) and show loss of lipid droplets[34,36].

Their importance in the stromal reaction has been shown by *Bachem et al* who showed increased stroma in orthotopic nude mouse cancers when cancer cells were transplanted along with pancreatic stellate cells as opposed to in isolation[37]. *Vonlaufen et al* also noted stellate cells along with cancer cells in liver metastases from cancer cells transplanted with pancreatic stellate cells in an orthotopic nude mice model, suggesting co-migration and a possible role for stellate cells in promoting a favourable microenvironment for migration and implantation[38].

Immune cells have been shown to make up approximately 50% of pancreatic tumour cell mass. *Clarke et al* showed that cells of the host immune system were present from the earliest stages of pre-invasive lesions but the dominant immune cells were those involved in immune suppression with an absence of activated effector T cells, with a corresponding lack of anti-tumour activity. This suggests that rather than the host immune response being overwhelmed following early immunosurveillance attempting to eliminate the tumour cells, the response is in fact undermined from the start[36,39,40].

The components of the ECM promoted by stellate cells include collagen, fibronectin, proteoglycans and hyaluronic acid (HA). The accumulation of these distorts the normal architecture of the pancreatic tissue. This increased rigidity leads to compression of blood and lymphatic vessels, leading to decreased perfusion[36].

Although most solid tumours contain areas of hypoxia as the high metabolic requirements of the tumour outstrip the developing vascular supply, pancreatic cancers actually appear to be globally hypoperfused, showing a paucity of blood vessels despite the hypoxic state and high levels of pro-angiogenic factors. This is demonstrated by the characteristic appearance on contrast enhanced cross sectional imaging of a lack of contrast uptake[36,40].

The observation that roughly 75% of vessels in pancreatic cancer appear to be collapsed may suggest the presence of high interstitial pressures,

exceeding the combined hydrostatic and oncotic pressures, along with the elastic forces of the vessel wall as described by Starling in 1896.

In normal tissues, interstitial fluid pressure (IFP) ranges from ~8mmHg in the head of the pancreas through ~2mmHg in muscle to ~0.1mmHg in the liver. These measurements are all significantly lower than typical arteriole (40-80mmHg) and capillary (15-40mmHg) pressures meaning adequate perfusion of the tissues.

This high IFP has been extensively investigated. For example, *Provenzano et al* used genetically engineered mouse models (GEMM), which, in contrast to xenograft tumour grafted mice, develop autochthonous tumours which faithfully replicate tumour structures in humans including the stroma formation. The IFP in such tumours was dramatically elevated, ranging from 75-130mmHg, which is similar to mean arterial pressure[41]. This explains the collapsed nature of vessels within the tumours.

The relevance of these findings of excessive ECM deposition and increased IFP within the stroma with regards to this thesis is the effect on resistance to systemic chemotherapy.

1.1.4 **Clinical presentation**

Early pancreatic cancer is often clinically silent which is the reason the disease often presents late at an incurable stage either once local disease is

advanced or distant spread has occurred. Vague symptoms of abdominal discomfort and nausea are common, but non-specific. Specific signs and symptoms can occur. Tumours of the pancreatic head are the most common and may cause obstructive jaundice by compression of the common bile duct, or more rarely, gastric outlet obstruction or gastrointestinal haemorrhage. Obstruction of the pancreatic duct may lead to pancreatitis. Patients with pancreatic cancer may also present with dysglycaemia, and this should be considered in anyone presenting with late onset diabetes mellitus[8,42,43]. However, although approximately 25% of patients with pancreatic cancer have diabetes at diagnosis, and another 40% have impaired glucose tolerance, most people with new late onset diabetes will not have pancreatic cancer[44–46].

Features of more systemic disease also occur in the form of asthenia, anorexia and weight loss, or less commonly, deep or superficial venous thrombosis[42].

1.1.5 **Investigations**

Initial investigations depend on the presentation but usually include routine blood tests which may confirm the presence of obstructive jaundice (raised serum bilirubin) or pancreatitis (raised serum amylase). Although carbohydrate antigen 19-9 (CA19-9) may be raised and levels of more than 100-200U/ml may predict unresectable disease or correlate with survival[42,47], it has shown limited benefit in the screening situation due to a lack of

specificity. Sensitivity is also impaired due to the fact that 10% of patients with pancreatic cancer are negative for Lewis antigen a or b and therefore cannot synthesize CA19-9, producing false negative results[8]. CA19-9 can be useful in confirmed cases of pancreatic cancer, particularly as a marker of early recurrence or progression during follow up[48].

Although first line imaging again depends on the presentation, and may include ultrasound or magnetic resonance imaging, the imaging of choice is a triple phase pancreatic protocol computed tomography (CT), along with a chest CT looking for pulmonary spread. This allows detection of both local disease and distant metastases[8].

When assessing disease stage, patients can be divided into those having resectable, borderline resectable, locally advanced/unresectable and metastatic disease. Local resectability depends on the relationship of the tumour to the surrounding vasculature; coeliac axis, superior mesenteric artery (SMA), superior mesenteric vein (SMV) and the portal vein (PV)[49]. While tumours which would require arterial resections are still considered unresectable other than in exceptional circumstances, vein resection and reconstruction is possible in the borderline group[50].

In cases where biliary drainage is required or CT findings are equivocal in terms of diagnosis, then endoscopic techniques may be used. Endoscopic retrograde cholangiopancreatography (ERCP) allow drainage via the placement of stents into the biliary tree and also to take brushings. This technique is unreliable in gaining a definitive cytological diagnosis due to a

poor sensitivity of 33-54%[51]. By comparison, the sensitivity of endoscopic ultrasound with fine needle aspiration is as high as 92% in specialist centres and is now the method of choice where tissue diagnosis is required[52].

1.1.6 **Staging**

The staging system for pancreatic cancer is based on the tumour, node, metastases (TNM) system used for all cancers but modified for the pancreas. This is provided by the union for international cancer control (UICC) and is currently up to its 8th edition[53]. This is shown in the following two tables.

	T=Primary tumour
TX	Primary tumour cannot be assessed
T0	No evidence of primary tumour
Tis	Carcinoma in situ (including PanIN3)
T1	Tumour restricted to the pancreas, <2cm greatest dimension
T2	Tumour restricted to the pancreas, >2cm greatest dimension
T3	Tumour extends beyond the pancreas, but not involving the SMA/coeliac axis
T4	Tumour involves the SMA or coeliac axis
	N=Regional lymph node status
NX	Regional lymph nodes cannot be assessed
N0	No regional lymph node metastases
N1	1-3 regional lymph node metastases
N2	4 or more regional lymph node metastases
	M=Distant metastases
M0	No distant metastases
M1	Distant metastases

Table 1: UICC TNM staging classification for pancreatic cancer. This table shows the descriptions of the individual T, N and M stage as applied to pancreatic cancer[53].

As can be seen from the second table below, the stage helps determine the potential surgical management of the patient. Resectable disease is any stage I or II disease. Stage III can be either borderline resectable or unresectable. Borderline includes disease with the tumour abutting $<180^0$ circumference of the SMA or coeliac axis, or involving a short segment of the hepatic artery, SMV, PV or confluence of the two[42].

Stage	TNM	% presenting cases
0	Tis, N0, M0	10%
IA	T1, N0, M0	
IB	T2, N0, M0	
IIA	T3, N0, M0	
IIB	T1, N1, M0 T2, N1 M0 T3, N1, M0	
III	T4, any N,N2, M0	30%
IV	Any T, any N, M1	60%

Table 2: UICC TNM staging classification for pancreatic cancer. This table shows how the separate T, N and M components combine to form a numbered stage. Also shown is how these correlate clinically as to whether the tumour is resectable and the percentage of patients presenting with pancreatic cancer who fall into each category[42,53].

1.1.7 **Surgery**

Surgery remains the only potentially curative treatment option for resectable pancreatic cancer. Overall 5-year survival rates have been increased from less than 5% to over 20% in specialist centres due to, amongst other things, improved surgical management oncological therapy[54–56].

Kausch reported the first successful two stage pancreaticoduodenectomy in 1912 performed for an ampullary carcinoma[57]. The first single stage resection was reported by Whipple in 1946[58]. It is these two surgeons who give their name to the procedure now termed a Kausch-Whipple pancreaticoduodenectomy. This involves removal of the gallbladder, common bile duct, duodenum and pancreatic head[59]. The operation has developed over time, and now having a pylorus preserving variant.

Tumours of the body and tail of the pancreas account for around a third of presenting patients and where resectable are treated by a left pancreatectomy combined with a splenectomy. Unfortunately, these tumours have an even more dismal prognosis compared to those affecting the head of the pancreas[60].

Laparoscopic resection of the pancreas is emerging as a potential alternative to the traditional open procedure[61]. A recent systematic review and meta-analysis concluded that, although minimally invasive resections are possible and reported results show improved outcomes, there is no robust evidence and no randomized or prospective studies yet available. Therefore, this cannot be recommended as standard practice at this time[62].

1.1.8 **Adjuvant therapy**

The use of chemotherapeutic regimes in pancreatic cancer was initially reported in the 1970s and 1980s, but only in locally advanced or metastatic disease[63]. The first randomised study looking at adjuvant chemotherapy following resection was published in 1993 by a Norwegian group[64]. This compared surgery alone with surgery plus adjuvant chemotherapy of 5FU, doxorubicin and mitomycin. Although median survival improved from 11 months to 23 months, this did not translate into long term survival.

The landmark ESPAC-1 trial[65] (European Study group for Pancreatic Cancer) was published in 2001 and was designed to determine whether adjuvant chemotherapy or adjuvant chemoradiotherapy improved survival following resection for pancreatic cancer. It was the first adequately powered randomised trial and recruited 541 patients in 61 international centres over a 6-year period. The patients were randomised either to a 2x2 design of chemoradiotherapy, chemotherapy, both or observation, or as individual treatment groups. The chemotherapy arms used folinic acid (initial IV bolus 20mg/m^2) and 5FU (425mg/m^2 on days 1-5 of a 28-day cycle for 6 cycles).

Initial analysis with a median follow up of 10 months suggested a significant improvement in survival for those randomised to receiving chemotherapy when compared to the entire study population (median survival 19.7 months vs 14 months, p=0.0005) but this significance was lost when looking at the 2x2 design alone (17.8 months vs 15.8 months, p=0.09).

Subsequent analysis of the 2x2 design published later in 2004 with a median follow up of 47 months showed median survival was now significantly improved in those receiving chemotherapy vs those not was; 20.1 months vs 15.5 months (HR=0.71 (0.55-0.92), p=0.009), with two and five year survival improving from 21% and 8% respectively to 40% and 21% for those receiving chemotherapy[66].

These results from ESPAC-1 established 5FU and folinic acid as the chemotherapy of choice in the adjuvant setting for pancreatic cancer.

In 2002, Takada et al[67] recruited 173 patients with pancreatic cancer as part of a larger study of 508 patients with various pancreaticobiliary malignancies. Randomisation was between adjuvant mitomycin C and oral 5FU or surgery alone. In the pancreatic subset, there was no significant improvement in survival.

In 2006, *Kosuge et al*[68] (JSAP-1 (Japanese Study group of Adjuvant therapy for Pancreatic cancer) reported randomising 89 patients with R0 pancreatic cancer resections to either cisplatin and 5FU or surgery alone which showed no significant impact on survival.

Following demonstration of a clinical benefit of using the nucleoside analogue gemcitabine over 5FU in palliative patients[69], *Oettle et al*[55] randomised patients to adjuvant gemcitabine vs observation alone following attempted curative pancreatic resection. The results were published as the CONKO-001 trial initially in 2007, with subsequent final results in 2008[70].

368 patients were randomised with a median follow up of 53 months performed. The results showed a significant increase in disease free survival from 6.9 months to 13.4 months, but unfortunately, while remaining significant, the overall survival only increased slightly from 20.2 months to 22.8 months (p=0.005). This may be due to the fact that those with recurrence in the observation group went on to receive gemcitabine for their relapse.

The JSAP-2 trial was published in 2009[71] and had randomised 119 patients to adjuvant gemcitabine and surgery alone. This showed an increase in median disease free survival (11.4 months vs 5months) but this did not convert into a significant difference in overall survival.

For ESPAC-3 patients had initially been randomised to adjuvant folinic acid and 5FU, adjuvant gemcitabine or surgery alone. However, publication of ESPAC-1 during the recruitment led to the surgery alone arm being abandoned and the study renamed ESPAC-3(v2).

The patients from ESPAC-3(v1) were placed in a meta-analysis with patients from ESPAC-1 which confirmed the benefit of the chemotherapy regime of folinic acid and 5FU as opposed to observation alone[72].

ESPAC-3(v2)[54] was published in 2010 and had randomised 1088 in 159 centres worldwide with a median follow up of 34.2 months. Although no difference was seen in progression free or overall survival between to two

adjuvant therapy regimes, there were significantly less treatment related adverse events in the gemcitabine arm.

The JASPAC-01[73], published in 2013, randomised 385 patients to either gemcitabine or the orally administered fluorinated pyrimidine S-1 following resection for pancreatic cancer. The oral drug was shown to improve disease free survival at 2 years from 29% to 49% compared to gemcitabine. However, this was an Asian population and concerns have been raised that due to genetic metabolic differences between Asian and Caucasian populations, the drug may be intolerable for the gastrointestinal tracts of western patients[74].

Recently, the results of the ESPAC-4 study have been published[75]. 730 patients were randomised to receive adjuvant chemotherapy following resection with either gemcitabine alone or in combination with the oral prodrug of 5-FU; capecitabine. The median overall survival was 28.0 months in the combined group vs 25.5 months in the gemcitabine alone group (HR=0.82, p=0.032). This significantly increased survival was achieved without any significant increase in grade 3-4 adverse events related to treatment.

The study concluded that the combination of gemcitabine with capecitabine should be the new standard of care for adjuvant therapy following attempted curative resection for pancreatic cancer. The results of the trials discussed are summarised in the table on the following page.

				Survival (95%CI)		
Year published	**Author/Group**	**Treatment arms (*n*)**	**R0 (%)**	**Median survival (months)**	**2-year survival (%)**	**5-year survival (%)**
1993	Bakkevold[64]	5FU,Doxorubicin MitomycinC (30)	100	23	70	4
		Surgery (31)		11 (p=0.02)	45	8 (=0.1)
2001	ESPAC-1[65] (All patients)	5FU/FA +/- CRT (238)	82	19.7 (16.4-22.4)	N/A	N/A
		No chemo +/- CRT (235)		14 (11.9-16.5) (p=0.0005)	N/A	N/A
2002	Takada[67]	5FU/MitomycinC (89)	58	n/a	N/A	11.5
		Surgery alone (84)			N/A	18 (log rank NS)
2004	ESPAC-1 (2x2 final analysis)[66]	5FU/Folinic Acid (147)	82	20.1 (16.5-22.7)	40	21
		No chemo +/- CRT (142)		15.5 (13-17.7) (p=0.009)	30	8
2006	JSAP-1[68] (Kosuge)	Cisplatin/5FU (45)	100	12.50	N/A	26.40
		Surgery alone (44)		15.8	N/A	14.9 (p=0.94)
2007	CONKO-001 [55](Oettle)	Gemcitabine (179)		22.1 (18.4-25.8)	47.5	22.5
		Surgery alone (175)	83	20.2 (17-23.4) (p=0.06)	42	20.5
2008	CONKO-001 Final [70](Neuhaus)	Gemcitabine (179)		22.8	N/A	21
		Surgery alone (175)		20.2 (p=0.005)	N/A	9
2009	JSAP 2[71] (Ueno)	Gemcitabine +/- RT (58)	84	22.3 (16.1-30.7)	48.3	23.9
		Surgery alone +/- RT (60)		18.4 (15.1-25.3) (p=0.19)	40	10.6
2009	Collated ESPAC data [72]	5FU/Folinic Acid (233)	75	23.2 (20.1-26.5)	49	24
		Surgery alone (225)		16.8 (14.3-19.2) (p=0.003)	37	14
2010	ESPAC-3(v2) [54]	5FU/Folinic Acid (551)	65	23 (21.1-25)	48.1 (43.8-52.4)	N/A
		Gemcitabine (537)		23.6 (21.4-26.4) (p=0.39)	49.1 (44.8-53.4)	N/A
2013	JASPAC-01[73]	S-1 (187)	87	46.3	70	N/A
		Gemcitabine (191)		25.5 (p<0.0001)	53 (p<0.0001)	N/A
2017	ESPAC-4[75]	Gemcitabine	40	25.5 (22.7-27.9)	52.1 (46.7-57.2)	N/A
		Gemcitabine/ Capecitabine		28 (23.5-31.5) (p=0.032)	53.8 (48.4-58.8)	

Table 3: Major adjuvant chemotherapy trials in pancreatic cancer (adapted from Jones et al)[77]

As well as adjuvant chemotherapy, there has also historically been interest in the use of adjuvant chemoradiotherapy with or without additional chemotherapy to try and improve survival. A number of trials have addressed this and a meta-analysis in 2013 by Liao et al[76] attempted to clarify the findings.

The results of this study confirmed that adjuvant 5FU or gemcitabine improved survival (HR=0.65 (0.49-0.84) and 0.59 (0.41-0.83) respectively) compared with observation alone. Chemoradiation, on the other hand, resulted in worse survival than 5FU or gemcitabine (HR= 1.69 (1.12-2.54) and 1.86 (1.04-3.23) respectively). Furthermore, combining chemoradiation with chemotherapy resulted in significantly more haematological toxic side effects.

Therefore, there is now irrefutable evidence that adjuvant chemotherapy improves both disease free and overall survival. The current gold standard is based on gemcitabine and capecitabine. However, chemoradiation cannot be recommended at present[78].

1.1.9 **Palliative therapy**

Survival in advanced disease is expectedly poor. Locally advanced disease is associated with median survival of 8-12 months and metastatic disease with median survival of only 3-6 months[43]. These patients represent approximately 80% of those presenting with pancreatic cancer. Until 1997, 5FU was the agent of choice in the palliative setting but results were poor with response rates of less than 10%[79].

In 1997, 126 patients were randomised to 5FU or gemcitabine for advanced disease. gemcitabine was associated with a significantly better response rate of 24% vs 5% (p=0.0022) and an improved median overall survival of 5.6 months vs 4.4 months (p=0.0025)[69].

Since 1997, there have been a number of studies demonstrating the benefit of new regimes. Firstly, gemcitabine combined with erlotinib, an epidermal growth factor receptor (EGFR) inhibitor showed statistically significant improvement in overall survival but only of two weeks[80]. Understandably this regime was not adopted due to the limited improvement combined with added toxicity.

Next, a European trial found improved progression free survival and objective response rates when using gemcitabine plus capecitabine vs gemcitabine alone in advanced disease. This trial also suggested a trend towards improved overall survival (HR=0.86; 0.72-1.02; p=0.08)[81].

More recently, 2 studies have shown improved survival when comparing single agent chemotherapy with gemcitabine compared with newer combined regimes[82,83]. In 2011, Conroy et al[84] showed FOLFIRINOX (folinic acid, 5FU, irinotecan (topoisomerase inhibitor) and oxaliplatin) plus gemcitabine to improve progression free survival (6.4 vs 3.3 months, p=<0.001) and overall survival (11.1 vs 6.8 months, p=<0.001) compared to gemcitabine monotherapy. Then in 2013, von Hoff et al[85] reported that adding nanoparticle albumin bound (nab)-paclitaxel (a taxane agent) to gemcitabine improved overall survival to 8.5 months from 6.7 months when

gemcitabine alone was used (p=<0.001). Nanoparticle albumin bound (nab)-paclitaxel (trade name Abraxane) uses albumin as a 'stealth coating' to aid delivery of the therapeutic agent into the tumour microenvironment.

These have left combined regimens with gemcitabine plus either FOLFIRINOX or nab-paclitaxel as the standard treatment for palliative disease[86].

1.2 Gemcitabine

PDAC is a significant problem with a dismal prognosis and although surgery is the only form of cure, only around 20% of patients are suitable for surgery at presentation. Chemotherapy is therefore the mainstay of treatment for most patients and the most commonly used agent is gemcitabine. Gemcitabine is also widely used in the adjuvant setting.

1.2.1 Indications, administration and side effects

gemcitabine (2',2'difluorodeoxycytidine) is an analogue of the natural nucleoside cytidine in its deoxygenated form. It differs from deoxycytidine by the addition of 2 fluorine atoms.

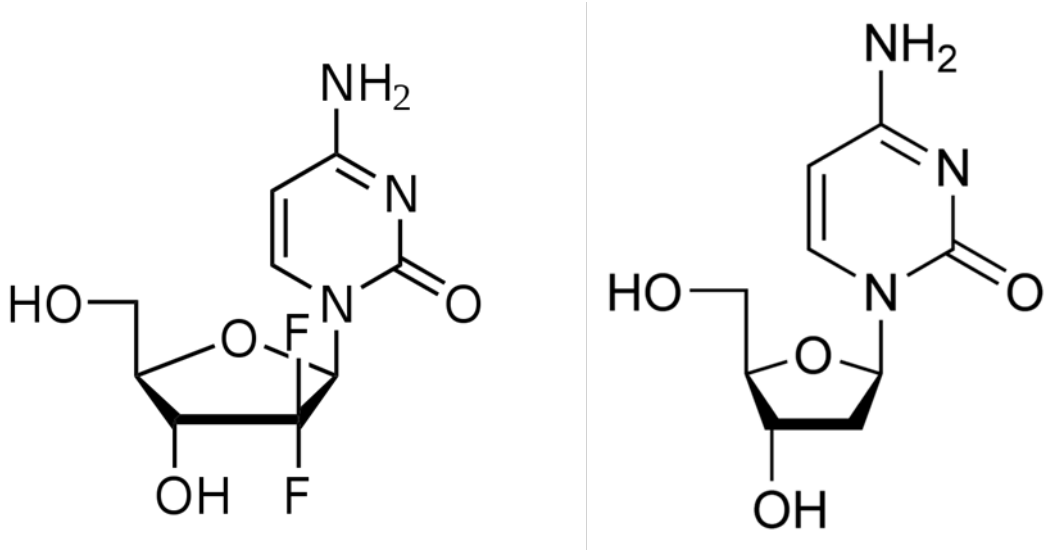

Figure 5: Molecular structure of gemcitabine (left) and Deoxycytidine (right)

Gemcitabine is used as chemotherapy for several solid tumours including non-small cell lung, ovarian, bladder, breast and head and neck cancers[87].

It is now also used as the gold standard for pancreatic cancer in both the adjuvant and palliative settings[88].

It is given via the IV route at a dose of 1000mg/m2 over 30 minutes, given weekly for 3 weeks followed by a week break[89]. Standard therapy in pancreatic cancer previously involved using gemcitabine alone but newer combinations of drugs are becoming more common[90].

Haematological side effects include anaemia, neutropenia and thrombocytopenia whereas non-haematological side effects include oedema, rash, fever and dyspnoea [89].

1.2.2 **Mode of action (see figures 6 and 7)**

Gemcitabine (difluorodeoxycytidine, dFdC) is transported into the cells by a variety of nucleoside transporters including Human Equilibrative Nucleoside Transporter 1 (hENT-1) and Concentrative Nucleoside Transporters 1 and 3 (CNT-1, CNT-3), where it is phosphorylated into its monophosphate form (diflurodeoxycytidine monophosphate, dFdCMP) by deoxycitidine kinase (DCK).

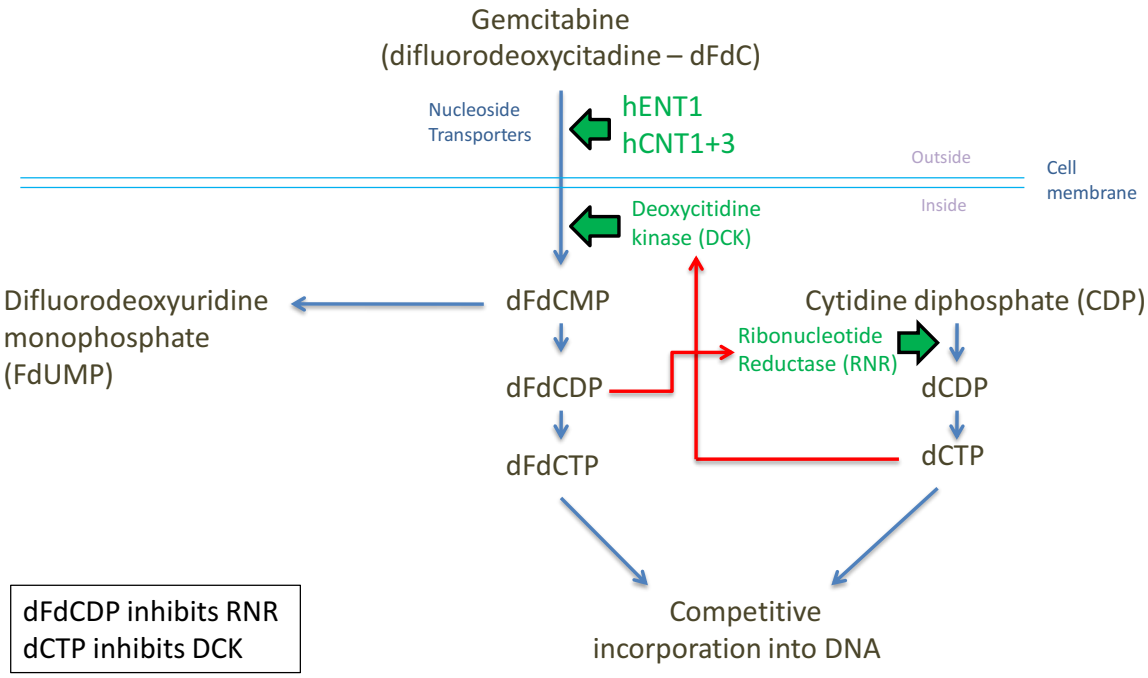

Figure 6: Uptake and metabolism of gemcitabine[87]

dFdCMP is then further phosphorylated to di and tri-phosphate forms (dFdCDP and dFdCTP respectively) by nucleoside mono and di-phosphate kinases. dFdCTP is the active metabolite which exerts its primary effect by being incorporated into DNA by DNA polymerase. This process happens competitively against the naturally occurring nucleoside Cytidine. Once incorporated into DNA, Gemcitabine only allows one further base to be attached to the DNA chain, after which DNA polymerase is dislodged from the DNA strand and replication arrests. This 'masking' of gemcitabine by the extra nucleotide makes the break site unattractive to DNA repair enzymes, increasing the effect. This leads to apoptosis[91] (see figure 7).

Gemcitabine is also known to cause 'topoisomerase poisoning'. This is a term used to describe enhanced topoisomerase-1 cleavage during DNA replication and maintenance, which also leads to cell death via single and double DNA breaks[92].

Gemcitabine is inactivated at two stages within the cell. Once transported into the cell, over 90% of gemcitabine (dFdC) is converted to difluorodeoxyuridine (dFdU) by cytidine deaminase (CDA) which is removed from the cell. The monophosphate form of gemcitabine is converted to difluorodeoxyuridine phosphate (dFdUMP) by deoycytidylate deaminase (DCTD) which is subsequently converted to dFdU and removed from the cell. Nucleotidases also reduces the phosphorylated forms of gemcitabine providing another method of inactivation.

Gemcitabine also aids its cytotoxic effect in other ways. dFdCTP self-potentiates by having a negative effect on DCTD, thereby increasing the amount of phosphorylated gemcitabine. Gemcitabine also has a negative effect on Ribonucleotide Reductase (RNR).

RNR is an enzyme made up of 2 subunits: RRM1 containing the binding site and RRM2 containing the organic free radical for enzymatic activity[93]. It catalyses the conversion of the natural nucleotide cytidine diphosphate (CDP) to deoxycytidine diphosphate (dCDP) which goes on to be further phosphorylated before being incorporated into DNA by DNA polymerase in competition with gemcitabine. By having a negative effect on RNR,

gemcitabine decreases the amount of active natural nucleotide and therefore decreases the biosynthesis of DNA[94] (see figure below).

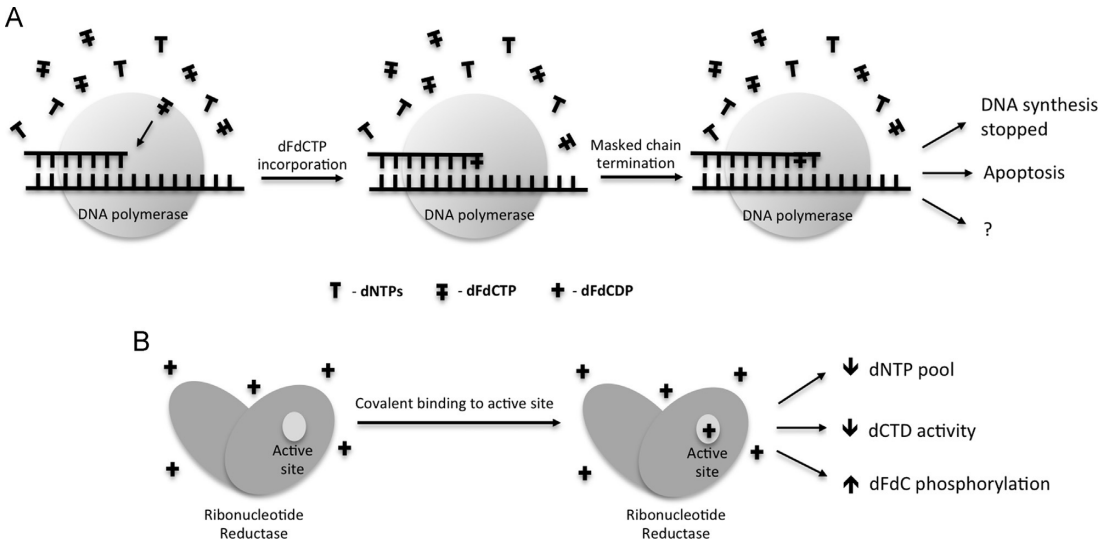

Figure 7: Main mechanisms of action of gemcitabine. A shows gemcitabine (dFdCTP) being incorporated into the DNA chain by DNA polymerase followed by a natural nucleotide triphosphate base (dNTP). This terminates elongation of the chain as DNA polymerase is unable to proceed. Some downstream pathways are not well understood. B shows gemcitabine diphosphate (dFdCDP) covalently binding to ribonucleotide reductase (RNR) which inactivates it, and subsequently decreases the pool of natural nucleotides, decreases deoxycytidine deaminase activity, and increases dFdCTP production. Taken from De Sousa et al without permission[95].

Two other interactions are of particular note. The first is the negative effect that dCTP has on DCK. Therefore, the more active natural nucleotide (dCTP) available, the less gemcitabine will be phosphorylated to its active forms.

The second is that the tri-phosphate form of gemcitabine (dFdCTP) has a negative effect on DCTD and therefore reduces the conversion of dFdCMP to dFdUMP. This is therefore a further self-potentiating effect of gemcitabine.

1.2.3 **Mechanisms of Resistance**

1.2.3.1 Membrane transporters

Due to the hydrophilic nature of gemcitabine, it does not readily diffuse across the cell membrane, instead requiring transport by various nucleoside transporters. These include the sodium independent hENT-1 which allows movement in both directions across the membrane and the sodium dependent CNT-1 and CNT-3 which concentrate gemcitabine within the cell[96,97].

These transporters have been an area of much investigation as they directly affect the amount of gemcitabine available within the cell to exert its cytotoxic effects.

hENT-1 is one of the primary transporter of gemcitabine and a number of studies have now shown levels to affect sensitivity and survival both in vitro and in vivo. Mackey et al 1998[96] used pharmacological inhibition of hENT-1 and showed that this increased resistance to gemcitabine in vitro up to 1000 fold in some cell lines.

However, Nakano et al 2007[93] showed that expression of the mRNA for hENT-1 did not alter in vitro with changes in resistance. The hENT-1 levels were significant when examined in combination with other genes concerned with gemcitabine transport and metabolism but this will be discussed in a later section. This negative result appears to contradict the majority of the studies to date.

A number of in vivo studies have been performed using either RT- PCR or immunohistochemistry to assess the expression of nucleoside transporters in patients receiving adjuvant therapy for pancreatic cancer.

Giovanetti et al 2006[98] used qRT-PCR to assess expression of hENT-1 in tumour tissue taken from biopsies or surgical resections. The patients included those having surgery or those treated palliatively with chemoradiation. They showed high levels of hENT-1 to be associated with a significantly longer overall survival compared to lower levels. Similar results were gained for time to disease progression and disease-free survival. On multivariate analysis, hENT-1 was found to be independently significant with regards to prognosis. Kim et al 2011[99] also retrospectively isolated RNA from surgical specimens and performed qRT-PCR looking for levels of hENT-1. They showed that low hENT-1 levels were significantly associated with poor progression free and overall survival on the univariate analysis, but only significantly associated with poor progression free survival in the multivariate analysis.

Spatlin et al 2004[100] looked at tissue samples from 21 patients with pancreatic cancer treated with gemcitabine, using immunohistochemistry to stain for hENT-1 and CNT-3. They found that patients whose tumours consistently expressed hENT-1 in all cells (normal glandular cells did not express hENT-1) had a significantly longer overall survival compared to lower levels of expression. They also found that CNT-3 showed high staining throughout all tumours.

Maréchal et al[101] also looked at hENT-1 and CNT-3 in 45 patients treated adjuvantly with gemcitabine based chemoradiation after curative resection. Using immunohistochemistry they found that high expression of hENT-1 was associated with longer progression free and overall survival whereas high CNT-3 expression was associated with overall survival only. Farrell et al 2009[102] looked at 229 patients treated in the RTOG9704 trial. This was a prospective randomised trial where post-surgery patients were randomised to treatment with gemcitabine or 5-FU pre and post chemoradiation therapy with 5-FU. Immunohistochemistry was used to stain for hENT-1 on a tissue microarray containing samples of all 229 patients. This showed once again that increased hENT-1 expression was associated with increased disease-free and overall survival in those patients treated with gemcitabine. However, those treated with 5-FU showed no such association.

Morinaga et al 2011[103] recently published a study using immunohistochemistry to assess hENT-1 expression in patients receiving adjuvant therapy with gemcitabine alone. Of the 27 patients, 16 were judged to have high levels of hENT-1 expression and these were found to have significantly longer disease-free and overall survival. hENT-1 expression was confirmed to be a significant prognostic factor for overall survival on both univariate and multivariate analysis.

In 2013, *Greenhalf et al*[104] reported retrospectively analysing tissue from 434 patients from the ESPAC-3 and ESPAC-1 trials for expression of hENT1. These patients had undergone potentially curative surgery and were randomised to receive either adjuvant gemcitabine or adjuvant 5FU post

operatively. Patients receiving gemcitabine with low expression of hENT1 had significantly worse median overall survival than those who had high expression of hENT1 (17.1 months vs 26.2 months; p=0.002). There was no such significant difference in the patients who had received adjuvant 5FU (25.6 months vs 21.9 months; p=0.36). This study concluded that other treatment regimes should be considered for patients with low hENT1 expression.

A recent systematic review concluded that immunohistochemically detected hENT1 expression was significantly associated with disease free survival (HR=0.58; 0.42-0.79) and overall survival (HR=0.52; 0.38-0.72) for those patients receiving adjuvant gemcitabine, and was therefore a suitable prognostic biomarker[105].

So there is now convincing evidence to show that high hENT-1 levels have a significant effect on the transport of gemcitabine into pancreatic cells and allows it to exert its cytotoxic effect.

1.2.3.2 Gemcitabine metabolism

Once transported into the cell, gemcitabine is phosphorylated to its monophosphate form (dFdCMP). Two further phosphate groups are added to create the active forms of gemcitabine (dFdCDP and dFdCTP). The initial phosphorylation is the rate limiting step[106] whereas the second and third

phosphate groups are added in reactions catalysed by non-specific nucleotide kinases.

The rate limiting step is primarily catalysed by deoxycytidine kinase (dCK). dCK has a much higher affinity for gemcitabine compared to the natural nucleoside deoxycytidine (dCyd) as shown by its K_m value of 4.6μM versus 1.5μM[107](the K_m value is the substrate concentration at which the reaction rate is half maximum). Gemcitabine is also phosphorylated by the mitochondrial enzyme thymidine kinase 2 (TK2). However, the substrate specificity for gemcitabine is only 5-10% that of dCyd[108].

dCK has long been linked with acquired resistance to gemcitabine in vitro. The earliest report was by Ruiz van *Haperen et al* in 1994. They created ovarian cancer cells resistant to gemcitabine by gradual exposure to increasing concentrations producing a 30,000-fold increase in resistance. They then showed that there was no detectable dCK protein in the resistant cells on western blot compared to normal levels in the sensitive cells[109].

Following this further work demonstrated a similar correlation between gemcitabine resistance and dCK activity in various solid tumour cell lines in vitro[110] and in vivo[111]. Specifically, *Blackstock et al*[112] looked at the in vivo effects in xenografts. They developed human colon cancer xenografts in nude mice which were developed with and without transfection with a retroviral vector containing dCK, thereby creating wild-type tumours and tumours overexpressing dCK. Following treatment with gemcitabine, they showed increased accumulation within the tumour cells overexpressing dCK of

dFdCTP as well as a more marked tumour growth delay than in wild type tumours.

More recently, studies specifically looking at pancreatic cancer have emerged. In vitro, Nakano et al 2007[93] developed resistant pancreatic cancer cell lines and looked at the expression of 4 genes associated with gemcitabine metabolism and transport (namely hENT-1, dCK, RRM1 and RRM2). This showed that with increasing resistance, dCK RNA levels initially increased slightly but then fell to undetectable levels as cell lines developed more resistance. *Ohhashi et al*[113] looked at the same 4 genes in cells developed to acquire resistance to gemcitabine, but then went on t0 inhibit these genes via RNA interference with siRNA. They found once again that expression of cDK was significantly reduced in the resistant compared to the parental cell line. They also showed that down regulation of dCK enhanced resistance to gemcitabine.

Tang et al 2011[114] initially looked at the effect of overexpressing dCK via recombinant adenovirus vectors and found that this increased sensitivity to gemcitabine. They then went on to perform intratumoral injections of these vectors into established subcutaneous pancreatic cancer models in nude mice. This caused tumour inhibition and an increase in apoptosis.

Fujita et al 2010[115] retrospectively examined 40 human cancers treated with gemcitabine looking for levels of dCK amongst other genes of gemcitabine metabolism and transport. They performed qRT-PCR and found high dCK levels to be associated with significantly longer disease free survival.

These findings represent compelling evidence as to the importance of dCK in the metabolism of, and subsequently the resistance of cells to gemcitabine.

There is some evidence that TK2 may also have a role despite playing a secondary role to dCK in gemcitabine phosphorylation. This is because TK2 phosphorylates dCyd far more efficiently than it does gemcitabine. Deoxycytidine monophosphate is then converted to its diphosphate (dCDP) and subsequently its active triphosphate form (dCTP). This has 2 effects on the action of gemcitabine: firstly, the increased pool of dCTP competes with gemcitabine for incorporation into DNA, and secondly dCTP inhibits dCK, thereby reducing the active metabolite of gemcitabine.

This inhibition of dCK by dCTP has been suggested as the means for acquired resistance in human oropharyngea[116]l and human small cell lung cancer[117].

It has also been reported that inhibiting the deamination of gemcitabine by CDA may increase sensitivity to the drug. Significant increases in sensitivity to gemcitabine were observed in various human cancer cell lines following treatment with tetrahydrouridine (an inhibitor of CDA activity)[118,119]. Furthermore, neuroblastoma cell lines highly sensitive to gemcitabine were found to have low levels of CDA mRNA.

1.2.3.3 Inhibition of Ribonucleotide Reductase (RNR)

As described above, RNR is responsible for the conversion of cytidine diphosphate (CDP) to deoxy-cytidine diphosphate (dCDP), which is a vital step in the production of the natural nucleotide base pool for incorporation

into DNA competitively against gemcitabine. The action of RNR is inhibited by gemcitabine. Therefore, alterations in the expression of either of the two subunits of RNR (RRM1 and RRM2) could be expected to affect resistance to gemcitabine[95].

This hypothesis has been confirmed in numerous studies. Increased expression of RRM1 has been shown in relatively gemcitabine resistant cell lines in a variety of different cancers including pancreatic, colonic, biliary and non-small cell lung cancer[93,120–123]. Equally, siRNA knockdown of RRM1 in the resistant MiaPaCa pancreatic cancer cell line, increased sensitivity[120]. Similar results were shown for RRM2 with overexpression associated with resistance to gemcitabine and knockdown reducing this resistance in vitro[124].

1.2.3.4 Gemcitabine induced DNA damage and induction of apoptosis

As discussed above, when gemcitabine is incorporated into the DNA chain, a further nucleotide is subsequently attached before DNA polymerase is dislodged. This 'masking' of gemcitabine potentiates its effect as this makes it more difficult for DNA repair genes to excise mismatched deoxyribonucleotides from DNA[125]. Some repair enzymes are able to tackle this problem and may therefore be related to resistance. Excision repair cross-complementation 1 (ERCC1) is a DNA endonuclease which incises DNA at the site of double strand breaks, meaning it can repair gemcitabine induced damage. It has been shown that overexpression of ERCC1 is associated with poor response to gemcitabine[126,127].

Where DNA can be repaired after damage by gemcitabine, Polo-like kinase 1 (Plk1) is involved in entering the cell in to mitosis. When Plk1 levels are inhibited, sensitivity to gemcitabine increases[128].

The effect of gemcitabine on topoisomerase-1 cleavage to produce topoisomerase poisoning has been investigated showing that acute myeloid leukaemia cells deficient in topoisomerase 1 are resistant to gemcitabine[92].

In regards to apoptosis, a variety of pathways have been found to interact with gemcitabine activity. Examples include p53 mutations reducing increasing resistance[94], the cytotoxic effect of gemcitabine being mediated by p38 and leading to MAPK-caspase dependent apoptosis[129], and gemcitabine resistance being associated with over activation of the PI3K/Akt pathway[130].

1.2.3.5 Stroma

One of the important factors in gemcitabine resistance in pancreatic cancer is the tumour environment characterised by the dense surrounding stroma and subsequent poor vascularisation due to high pressures. Among all epithelial tumours, pancreatic cancer possesses the most extensive desmoplastic reaction which can account for up to 90% of tumour volume[131]. This limits both drug delivery to the tumour cells and also the immune system[95].

A vital pathway for the development of the stroma is hedgehog (Hh) signalling. This is known to promote tumorigenesis and the characteristic desmoplastic reaction seen in pancreatic cancer, by affecting the motility and

differentiation of stromal cells, causing the extracellular matrix composition to be modified[132].

It has also been shown that inhibiting the Hh signalling pathway, stroma related gemcitabine resistance could be partially overcome, by increasing vascularity and drug delivery to the tumour by up to 60%[133].

Further studies have also shown a synergistic effect between inhibition of the Hh pathway and gemcitabine in pancreatic cancer cell lines and mouse xenograft models[134–136].

1.2.3.6 EMT phenotype

Epithelial to mesenchymal transition (EMT) plays an important role in many solid tumours, including pancreatic cancer. gemcitabine resistant cells have been shown to have lower expression of epithelial markers such as E-cadherin and higher expression of mesenchymal markers such as vimentin[137].

It has also been demonstrated that repressors of E-cadherin such as ZEB1 and slug can cause gemcitabine resistance in pancreatic cancer and conversely that downregulation of ZEB1 induced reversal of EMT characteristics of Gemcitabine resistant cells[138,139].

However, although it is now well known that the EMT phenotype is linked to resistance, the diversity of EMT causing transcriptional factors may enable cancer cells to adapt and survive a single targeted therapy. Therefore, this remains an emerging area of research[140].

1.3 PDAC immortal cell lines

The laboratory cell work utilised immortalised pancreatic cancer cell lines in regular use within the department of molecular and clinical cancer medicine at the University of Liverpool. The origins and characteristics of the various cell lines are described below.

1.3.1 **Suit-2**

These cells have the following mutations:

K-RAS alteration	P53 alteration	P16 alteration	SMAD4 alteration
p.G12D	p.R273H	69 GAG-TAG Product Glu – stop	None Wild type

Table 4: Mutations in SUIT-2 cell line

SUIT-2 cells are derived from a metastatic liver tumour of human pancreatic carcinoma. These cells grow in monolayered sheets and histologically closely resemble the original moderately differentiated pancreatic tubular adenocarcinoma. The cells produce both carcinoembryonic antigen (CEA) and carbohydrate antigen 19-9 (CA19-9), and propagate even in serum free medium[141]. Parental SUIT-2 cells were given the abbreviation AS.

1.3.2 **BxPC3**

These cells have the following mutations:

K-RAS alteration	P53 alteration	P16 alteration	SMAD4 alteration
None Wild type	p.Y220C	Homozygous deletion	Homozygous deletion

Table 5: Mutations in BxPC3 cell line

BxPC3 are derived from an adenocarcinoma of the pancreatic body from a 61-year-old female. They express CA 19-9 and CEA.

1.3.3 **Panc1**

These cells have the following mutations:

K-RAS alteration	P53 alteration	P16 alteration	SMAD4 alteration
p.G12D	p.R273H	Homozygous deletion	None Wild type

Table 6: Mutations in the Panc1 cell line

Panc1 are derived from an adenocarcinoma of the head of the pancreas of a 56-year-old male. They do not express CA19-9 or CEA.

1.3.4 **MiaPaCa**

These cells have the following mutations:

K-RAS alteration	P53 alteration	P16 alteration	SMAD4 alteration
p.G12C	p.R248W	Homozygous deletion	None Wild type

Table 7: Mutations in the MiaPaCa cell line

MiaPaCa are derived from an adenocarcinoma of the pancreatic body and tail of a 65-year-old male. They do not express either CA19-9 or CEA.

1.4 Previous work

1.4.1 Development of resistant cell lines

The wild-type SUIT-2 cell line was grown in increasing concentrations of gemcitabine and 5-FU to create resistant cell lines. Initial MTS assays were performed on the original line and from this, IC50 values were obtained. This value was used to give an initial concentration of chemotherapy to use.

For gemcitabine, the initial concentration was 5nM of gemcitabine in the 20mls of full media used with T-75 flasks. The cells were passaged 3 times in the initial concentration and the concentration was then doubled up to a maximum of 1000nM.

For 5-FU, the initial concentration was 1μM and increased up to a maximum of 50μM.

Both gemcitabine and 5-FU were diluted in fresh full media and were produced from master stock frozen at -80°C.

This process produced a cell line which could be cultured in 1μM gemcitabine but lost this resistance when cultured without gemcitabine for multiple passages. These cells were named KR and were used for the microarray experiments.

From this population of transiently resistant cells, a clonal population was created by initially growing KR cells in 5μM gemcitabine and then serially diluting the cells to a concentration of 1-2 cells per well in a 96-well plate. After incubation until the well was confluent, the well was trypsinised and the cells once again serially diluted to seed at 1-2 cells per well in a 96-well plate. This was repeated for a third time and the cells allowed to grow to a larger population in culture medium with 5μM gemcitabine. This produced a cell line which tolerates higher levels of gemcitabine (5μM) and maintains resistance to gemcitabine even when cultured without gemcitabine for 6 months. This cell line was termed GR.

Unfortunately, it was not possible for me to use this KR cell line fully during my experiments. I was provided with cell lysate to perform western blots upon, but when the frozen stores of the cells were defrosted and culture attempted, it became apparent that they had developed a mycoplasma infection and could not be used.

Therefore, my experiments used cell lysate for the KR Suit-2 cell line provided to me only. Thankfully the GR Suit-2 cell line was unaffected by these problems and could be used freely.

1.4.2 **Determination of gemcitabine sensitivity**

An MTS assay was performed to confirm the resistance of the clonal resistant cell line (GR) cell line relative to the parental SUIT-2 cell line (AS).

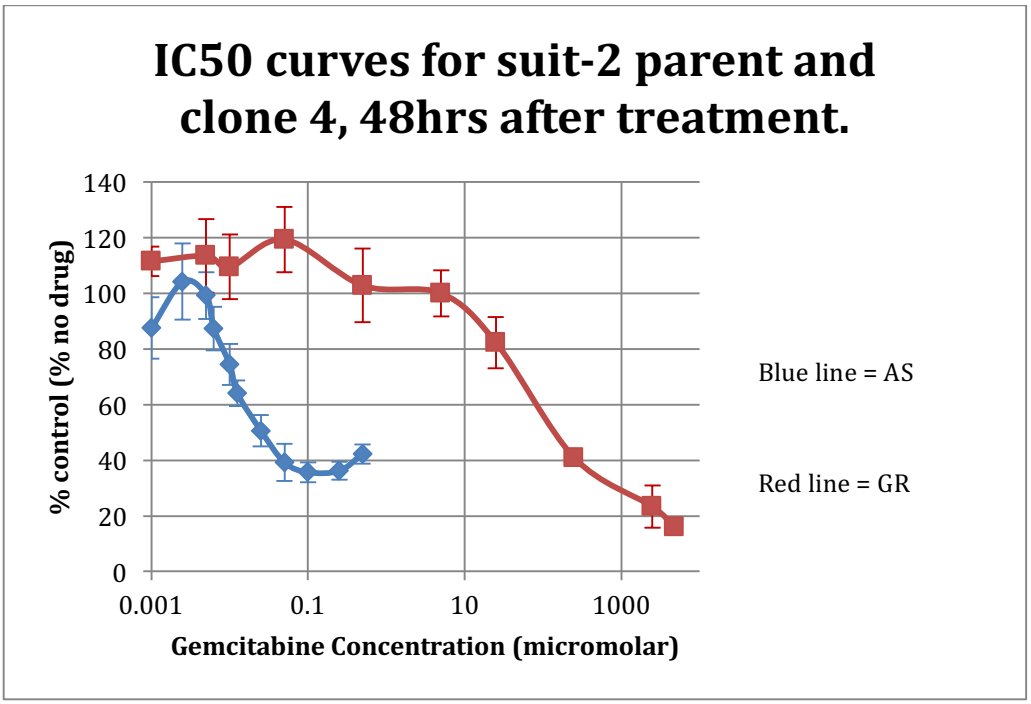

Figure 8: ***Cytotoxicity curves for AS and GR cell lines treated with gemcitabine. Percentage of cells alive vs control are plotted against concentration of gemcitabine (Dajani, unpublished)***

The above cytotoxicity studies were taken after 48 hours' treatment of cells with varying concentrations of gemcitabine. The error bars represent one standard deviation. This confirms that the resistant cells tolerate gemcitabine in much higher levels than the sensitive cells. IC50 values

represent the concentration of gemcitabine which kills half the cells and the IC50 values in this experiment are ~0.025μM for AS and >100μM for GR.

This cytotoxicity study for the transiently resistant cell line KR vs parental Suit-2 (AS) shows an increase in the level of resistance to gemcitabine but not to the level of the GR resistant cell line in the previous figure. The IC50 values for gemcitabine determined from the curves are 35nM for AS cells and 400nM for KR cells.

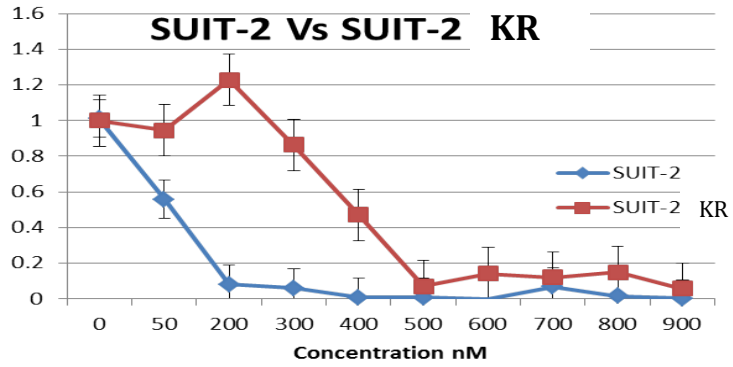

Figure 9: ***Cytotoxicity curves for AS and KR cell lines treated with gemcitabine. In this graph, the percentage of cells alive is plotted as relative to 1=100%, against concentration of gemcitabine. Suit-2 (blue line) represents the parental Suit-2 cell line called AS in my work, and Suit-2 KR (red line), the resistant cell line termed KR in this thesis. (Dajani, unpublished)***

1.4.3 Microarray

The sensitive cell line AS and the first resistant cell line KR were used for microarray experiments. Total protein was extracted from cultured cell lysate and hybridised to 810 Protein Antibody Arrays to compare differential protein expression[142]. RNA was extracted from cultured cells and hybridised to Illumina Human v3 Bead Arrays to compare gene expression.

1.4.4 Bioinformatics

The microarray results were examined by the resident bioinformatics expert in the Department of Molecular and Clinical Cancer Medicine in Liverpool, Dr Brian Lane. The following genes and proteins were found to be significantly differentially expressed:

Genes/RNA	Proteins
BEX4	Glutathione S-transferase P
LOC439949	Zinc finger protein 593
SERPIN A1	Occludin
SNAR-A1	Folate receptor alpha
	Ribonucleotide reductase subunit M2 (RRM2)

Table 8: Differentially expressed genes and proteins in microarrays

1.5 Genes and proteins of interest

1.5.1 Genes of interest

1.5.1.1 SERPIN A1

The serpins are a super-family of proteins whose membership is based on the presence of a common core comprising of three β-sheets and 8-9 α-helices. Despite the common core, they have a wide variety of functions and properties. The family is subdivided into 16 'clades' which are each assigned a letter. SERPIN A1 is the first such member of the A clade which represents a group of proteinase inhibitor[143].

The gene termed SERPIN A1 codes for the protein α-1-antitrypsin (A1AT), which is also sometimes referred to as α-1-proteinase inhibitor. It is a 52kDa acute phase protein which inhibits serine proteases and is released from human neutrophils during the inflammatory process. Deficiency of A1AT is associated with both chronic liver disease and pulmonary emphysema[144]. Although the main site of production is in the liver, it has been shown to be produced by pancreatic islet cells[145].

A1AT has long been suspected as being a potential biomarker of pancreatic cancer[146], however others have argued that the fact it is involved in the acute phase response makes its usefulness as a specific marker of the disease unlikely[147]. Conversely, it has also been shown to inhibit angiogenesis in the corneas of rats and to reduce subcutaneous tumour growth in mice[148].

More specific to pancreatic cancer and gemcitabine, high levels of A1AT were shown to predict short overall survival in patients with advanced pancreatic cancer receiving gemcitabine monotherapy[149]. SERPINA1 was also shown to have high expression in pancreatic cancer cell lines with intrinsic sensitivity to gemcitabine and also have low expression in cell lines with acquired gemcitabine resistance[150]. Although these two results seem contradictory, they do suggest some association between SERPINA1 and gemcitabine resistance.

More recently, A1AT has been suggested as an immunohistochemistry staining marker (along with three others as a panel of four) for serous cystadenoma of the pancreas[151], and the ratio of serum trypsin to A1AT has been shown to be higher in pancreatic cancer patients with PRSS1 mutations compared to healthy controls[152].

Combining all the evidence available as well as the ingenuity pathway above, SERPIN A1 and A1AT were felt to represent a good avenue of investigation.

1.5.1.2 Other genes

Three other RNAs were identified by the arrays as being differentially expressed. First the small ILF3/NF90-associated RNA A1 (SNAR-A1) is a small non-coding RNA which binds to NF90. There is no literature available on the function of this RNA.

Secondly, brain expressed X-linked 4 (BEX4) is a member of a group of pro-apoptotic genes. At the time of reporting of the arrays, there was no available literature on the BEX4. Very recently, decreased expression has been linked with growth of oral squamous cell cancers and neuroblastomas[153,154].

The final RNA has the name LOC439949 and codes for a hypothetical protein only.

Given the lack of literature noted and the limited resources available, these three differentially expressed RNAs were not investigated.

1.5.2 **Proteins of interest**

1.5.2.1 Glutathione S-transferase P

Glutathione S-transferases (GSTs) are a family of enzymes which play an important role in detoxification of carcinogens. Carcinogen metabolism involves phase I metabolic activation and phase II detoxification involving a variety of enzymes. GSTs are the principal phase II enzymes which catalyse the conjugation of toxic and carcinogenic electrophilic molecules[155]. There are four main classes of which glutathione S-transferase P (or Pi) is one (GSTP). It is a 23kDa protein.

Given the link with carcinogen metabolism, GSTP is an obvious source of interest for oncological research. However, although one study looking at the gene expression from five human pancreatic cancer patients showed upregulation of GSTP[146], subsequent studies looking at much larger

populations have shown no such differential expression when compared with healthy controls[156,157]. GSTP was selected to be investigated further.

1.5.2.2 Occludin

Occludin is a 59 kDa protein which is an integral plasma membrane protein located at the tight junctions between cells. It has therefore been implicated in as playing a vital role in the cell dissociation which leads to tumour invasion and metastases in pancreatic cancer[158]. It has also been suggested that occluding plays a role in the development of the EMT phenotype noted in pancreatic cancer[159–162].

Occludin was therefore considered a suitable candidate for further study.

1.5.2.3 Folate receptor α

Folate receptor α (FOLR) is a member of the folate receptor family which mediate delivery of 5-methyltetrahydrofolate into cells. This is the biologically active form of folate used for DNA production and the cysteine cycle. The α form is usually only expressed on luminal epithelial cells of the kidney, lung, choroid plexus and placenta, so is not in contact with circulating folate. It has been shown to be overexpressed in numerous solid organ tumours including kidney, brain, lung, endometrial, ovarian, colorectal, gastric, and pancreatic[163].

The main area of interest at present for FOLR is in ovarian cancer, where a monoclonal antibody called farletuzumab has reached as far as Phase III

trials as part of combination therapy[164,165]. In pancreatic cancer, the folate receptor family has been developed as a potential target folate-gemcitabine nanoparticle to target drug delivery, but this remains in early stages of development[166]. FOLR was also chosen as a candidate for further study.

1.5.2.4 Ribonucleotide reductase subunit molecule 2 (RRM2)

RRM2 is the smaller of the two subunits which make up the ribonucleotide reductase enzyme. The function of this molecule as described above is to increase the pool of natural nucleotide triphosphates, for incorporation into DNA in competition with gemcitabine.

As early as 1999, overexpression of RRM2 was being described as a mechanism of resistance to gemcitabine in oropharyngeal epidermoid carcinoma[116]. In 2004 it was shown that siRNA knockdown of RRM2 could both attenuate pancreatic cancer invasiveness and gemcitabine resistance in vitro[167], as well as suppress tumour growth and inhibit metastases in an orthotopic xenograft model in vivo[124].

In 2007, *Itoi et al*[168] looked at EUS-FNA biopsies taken from 31 patients with unresectable pancreatic cancer and assessed them for RRM2 expression. They found that the median survival of patients with low levels of RRM2 was 8.8 months vs 5.0 months for those patients with high levels of RRM2 (p=0.01). The overall response rate to gemcitabine was also significantly higher in low vs high expression of RRM2 (50.0% vs 7.7%, p=0.013).

Around the same time, a number of groups were assessing RRM2, along with other well-known proteins associated with gemcitabine metabolism. RRM2 was consistently shown to be related to gemcitabine sensitivity[93,115,169]. A subsequent meta-analysis of this collection of studies showed that RRM2 levels were associated with overall survival (HR=2.13 (1.00-4.52), p=0.05) but not disease or progression free survival (p=0.227 and 0.19 respectively)[170].

Meanwhile another group again showed that siRNA knockdown could decrease resistance to gemcitabine[113].

Xie et al[171] examined resected tumours of 117 patients for levels of RRM2, they showed no prognostic benefit of low levels. However, only 44 patients received adjuvant gemcitabine, but even in this subset neither progression free nor overall survival were significantly different whether high or low levels of RRM2 were seen. This study may have been underpowered to show a result, given there were only 8 patients in the high expression group given adjuvant gemcitabine.

In comparison to these relatively low patient numbers, *Farrell et al*[172] looked at 229 patients from the Radiation Therapy Oncology Group (RTOG) trial who received gemcitabine. They claim that RRM2 was associated with survival in these patients and tentatively suggest that RRM2 should 'possibly' be pursued further as a biomarker of gemcitabine resistance. However, the data in the actual paper could be viewed as equivocal. It should be noted that the patients in this trial received combination chemo-radiotherapy both pre-

and post-operatively which may have an effect on the biology of tumours not seen outside the US where radiotherapy is not standard practice, and may also have affected the tumour biology prior to the samples being taken due to neo-adjuvant treatment.

Given all the interest, RRM2 was an obvious candidate for further study. Also, to date no study has shown a survival difference in RRM2 levels in patients with resected tumours prior to treatment with gemcitabine, i.e. prior to adjuvant therapy without any neoadjuvant therapy pre-operatively. This could be a viable route of enquiry with the facilities and bio-bank available at Liverpool university.

1.5.2.5 Interleukin 1β

Interleukin 1-β (IL1β) is a member of the interleukin 1 family of cytokines. It is produced by macrophages and is a mediator of the inflammatory response which is involved in a wide variety of cellular activities. Its role in chronic inflammation, carcinogenesis and angiogenesis, plus the availability of IL1 blocking drugs and evidence from animal models, have led some to suggest using reducing IL1 activity in human malignancies, particularly metastatic disease[173].

In pancreatic cancer, interleukin 1 receptor antagonist levels have been associated with disease severity[174,175], and increased levels can activate the hedgehog pathway, affecting tumour development and stroma formation[176].

Given the prominent function of IL1β in various cellular processes including the inflammatory response, a specific role within a pathway of gemcitabine resistance may be difficult to identify. However, the initial ingenuity pathway showed an interaction with SERPIN A1, and so IL1β was selected for further study.

1.5.2.6 Zinc finger protein 593

Although the phrase zinc finger protein is now used to describe a wide variety of protein structures, when a literature search was performed specifically looking for zinc finger protein 593, no results were found. Therefore, in view of limited resources, this protein was not investigated further.

1.6 Summary

Pancreatic cancer is a devastating disease with an extremely poor prognosis, due to a combination of late presentation in approximately 80% and high levels of recurrence for the few deemed suitable for curative resection.

Gemcitabine based chemotherapies remain the current gold standard, but many tumours have innate resistance or progress despite treatment.

The previous work done within the department at the university of Liverpool identified SERPIN A1 and a number of proteins of interest which required further investigation, which was the aim in this research.

2 Aims and Objectives

The aim of this study is to examine the results of the microarray and identify a novel pathway for gemcitabine resistance. Once candidate genes and proteins have been validated, they will be manipulated to assess their effect on resistance to gemcitabine. If a link with resistance can be confirmed, the candidate genes and proteins could, in the future, be interrogated for their potential effect on patients treated with gemcitabine from the bank of pancreatic cancer tissue microarrays available within the department. If an effect on recurrence or survival could be established this could lead to personalised chemotherapy or potential targets for novel treatments.

Objectives:

1 To establish levels of gemcitabine resistance and levels of proteins previously associated with gemcitabine metabolism and resistance.

2 To validate the results of the RNA and protein microarrays.

3 To knockdown the differentially expressed genes and proteins of interest to assess an effect on resistance.

4 To optimise immunocytochemistry and immunohistochemistry of any genes or proteins affecting resistance to allow further studies on human tissue to assess any effect on recurrence or survival.

3 Materials and Methods

3.1 Materials

3.1.1 Chemical or Reagent

Chemical or reagent	Supplier
Acrylamide-bis ready-to-use solution 30% for electrophoresis	*VWR international, Lutterworth*
Albumin from Bovine Serum	*Sigma Chemical Co, Poole*
Ammonium persulfate	*Sigma Chemical Co, Poole*
Blotting paper Whatman GB004	*VWR international, Lutterworth*
β-actin Primary Antibody	*Cell Signalling, Hitchin*
Bradford dye reagent	*BioRad, Hemel Hempstead*
Coomassie Blue	*Sigma Chemical Co, Poole*
Dimethyl Sulfoxide (DMSO)	*Fisher Scientific, Loughborough*
Distilled water	*University of Liverpool stores*
DL-Dithiothreitol (DTT)	*Sigma Chemical Co, Poole*
dNTP mix	*Life technologies, Paisley*
Ethanol	*University of Liverpool stores*
EZ4U Assay	*Biomedica, Austria*
Foetal Bovine Serum (FBS)	*Life technologies, Paisley*
Gemcitabine	*Eli-Lilly, Basingstoke*
Glycine	*Fisher Scientific, Loughborough*
Hydrochloric acid	*University of Liverpool stores*
L-glutamine	*Life technologies, Paisley*

Chemical or reagent	Supplier
LightCycler® 480 SYBR Green I Master mix	*Sigma Chemical Co, Poole*
Lipofectamine 2000	*Invitrogen, Renfrew, UK*
Non-fat Dry Milk, Blotting Grade	*BioRad, Hemel Hempstead*
OPTIMEM® I Reduced Serum Medium (1X), liquid - with L-Glutamine	*GE Healthcare, Amersham*
Restore™ Western Blot Stripping Buffer	*Thermo Scientific, Loughborough*
PCR buffer 10X	*Life technologies, Paisley*
Phosphatase Inhibitor Cocktail Tablets	*Roche Applied Sciences, Burgess Hill*
Phosphate Buffered Saline (PBS) Tablets	*Fisher Scientific, Loughborough*
Penicillin-streptomycin	*Sigma Chemical Co, Poole*
Protease inhibitor tablets, EDTA-free	*Roche, Welwyn Garden City*
Protein ladder	*Life technologies, Paisley*
Random primer for PCR	*Life technologies, Paisley*
RNAse A	*Thermo Scientific, Loughborough*
RNAse free water	*Life technologies, Paisley*
RNase inhibitor	*Life technologies, Paisley*
RPMI-1640 Media	*Sigma Chemical Co, Poole*
SMARTpool SiRNA GSTP	*Dharmacon Inc., Chicago*
SMARTpool SiRNA RRM2	*Dharmacon Inc., Chicago*
SMARTpool SiRNA SERPIN A1	*Dharmacon Inc., Chicago*
Sodium chloride	*Sigma Chemical Co, Poole*
Sodium Dodecyl Sulfate (SDS)	*Fisher Scientific, Loughborough*

Chemical or reagent	Supplier
SuperScript® II Reverse Transcriptase	*Life technologies, Paisley*
Taq DNA polymerase	*Life technologies, Paisley*
TEMED(N,N,N′,N′-Tetramethylethylenediamine)	*Sigma Chemical Co, Poole*
Tris Base	*EMD Chemicals, San Diego*
Tris HCL	*Sigma Chemical Co, Poole*
Tween® 20	*Sigma Chemical Co, Poole*
Trypsin	*Sigma Chemical Co, Poole*
Virkon	*Antec International, Sudbury*
Western Lightning Plus ECL	*PerkinElmer, Cambridge*

3.1.2 **Equipment**

Equipment	Supplier
Cell Counting Slides	*BioRad, Hemel Hempstead*
Centrifuge (Heraeus)	*Thermo Scientific, Loughborough*
Dako EnVision+ System	*DAKO, Cambridge*
Falcon Tubes - 15 and 50ml	*Corning Inc., New York*
GBX Developer and Fixer	*Kodak*
High Pure RNA Isolation Kit	*Roche Applied Sciences, Burgess Hill*
LightCycler 480	*Sigma Chemical Co, Poole*
LightCycler 480 96 Multiwell Plate and sealing foil	*Sigma Chemical Co, Poole*
Microcentrifuge tubes (0.5ml/1ml)	*Eppendorf, Stevenage*
Multiskan EX spectrophotometer	*Thermo electron corporation*
PageRuler Prestained Protein Ladder	*Fermentas, York*
pH Meter Seven Compact	*Mettler-Toledo, Beaumont Leys*
X-Ray Kodak Film 18x24 cm	*Thermo Scientific, Loughborough*
Pipettes - 5, 10, 25ml	*Corning Inc., New York*
Pipette tips	*Starlab, Milton Keynes*
Plates (96-well)	*Corning Inc., New York*
Procell Incubator	*JenconsScientificLtd,Leighton Buzzard*
Sonicade	*Branson Ultrasonics, Connecticut*
Trans-Blot® Turbo™ Transfer System	*BioRad, Hemel Hempstead*
T25 and T75 Flasks	*Thermo Scientific, Loughborough*
Vortex Genie 2	*Scientific Industries, New York*
Water Bath JB Aqua 26 Plus	*Grant, Shepreth, Cambridgeshire*
Weighing Scales	*VWR, Lutterworth*

3.1.3 **Preparation of Solutions**

1M DL-Dithiothreitol (DTT)

0.154g DTT, 1ml distilled water. Storage: Aliquoted and stored at -20°c

1M Tris

30.29g Tris HCl, 200ml distilled water, pH as required. Storage: Room temperature

Running Buffer x10

50ml 20% Sodium dodecyl sulphate (SDS), 144g Glycine, 30g Tris Base, Make up to 1L with distilled water. Storage: Room temperature

PBST x1

10 phosphate buffered saline (PBS) tablets, 1L distilled water, 1ml Tween per 0.1% concentration desired. Storage: Room temperature

TBST x10

87.66g Sodium chloride, 121g Tris Base, 1L distilled water, pH to 7.5 with sodium chloride and/or sodium hydroxide, titrate to x1 with distilled water, then add 1ml Tween per 0.1% concentration desired. Storage: Room temperature

Reducing Sample Buffer x5

1g Sodium dodecyl sulphate (SDS) powder, 3ml 1M Tris HCl pH 6.8, 5ml Glycerol, 2ml distilled water, 0.05g bromophenol blue. Storage: Aliquoted and stored at -20°c

RIPA Buffer

50nM Tris HCL pH 8, 150mM NaCl, 1% NP-40, 0.5% Sodium deoxycholate, 0.1% SDS. Storage: Stored at 4°c. 10ml aliquoted when required with a protease inhibitor tablet added

Freezing Media

90% Foetal bovine serum, 10% DMSO. Storage: Aliquoted and stored at -20°c

3.2 Methods

3.2.1 Cell culture methods

3.2.1.1 Culturing and Sub-Culturing

All cell culture work was performed under a class 2 laminar flow tissue culture cabinet using standard aseptic technique. All liquids used in cell culture were pre-warmed to 37°C.

All cell lines were cultured in 75cm^2 filter capped flasks (T-75) with RPMI-1640 media with 10% Foetal Bovine Serum (FBS), 5mls of 2500iu penicillin/5µg per ml streptomycin solution, and 5mls of 2mM L-glutamine, and incubated at 37°C in 5% CO_2. Once the cells had formed a monolayer which was about 80% confluent they were split.

Splitting involved removing the media with a pipette and replacing with 10mls Phosphate Buffered Saline (PBS). The flask was agitated for a few seconds to wash the remaining media from the cells and the PBS removed with a pipette. 2mls of Trypsin was then added to the flask with a pipette and the cells were then incubated at 37°C/5% CO_2 for between two and five minutes, until all the cells had detached from the bottom of the flask. The Trypsin and cells were made up to 10mls with fresh media with a pipette to inactivate the Trypsin and the mixture removed from the flask in a pipette and a proportion of the total cells either replaced in the same flask or

transferred to further flasks. Media was then added up to a total volume of 20mls (for T-75 flasks) and the flasks replaced in the incubator.

Cells were usually split 1:10 approximately twice per week (i.e. 1ml of the 10ml mixture of media, Trypsin and cells returned to the flask). Flasks were changed every 2-3 weeks.

Mycoplasma testing was performed routinely throughout the work by laboratory technicians within the department at approximately six monthly intervals. Similarly, genotyping on all cell lines was performed by laboratory technicians at the commencement and end of the work.

3.2.1.2 Long term Cryostorage of Cells

When fully confluent, cells were washed with PBS and trypsinised as with standard culture and then the 10mls of cells, Trypsin and media placed in 15ml flacon tubes and centrifuged for 5 minutes at 1000rpm to form a cell pellet. This pellet was resuspended in 10mls of PBS to wash the Trypsin from the cells and re-pelleted by further centrifuge in a 15ml falcon tube for 5minutes at 1000rpm. The FBS was then removed and the cells were then resuspended using a 5ml pipette in 1-10mls of full media depending on the size of the pellet. The suspension was split between NUNC cryotubes placing 1ml in each tube with a 1000µl pipette and placed on ice for 10 minutes. 0.25mls of freezing media was added and the cells placed back on ice for 5 minutes. A further 0.25mls of freezing media was added and the cells placed

on ice for a final 20 minutes. They were then transferred to a -80°C freezer for at least 3 days prior to being stored long term in liquid nitrogen at ~-200°C.

3.2.1.3 Recovery of cells from cryostorage

Cells were thawed in a water bath at 37°C and, once warmed, were pipetted into a 25cm2 filter capped flask (T-25) and supplemented with 10mls of media. The cells were then incubated at 37°C and 5% CO2. The media was removed with a 25ml pipette and replaced with fresh media at 24 hours to remove any remnant of DMSO (from the freezing media) and the cells transferred to T-75 flasks after 72 hours. Once established, all cells were passaged (split) at least 3 times prior to being used for experiments.

3.2.2 **Cytotoxicity studies using MTS assay methods**

Cytotoxicity studies with MTS (3-(4,5-dimethylthiazol-2-yl)-5-(3-carboxymethoxyphenyl)-2-(4-sulfophenyl)-2H-tetrazolium) utilise the ability of mitochondrial dehydrogenase to convert the tetrazolium ring of MTT (a yellow liquid) to a formazan product which is a darker orange colour with an absorbance wavelength or 490nm. The number of surviving, respiring cells is therefore proportional to the colour of the solution which is measured with a spectrophotometer.

Cell were grown to confluence in T75 flasks and then a cell pellet produced as above (3.2.2). The pellet was resuspended in 10mls of media and 10µl placed in the BIO-RAD TC10 Automated Cell Counted to find out the concentration of the cells. The cells were then diluted by the required amount to produce a concentration of $1.5x10^4$ cells per ml. 200µl of this solution was then seeded into each well of a 96-well plate (i.e. $3x10^3$ cells per well). The cells were then incubated overnight at 37°C and 5% CO_2.

After 24 hours, solutions of varying concentrations of chemotherapy were prepared. The concentrations were prepared by diluting the premade stock in full media. The media in the 96-well plate was removed with a suction device. The 96-well plate was divided into 12 lanes of 8 and the varying concentrations of chemotherapy and media each added to a lane of 8 wells, as well as a control lane of cells with no chemotherapy and a lane of media without any cells as a negative control. The cells were incubated at 37°C and 5% CO_2 for 72 hours.

The MTS assay was performed at 72 hours using a kit from Biomedica (EZ4U). The kit was used as per the manufacturer's instructions and involved mixing the 2.5mls of the activator liquid with the substrate powder. This produces a yellow liquid and 20µl of this was added by pipette to each of the 96 wells. Readings were then taken at 0, 1, 2, 3 and 4 hours using the Multiskan EX spectrophotometer (Thermo electron corporation). The Multiskan Ex takes readings of absorbance at wavelengths of 450nm and 620 nm. The 620nm reading is a control for light outside the range produced by the purple formazan and can therefore be subtracted from the 450nm reading to produce a reading specific to the formazan.

The readings were then standardised relevant to the positive and negative controls to produce values between 0-100% of cells viable and plotted against concentration. This produced 'so-called' IC50 curves showing decreasing viability with increasing concentrations of gemcitabine. These curves could in turn be used to find IC50 values, which is the concentration of gemcitabine needed to kill 50% of the cells.

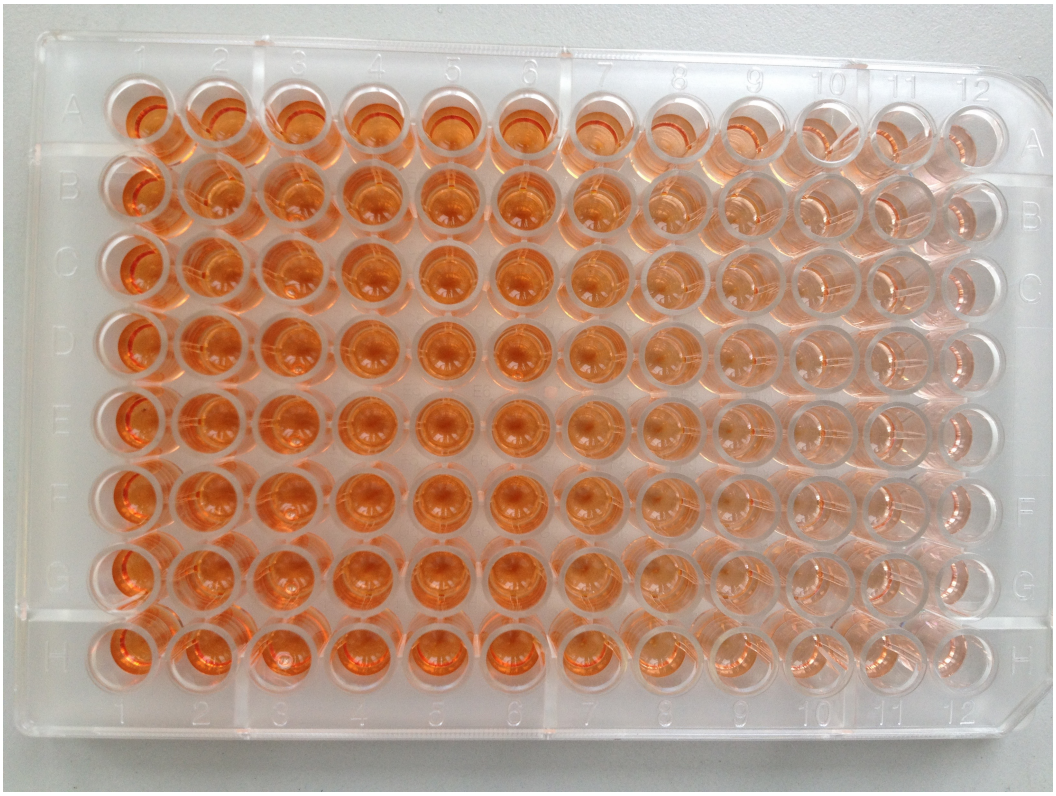

Figure 10: ***An example of a 96-well plate following MTS assay. The 12 columns are treated similarly, allowing 8 repeats of each condition and statistical analysis if required. The concentration of gemcitabine increases from left to right, with no gemcitabine in the left-hand column and no cells seeded in the right-hand column. This allows comparison between a presumed 100% of cells alive (respiring) vs 0% cells alive. The depth of colour is greater the more cells are respiring. The colour can be seen to decrease from left to right as concentration of gemcitabine increases. This colour change can be measured with a spectrophotometer and converted to numerical values and then survival curves.***

3.2.3 **Western Blot methods**

3.2.3.1 Antibodies and controls used

Target	Company and code	Size in kDa	% Gel	Dilution for primary antibody	2º antibody and dilution	Dilution/ blocking agent	Control
IL-1β	Abcam Ab45692	17	15	1:5000	Rabbit 1:2000	5% milk/ PBS	Abcam (ab9617)
α-1-anti-trypsin	Abcam Ab9399	52	12	1:5000	Mouse 1:3000	5% milk/ TBS	Pooled human serum
hENT1	Mackay antibody	40	12	1:500	Mouse 1:2000	3% BSA/ PBS	None
CNT1	Santacruz SC49284	72	12	1:1000	Mouse 1:2000	3% BSA/PBS	None
DCK	Abcam	30	12	1:500	Rabbit 1:2000	3% BSA/PBS	None
CDA	Abcam 82346	-	-	-	-	-	Abcam Ab99441
DCTD	Abcam Ab103988	20-22	15	1:5000	Rabbit 1:2000	5% BSA/PBS	Abcam Ab96766
RRM1	Abcam Ab81085	80	12	1:2000	Rabbit 1:2000	5% milk/PBS	None
RRM2	Abcam Ab57653	45	12	1:5000	Mouse 1:3000	5% milk/TBS	Abcam Ab99137
Il-15	Abcam Ab40668	31	12	1:1000	Rabbit 1:3000	5% BSA/PBS	Abcam Ab73500
GSTP	Abcam Ab47709	23	15	1:2000	Mouse 1:3000	5% Milk/PBS	Cell lysate
Occludin	Abcam Ab31721	59	12	1:250	Rabbit 1:3000	5%BSA/ PBS	Cell lysate

Table 9: Antibodies, controls and conditions used for western blot

The table above shows the antibodies and conditions used in Western Blotting along with order numbers where these were purchased commercially.

3.2.3.2 Production of protein from whole cells

Cells were grown to full confluence, the media removed and the cells washed with PBS. They were then incubated with Trypsin until the cells were detached from the base of the flask. The cells were then drawn up in media and centrifuged (5 minutes at 1000 rpm) to produce a cell pellet. The cell pellet was then resuspended in 1ml of PBS, centrifuged again and the PBS removed. Lysis buffer was then added (50-100µl depending on the size of the cell pellet) and the solution was sonified for 10 seconds to disrupt the cell membranes (Sound Enclosed Sonifier, Branson Ultrasonics, Shanghai, China). The resulting solution was then centrifuged for 10 minutes at 10,000 rpm and the lysate removed by pipetting from the cell pellet. The lysate was stored at -80°C and the cell pellet discarded.

Cell lysate was produced as above and the amount of total protein in the lysate then determined by Bradford assay prior to Western blotting to ensure consistent loading between samples (described below).

3.2.3.3 Production of supernatant from cultured cells

Cells were initially grown until confluent in full media including FBS. The media was then removed and the cells washed with PBS before placing in serum free media for 24 hours. The media was again removed and the cells

washed with PBS before placing in small amounts of serum free media overnight (5mls of media for one T75 plate).

The supernatant was then removed and filtered through a Spin-XUF 20ml (Corning, order no.431491) for 10 minutes at 3000rpm. This filter is designed to only allow substances less than 100kDa to pass through it.

The cells were then harvested and counted to allow standardisation of the amount of supernatant to be loaded in further experiments per cell line.

3.2.3.4 Protein quantification with Bradford assay

The Bradford assay is a colorimetric protein assay which uses the change in colour of Coomassie blue dye from its red form to its blue form when it binds to protein. The blue form of the dye has an absorbance spectrum of 595nm which increases proportionally to the amount of dye bound to protein and therefore the amount of protein.

Solutions of standard protein concentration were made up by diluting Bovine Serum Albumin (BSA) in distilled water (dH_2O). An initial stock was made of 5mg/ml by diluting 0.05g BSA in 10mls dH_2O. This stock was further diluted as shown on the next page.

2µl of the standards and the lysate samples (in triplicate) were added to 798µl dH_2O and 200µl of Coomassie blue solution and assayed by spectrophotometry at 595nm. The standards were used to produce standard curves and the protein concentration in the lysate estimated.

Volume of 5mg/ml BSA standard in µl	Volume of dH_2O in µl	Final concentration of BSA in mg/ml
100	0	5
70	30	3.5
50	50	2.5
20	80	1
10	90	0.5

Table 10: Making up standards for Coomassie blue staining

3.2.3.5 Polyacrylamide Gel Production

Different percentage gels were used depending on the molecular weight of the protein being tested for according to the following table:

Molecular weight of protein	% gel
>150 kDa	6%
90-150 kDa	8%
60-90 kDa	10%
30-60 kDa	12%
<30 kDa	15%

Table 11: Percentage gels used for western blot depending on molecular weight of protein

The gels consist of a resolving section for the separation of proteins and a stacking gel for the alignment of proteins prior to entering the resolving gel. The different gels were produced using varying amounts of dH2O, 30% acrylamide, Tris solution, 10% sodium dodecyl-sulphate (SDS), 10% ammonium persulphate (APS) and N, N, N', N'-tetramethylethylenediamine (TEMED) according to the table below depending on the protein being blotted for.

% gel	6	8	10	12	15
H_2O	2.6	2.3	1.9	1.6	1.1
30% acrylamide mix	1.0	1.3	1.7	2.0	2.5
1.5M Tris (pH 8.8)	1.3	1.3	1.3	1.3	1.3
10% SDS	0.05	0.05	0.05	0.05	0.05
10% APS	0.05	0.05	0.05	0.05	0.05
TEMED	0.004	0.003	0.002	0.002	0.002

Table 12: Ingredients (in mls) per percentage for one resolving gel (5mls total)

H_2O	1.4
30% acrylamide mix	0.33
1.0M Tris (pH6.8)	0.25
10% SDS	0.02
10% APS	0.02
TEMED	0.002

Table 13: Ingredients (in mls) for one stacking gel (2mls total)

Bio-Rad mini gel apparatus was used for gel production, electrophoresis and transfer. The resolving gel mixture was made, vortexed and 4mls pipetted between two glass plates to produce a 0.75mm flat gel. The glass plates were sealed below and at the sides and placed vertical leaving room for the subsequent stacking gel. Once this had set (20 minutes at room temperature) the stacking gel mixture was made, vortexed and 1.5mls pipetted into the space left on top of the resolving gel. A comb was then placed into the stacking gel to create lanes into which the protein could be loaded. Once set, the comb was removed and the gel used that day, or kept hydrated in the fridge overnight.

3.2.3.6 Electrophoresis

Protein samples were prepared for electrophoresis in the following manner. 3µl loading buffer was added to the volume of lysate required depending on the Bradford assay and the amount made up to 15µl with 1x RBB in 0.5ml epindorfs.

These samples were warmed at 96°C for 15 minutes to denature the proteins and centrifuged at 13,000 rpm for a few seconds. While warming the samples, a Mini Protean III electrophoresis chamber (Bio-Rad) was set up and the glass plates containing the gels placed vertically within it and running buffer poured in to completely cover the gels. Any air bubbles within the lanes of the gels were removed with a needle and syringe containing running buffer.

A commercial pre-made protein ladder (New England Biolabs) stored at -20°C was then thawed and 5µl loaded by pipetting into the end lane. The protein samples were then loaded into the remaining lanes.

The electrical input was then attached to run through the gel top to bottom and a current of 25-55 mA applied until the lightest proteins of the protein ladder had reached the bottom of the gel (~one hour).

3.2.3.7 Transfer

Proteins were then transferred from the polyacrylamide gels to Hybond Enhanced Chemo-Luminescence nitrocellulose membranes. The gels were removed from the glass plates and trimmed to size. They were then placed in transfer cassettes adjacent to the membranes and flanked by Whattman chromatography paper and sponge. The cassettes were then placed into transfer chambers and immersed in transfer buffer. A magnetic stirrer was placed in the bottom of the chamber and the chamber sat on the base unit of the magnetic stirrer, and an ice block placed in the chamber to prevent overheating when a voltage was applied. A potential difference of 100V was then applied for between 30minutes depending on the size of the cassette.

3.2.3.8 Immunoblot

The membranes were removed from the chamber after transfer and blocked as per the above protocols prior to applying the primary antibody. The choice of blocking agent was dependent on preliminary trials of the antibody and its optimum experimental design, and involved rocking the membrane at 25rpm in the chosen solution for at least one hour.

The primary antibody was diluted in the same solution used for blocking to a concentration determined by the optimisation experiments and rocked at

25rpm for either 1-2 hours at room temperature or in a cold room at 4°C overnight.

After removal of the primary antibody, the membranes were washed in plain TBS or PBS dependent on the above solutions. At least 4 washes of 15 minutes each, rocking at 25rpm were used.

The secondary antibody was chosen dependent on the primary (rabbit or mouse) and was then diluted in the blocking solution as above. The solution again depended on the optimisation experiments. This was added to the membrane which was then rocked at 25rpm for 90 minutes.

A further 4 washes of 15 minutes each were performed as above.

Following the final wash, the solution was removed and Amersham 'Western Lightning' Enhanced Chemo-Luminescence (ECL) was used to visualise the blot. 2.5mls of the two separate ECL components were mixed separately in falcon tubes and added to the membrane for 5 minutes. Following this the ECL was removed and the membrane placed in a light proof cassette between 2 pieces of transparent acetate. Tracking tape was placed alongside the gel and the protein ladder levels marked onto the tape with a permanent black marker to allow them to be seen on the developed film.

The light proof cassette was then moved to a dark room and Kodak Biomax light film placed onto the membrane for various exposure times dependent on the strength of the luminescence. The film was then developed for 1

minute and fixed for the same length of time before being washed in tap water and dried.

3.2.3.9 Quantification of protein loading

β Actin is a relatively stable cytoskeletal protein present in constant levels in all mammalian cells. Therefore, it can be used as a control to ensure that there was consistent loading of protein from well to well in the Western Blot.

Following the above immunoblot, the membranes were stripped of the antibodies by placing in an oven with stripping buffer for 30-60 minutes. The stripping buffer was then washed off with at least 4 washes of 15 minutes rocking at 25rpm.

The β Actin immunoblot was then performed in the same way as the initial experiment above using the same blocking/dilution agent and the following concentrations; block, primary antibody (β Actin at 1:10,000 dilution), wash, secondary antibody (Mouse at 1:2,000 dilution), wash, develop.

Even loading was seen as equal size and densities of bands at 42kDa (molecular weight of β Actin).

3.2.4 **Polymerase chain reaction**

To allow quantification of levels of RNA, RNA was first extracted and purified from cells, from which cDNA could be produced. Primers to be used for PCR were then tested and conditions optimised with reverse transcription PCR (RT-PCR). Following this, quantitative real-time RT-PCR was performed, using GAPDH as a loading control.

3.2.4.1 Extraction of RNA from animal cells

RNA was purified from cells using the RNeasy Mini Kit equipment from QUIAGEN. This contained Buffer RLT, QIA shredder, RNeasy column, Buffer RW1, Buffer RPE, RNase free water and 1.5ml and 2ml collection tubes.

Cells from a fully confluent T-75 flask were trypsinised as per the splitting procedure (section 3.2.1). Instead of replacing a certain amount of the 10mls of cells, media and Trypsin back to the flask, it was placed into a 15ml falcon tube and centrifuged at 500rpm for 5 minutes to produce a cell pellet. The media was removed by pipetting and the cells resuspended in 10mls of PBS to wash them before being centrifuged again to produce a cell pellet and the PBS removed.

The cells were then disrupted/lysed by adding 600 µl of Buffer RLT. The lysate was then homogenised by adding it to a QIA shredder in a 2ml collection tube and centrifuging at 10,000rpm for 15 seconds. The QIA shredder was discarded and 600µl of 70% ethanol was added to the flow through and mixed by pipetting. The solution was then transferred to an

RNeasy column and centrifuged for 15 seconds at 10,000rpm. This time the flow through was discarded and the RNeasy column transferred to a new 2ml collection tube.

700µl of Buffer RW1 solution was added to the RNeasy column and centrifuged at 10,000rpm for 15 seconds to wash the column and the flow through discarded. Following this 500µl of Buffer RPE was added to the column and the column centrifuged (15 seconds at 10,000rpm) and the flow through again discarded. A further 500µl of Buffer RPE was then added and the column centrifuged at 10,000rpm but for 2 minutes.

The flow through was again discarded and the column transferred to another new 2ml collection tube and centrifuged at 10,000rpm for 1 minute to dry the column. Finally, the RNeasy column was placed in a new 1.5ml collection tube and 50µl of RNase free water added prior to centrifuging for 1 minute at 10,000rpm to elute the RNA from the column. The flow through was then retained as the purified RNA. A second eluting step could be performed if necessary.

The quality of the RNA produced was then tested using the Nanodrop ND-1000 spectrophotometer. This allowed quantification of the amount of RNA using the optical density at 260nm wavelength and the purity assessed using the 260/280nm optical density ration (greater than 2 considered acceptable).

Purified RNA was stored at -80°C.

3.2.4.2 Producing cDNA from RNA

2µl of the purified RNA was added to 1µl of random primers, 2µl of deoxynucleotide triphosphates (dNTP) mixture (5mM) and 8µl of RNase free water in 0.1ml Eppendorfs. This mixture was incubated at 65°C for 5 minutes and immediately chilled on ice before being briefly microcentrifuged (i.e. a few seconds) to collect all the condensation.

Then 4µl of First Strand buffer was added along with 2µl of DTT (0.1M) to each Eppendorf. The mixture was vortexed and incubated at 42°C for 2 minutes. 1µl of Reverse Transcriptase was then added before mixing by vortex, spinning briefly in a microcentrifuge and incubating at 25°C for 10 minutes. This was further incubated at 42°C for 2 hours and then heat inactivated at 70°C for 15 minutes.

This process produced 20µl of concentrated DNA which were diluted with RNase/DNase free water to produce a 200µl of a 1:10 master solution. These were further diluted as required below.

As a negative control, the above steps were also performed using 2µl of RNase free water instead of purified RNA at the initial step.

The cDNA was stored at -20°C.

3.2.4.3 Reverse Transcription PCR (RT-PCR)

Non-quantitative RT-PCR was used to test the primers produced a constant DNA segment of the anticipated length, and to create the optimal protocol for PCR prior to Quantitative RT-PCR.

Samples were made up as follows:

2.5µl Buffer, 1.56µl MgCl, 0.52µl dNTP, 0.52µl Primer 5', 0.52µl Primer 3', 0.129µl Taq polymerase, 16.151µl DNase free water, and 2µl of 1:10 cDNA.

These samples were mixed by vortex and then run on the G Storm GS1 Thermal Cycler (GRI thermal cyclers). The protocol varied depending on the primers (section 3.6.1) but the temperatures used for the housekeeping control gene GAPDH is shown below as an example (GAPDH is used as a control to ensure even loading of samples as it is uniformly present in all cells):

Initialisation step: 95°C for 12 minutes

Denaturation step: 95°C for 30 seconds (this step disrupts the hydrogen bonds between complimentary DNA strands producing single DNA strands)

Annealing step: 67°C for 30 seconds (this allows binding (annealing) of the primers to their complimentary bases on the single stranded DNA)

Elongation step: 72°C for 1 minute (this step allows the DNA polymerase to synthesise a new complimentary DNA strand to the primer-DNA complex)

The denaturation, annealing and elongation steps are repeated through multiple cycles (e.g. 40 times for GAPDH/SERPIN A1)

Final elongation: 72°C for 10 minutes

After performing RT-PCR, loading dye (to allow visualisation) was added to the DNA and the combination was electrophoresed through agarose gels. This allowed comparison of the size of the DNA produced against a standard 100 base pair DNA ladder.

Gels were made as follows. 60mls of TAE buffer and either 0.6g of agarose were mixed together to form 1% agarose gels. The solution was then microwaved on full power for 2 minutes, stopping to stir the mixture after 1 minute. After microwaving, 6µl of Gel Red Nucleic Acid Stain was added to the mixture which was stirred and poured into a rectangular plastic electrophoresing tray containing a comb to provide wells. This was left for 30 minutes to set.

The gel was covered with running buffer and the wells were loaded with mixtures of 13µl of the PCR samples with 2µl of loading dye. A further well was also filled with 2µl of loading dye with 3µl of 100 base pair DNA ladder to allow identification of the size of the DNA segments produced by the PCR.

A potential difference of 120V was set up across the gel and run for 30-40 minutes. When the run had finished, the buffer was poured off and the gel viewed under UV light.

3.2.4.4 Quantitative Reverse Transcription PCR (qRT-PCR)

qRT-PCR experiments were run on the 'Lightcycler® 480 Instrument' (Roche). For this, samples of 20µl were made up as follows:

7µl DNase free water, 10µl of LightCycler® 480 SYBR Green I Master (Roche), 0.5µl each of forward and reverse primer (1:10 dilution), and 2µl of cDNA. PCR controls were also made up with 2µl of DNase free water instead of cDNA.

The samples were loaded into LightCycler® 480 Multi-96-well Plate (Roche) in triplicate at least. Once the samples had been loaded, the wells were covered with sealing foil (provided with the Plates) and the plates were centrifuged at 1000rpm for 30 seconds to ensure the samples settled at the bottom of the wells. The plates were then loaded into the Lightcycler Instrument and run according to the protocols below:

qRT-PCR protocol

3.2.4.5 Quantification of total RNA/DNA

To ensure that the correct amount of cDNA was loaded into each well of the qRT-PCR experiments, quantification of the cDNA samples had to be performed.

This was performed by creating GAPDH curves with the qRT-PCR Lightcycler 480 machine. To do this, the master samples of cDNA were further diluted to produce 1:100, 1:500, 1:1000, 1:10,000, 1:50,000 samples. 20µl qRT-PCR samples (using GAPDH primers) were made up for each dilution of each cDNA sample in triplicate and these were loaded into the Multi-96-well Plate. The plate was then run on the GAPDH primer protocol. Using the computer software, this allowed the creation of GAPDH curves plotting dilution against the Crossing Point (CP) of the sample.

The CP represents the point (in cycles of PCR) of the exponential increase in the cDNA per sample. For 2 samples of equal quantities of starting DNA, the CP will be identical.

Therefore, using the above curves, the dilution required for each sample to produce an identical CP was worked out. The experiment was then repeated using each sample at its own dilution as found above loaded in triplicate with GAPDH primers once again and identical CPs confirmed.

The experiment with the primer of choice could then be performed using the same dilutions of the cDNA master samples in the knowledge that the samples contained equal amounts of cDNA.

3.2.5 **Gene Knockdown**

siRNA was purchased from Dharmacon RNAi technologies.

Knockdown was performed in three 6-well plates. One 6-well plate was used for knockdown with the siRNA of interest while the other two plates were used for two different negative controls. The 6-wells meant one could be used for post-knockdown RNA isolation/cDNA production/PCR experiments, two used for cytotoxicity experiments and three used to extract protein for Western Blot experiments.

Cells were grown to confluence in a T-75 flask and subsequently trypsinised and made up to 10mls with media to inactivate the trypsin. This 10mls mixture was then centrifuged in a 15ml falcon tube at 1000rpm for 5 minutes to produce a cell pellet. The media and Trypsin was removed with a pipette and the cells resuspended in 10mls of PBS to wash the cells. A cell pellet was again formed by centrifuge for 5 minutes at 1000rpm. The cells were then resuspended in 10mls of media and 10µl of this placed in the BIORAD automated cell counter to give the density of cells per ml. The cells were then seeded in three 6-well plates at a density of $1x10^5$ cells per well in 3mls of full media. These were then incubated overnight at 37°C, 5% CO_2. This resulted in approximately 40% confluence at 48 hours.

At 48 hours, the full media was initially replaced with 2.6mls of antibiotic free media per well. Then for each well the following were made up in two separate tubes: 200µl of OptimemI was added to 4µl of lipofectamine 2000

(tube 1) and a further 200µl of OptimemI was added to 10nM of siRNA (tube 2). The siRNA used was SERPIN A1 for 6 wells and the two negative control siRNA for 6 wells each (off-target and RISC free controls).

These tubes were incubated at room temperature for five minutes and then combined and mixed by flicking the tube to make a total of ~400µl per well. This mixture was incubated for a further 30 minutes at room temperature before being added in a drop wise fashion to each well.

Transfection occurred while the 6-well plates were incubated at 37°C and 5% CO_2 for the next 24 hours.

After 24 hours, the media was removed by pipette and 500µl of Trypsin added and the plates incubated for 2 minutes to detach the cells from the base of the wells. 2.5mls of fresh media was then added to the wells to inactivate the trypsin and the mixture of Trypsin media and cells aspirated with a pipette. This mixture could then be treated as per the experiments above to find the effect of the knockdown on protein and RNA expression or chemoresistance.

3.2.6 **Immunocytochemistry**

Immunocytochemistry (ICC) was used to demonstrate levels and position of protein within cultured cells.

1 Cells were grown to confluence in 2 T75 flasks, washed with PBS and trypsinised as per cell culture. Media was then added to the trypsin and centrifuged in a 50ml Falcon tube for 5 minutes at 500rpm. The media/Trypsin was removed and the cell pellet resuspended in 5mls of PBS to wash the cells, followed by centrifuging again at 500rpm for 5 minutes.

2 The pellet was resuspended in 4% formaldehyde (pH7) and left to sediment. After 2 hours, the formaldehyde was carefully pipetted off leaving the sedimented cells and fresh PBS used to resuspend the cells once more.

3 Following this the cells were applied to slides.

4 Primary antibody solutions (RRM2 1:1000) were made up using the diluent buffer (Dako) and the cells left in these solutions overnight at $4^{O}C$.

5 The following morning, the cells were washed with PBS and covered with HRP-labelled anti-mouse secondary antibody (Dako) and left on a shaker at 100rpm for 1 hour at room temperature.

6 The slides were then stained by covering in AEC+ chromagen substrate (Dako) and left on shaker at 100rpm for 10 minutes at room temperature.

7 The slides were washed with PBS and placed in Haematoxylin for 10 seconds. Slides were placed in 2% ammonium hydroxide for 5 seconds.

8 Slides were placed in 30% ethanol followed by 70%, 90% and 100% ethanol, all for 3 minutes each.

9 Slides were placed in Xylene for 5 minutes, 3 successive times.

10 Slides were then mounted on a coverslip to allow viewing.

3.2.7 **Immunohistochemistry**

Immunohistochemistry (IHC) was performed to show levels and position of protein within human tissue sections. The conditions were optimised using fresh frozen paraffin embedded (FFPE) blocks of human PDAC cut into 5μM sections on superfrost plus slides dried overnight at 37^{O}C. Sections from 3 patients were used from a store available in the department.

Optimisation experiments used varying concentrations of antibody based on the company recommendations, as well as positive and negative control (cytokeratin antibody and without primary antibody respectively). The RRM2 antibody concentration providing the best results was 1:1000. Dako EnVision^{TM}+ kits were used. The protocol was as follows:

1 Slides placed in Xylene for 5 minutes, 3 successive times to remove the paraffin.

2 Slides placed in 100% ethanol followed by 90%, 70% and 30% ethanol, all for 3 minutes each.

3 Slides placed in distilled water.

4 Slides put in metal rack and placed in pressure cooker containing 2 litres of boiling citrate buffer (4.2g citric acid in 2 litres distilled water, pH6) for 3 minutes.

5 Slides cooled with gentle stream of cold water for 5 minutes.

6 Slides placed in PBS and rocked at 20rpm for 3 x 2 minutes and subsequently dried using blue roll taking care not to wipe around rather than on the section.

7 A 'Dako Pen' (Dako) was used to create a water repellent circle around the tissue sections and this circle filled with peroxidise blocking solution (Dako), covering the tissue sections and left on shaker at 100rpm for 10 minutes.

8 Slides were then washed and dried as in step 6.

9 Tissue sections were then covered in primary antibody solutions (RRM2 1:1000) and left overnight at $4^{O}C$. Antibody solutions were created using diluent buffer (Dako).

10 The following morning, slides were then washed and dried as in step 6.

11 Tissue sections were covered with HRP-labelled anti-mouse secondary antibody (Dako) and left on a shaker at 100rpm for 1 hour at room temperature.

12 Slides were then washed and dried as in step 6.

13 Tissue sections were then stained by covering in AEC+ chromagen substrate (Dako) and left on shaker at 100rpm for 10 minutes at room temperature.

14 Slides were then washed and dried as in step 6.

15 Slides were placed in Haematoxylin for 10 seconds.

16 Slides were placed in 2% ammonium hydroxide for 5 seconds.

17 Slides placed in 30% ethanol followed by 70%, 90% and 100% ethanol, all for 3 minutes each.

18 Slides placed in Xylene for 5 minutes, 3 successive times.

19 Slides were then mounted on a coverslip to allow viewing.

4 Results

4.1 Confirmation of resistance and establishment of levels of proteins previously associated with gemcitabine metabolism and resistance

4.1.1 Overview

Cells from the various cell lines were first established using culture techniques. The cell lines were then treated with gemcitabine and subjected to MTS analysis to establish levels of resistance to gemcitabine. Western blot analysis was then performed on the cell lines to assess levels of the proteins described in the introduction already known to be associated with gemcitabine metabolism and resistance.

The aims were to confirm the resistance of the cell lines used and then to identify any significant differences in the levels of established proteins of interest which may be the cause of this resistance.

4.1.2 Gemcitabine resistance in cell lines

The cell lines were subjected to MTS analysis to assess their resistance/sensitivity to gemcitabine.

4.1.2.1 Suit2 (AS)

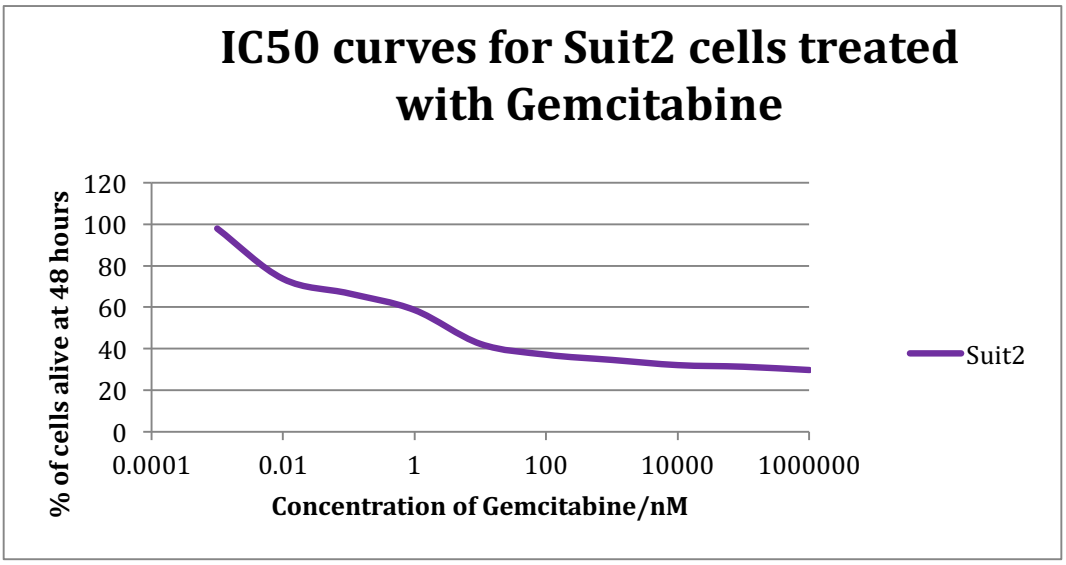

Figure 11: *IC50 curve for Suit2 cells treated with gemcitabine. Curves produced after 48 hours, showing concentration gemcitabine (nM) against % cells viable. IC50 value is 0.1 nM.*

4.1.2.2 BxPC3 (Bx)

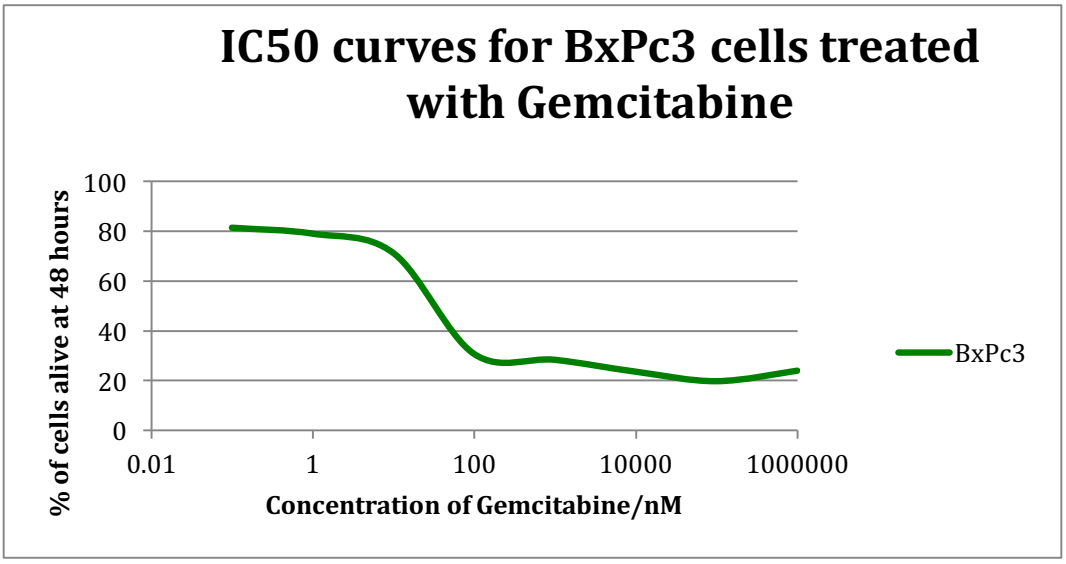

Figure 12: *IC50 curve for BxPc3 cells treated with gemcitabine. Showing concentration (nM) against % cells viable compared to control. IC50 value is 33.6nM.*

4.1.2.3 Panc1 (P1)

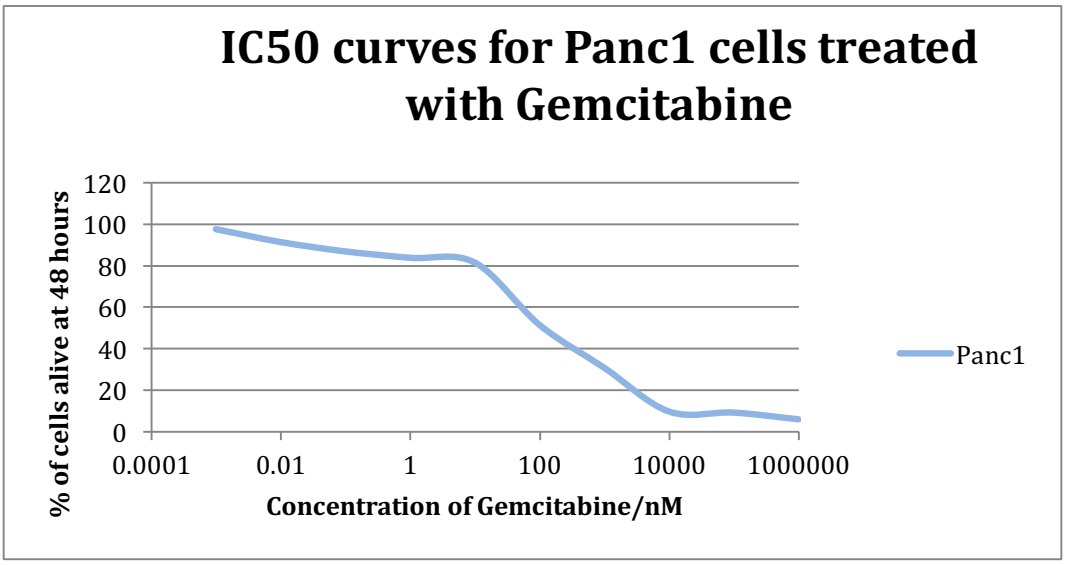

***Figure 13:** IC50 curve for Panc1 cells treated with gemcitabine. Curve produced after 48 hours showing concentration of gemcitabine (nM) against % cells viable. IC50 value is 103nM.*

4.1.2.4 MiaPaCa (MP)

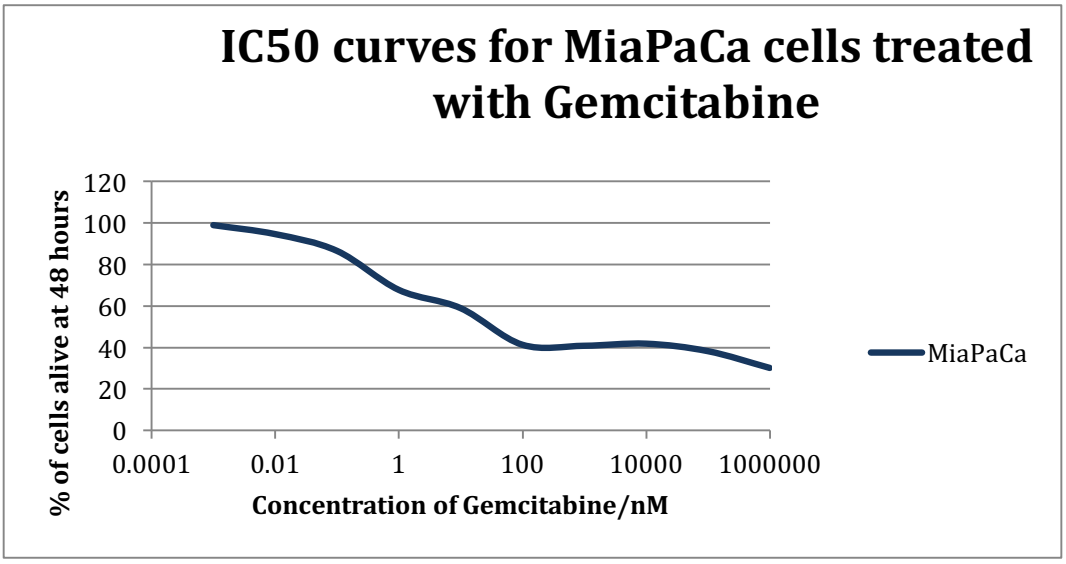

***Figure 14:** IC50 curve for MiaPaCa cells treated with gemcitabine. Curve produced after 48 hours showing concentration of gemcitabine (nM) against % cells viable. IC50 value is 0.8nM*

4.1.2.5 KR Suit2 (KR)

As discussed in the introduction, I was unable to perform any culture experiments with the transiently resistant cell line KR, due to a mycoplasma infection with the frozen supply. I did have a supply of cell lysate which could be used for the western blots shown further into the results section. Below is the cytotoxicity graph provided by my predecessor which is also shown in the previous work section of the introduction. Hence it is in a different format to the others and does not appear in the combined curves figure below.

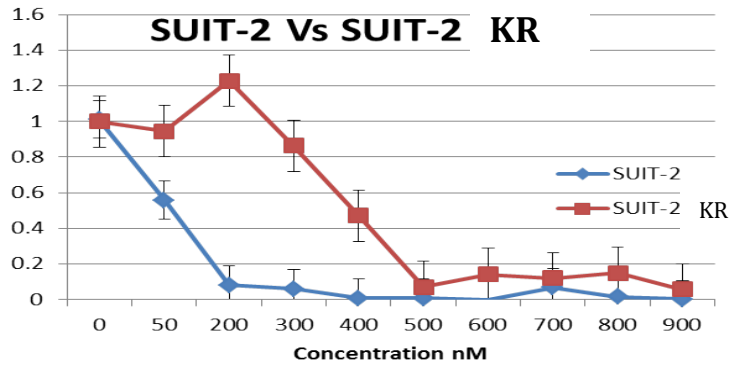

Figure 15: (provided by Dajani et al) Cytotoxicity curves for AS and KR cell lines treated with gemcitabine. In this graph, the percentage of cells alive is plotted as relative to 1=100%, against concentration of gemcitabine. Suit-2 (blue line) represents the parental Suit-2 cell line called AS in my work, and Suit-2 KR (red line), the resistant cell line termed KR in this thesis. (Dajani, unpublished). Also shown in introduction.

4.1.2.6 GR Suit2 (GR)

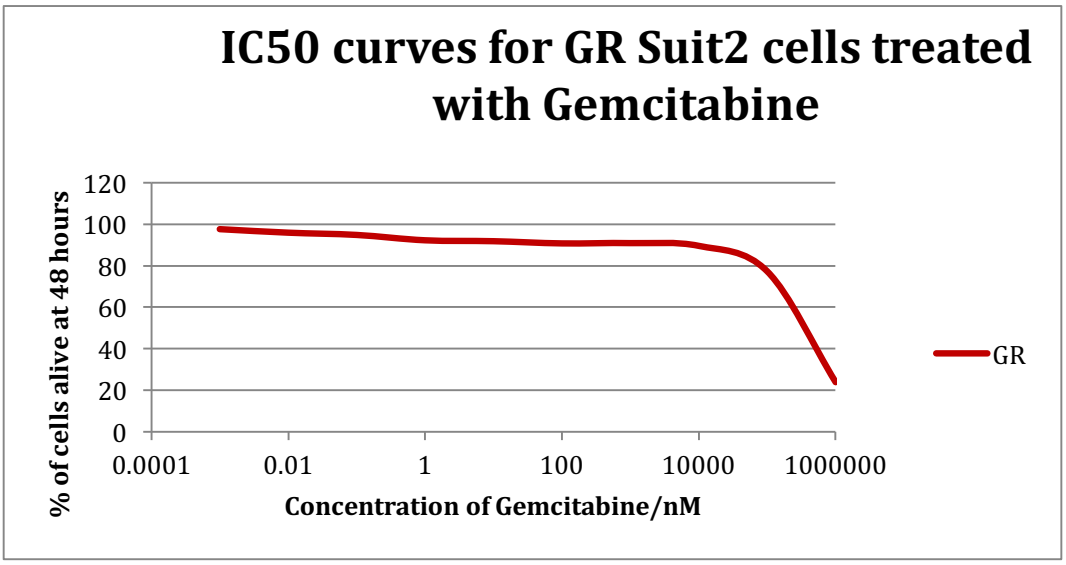

Figure 16: ***IC50 curve for clonal resistant Suit2 cells (GR) treated with gemcitabine. Curve produced after 48 hours showing concentration of gemcitabine (nM) against % cells viable compared to control treated with no gemcitabine. IC50 value is >300,000nM***

4.1.2.7 Combined IC50 curves and values

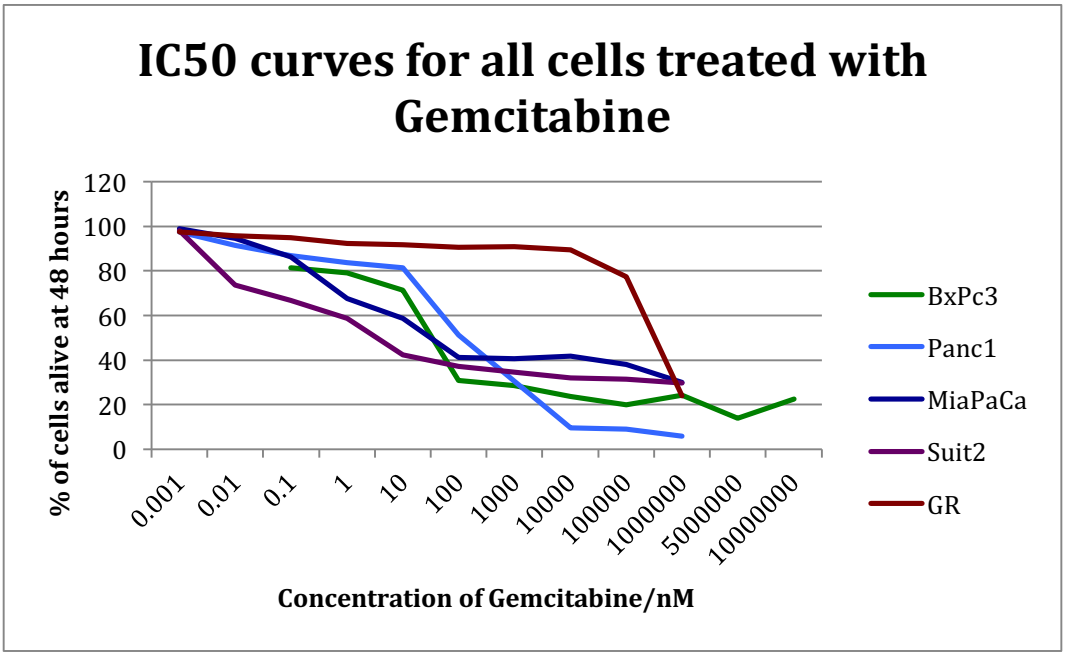

Figure 17: ***IC50 curves for all the cell lines combined when treated with gemcitabine. X-axis shows the concentration of gemcitabine (nM) used and the y-axis shows % viable cells after 48 hours compared with control cells of that type treated with standard media.***

Cell line	IC50 value for Gemcitabine/nM
Suit2	0.1
MiaPaCa	0.8
BxPc3	33.6
Panc1	103
GR Suit2	>300,000

Table 14: ***Summary of IC50 values for all cell lines used, treated with gemcitabine. This value represents the concentration of gemcitabine which renders 50% of the cells non-viable after 48 hours compared with minimum numbers of surviving cells.***

As can be seen from the figures and tables above, Suit2 cells are relatively sensitive to gemcitabine compared to the other original cell lines used by a factor of at least 10 (IC50 value of 3.42 compared with 33.6, 41.2 and 103).

However, the clonal resistant cell line GR Suit2 is far more resistant by a factor of 100,000 compared with the original cell line.

I have not added the transiently resistant cell line to this table as the experiment by my predecessor found a slightly higher IC50 value for the sensitive Suit-2 (35nM vs 3.42nM) which would be misleading when quoting the KR IC50 of 400nM gemcitabine. However, it is clear from my predecessor's curves that the KR cell line was relatively resistant compared to the parental cell line, probably in the region of 10 times more resistant.

Having shown that the developed cell line was indeed relatively resistant to gemcitabine, I then went on to explore the potential mechanism of resistance by looking at expression of various proteins and genes of interest.

4.1.3 Proteins previously associated with gemcitabine metabolism and resistance

As described in the introduction, there are a number of proteins already known to be relevant to gemcitabine metabolism and resistance. I therefore performed western blots to show baseline levels of some of these proteins in the various cell lines, which may be related to the levels of resistance shown above.

The blots were performed using the conditions described in the methods for each particular antibody. The protein ladder was always placed on the left followed by 3 different lines of Suit2 cells which were; parental Suit2, clonally resistant Suit2 (GR), transiently resistant suit2 KR. In addition, further lanes were used for the immortal pancreatic cancer cell lines BxPc3, Panc1, and MiaPaCa.

4.1.3.1 hENT-1

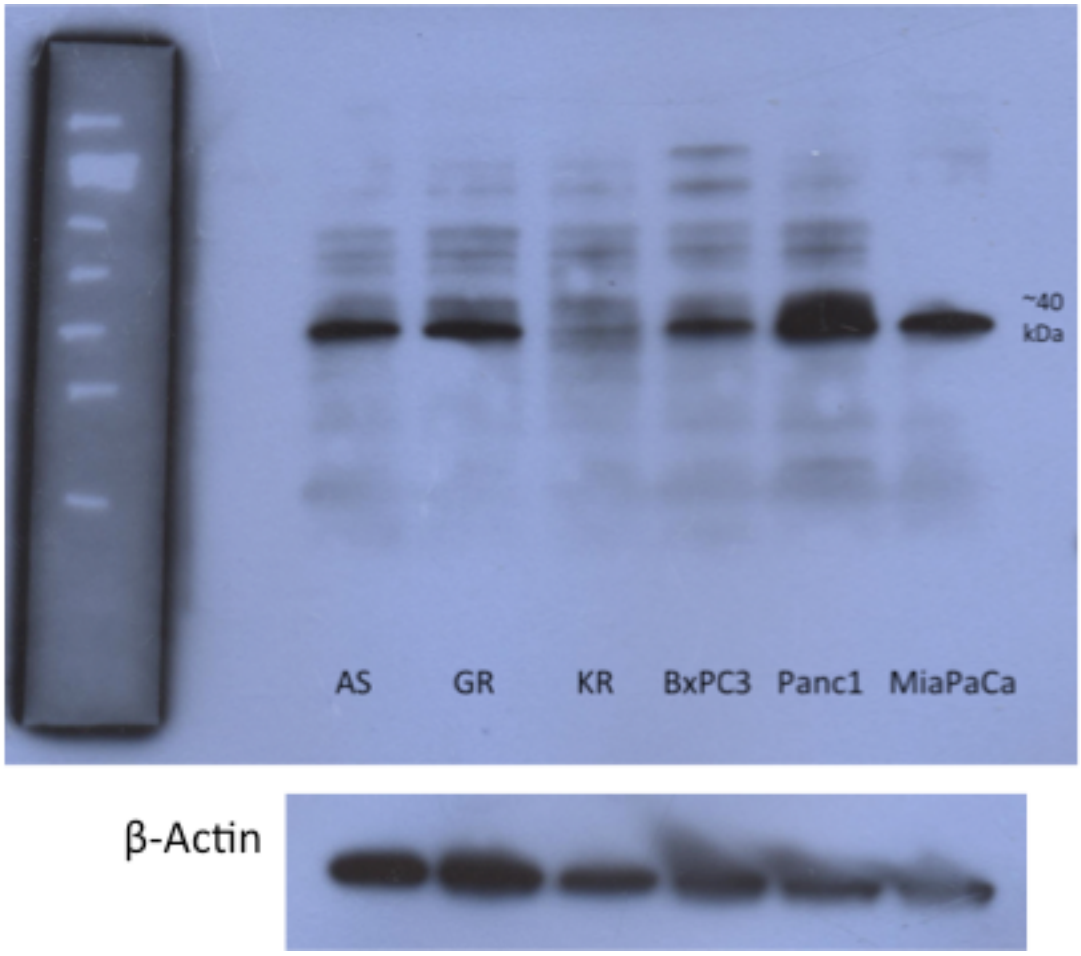

Figure 18: Western blot for hENT1. Bands demonstrated at approximately 40 kDa and the actin blot shown underneath. A blocking agent of 3% BSA diluted in PBS was used with a primary antibody concentration of 1:500 and a mouse secondary antibody concentration of 1:2000. No control lane was used as the bands are well expressed in the cell lines. The first lane is the control protein ladder and names of cell lines are shown underneath the relevant lanes.

The figure above is an example of a western blot for hENT1. This shows similar levels in the first 2 lanes representing AS and GR cell lines but a markedly lighter band in the third lane representing KR. The BxPc3 and MiaPaCa lanes show similar expression to AS and GR with a denser band in the Panc1 lane.

The actin shows slightly less overall protein in the last 4 lanes but not enough to account for the described differences.

4.1.3.1.1 CNT-1

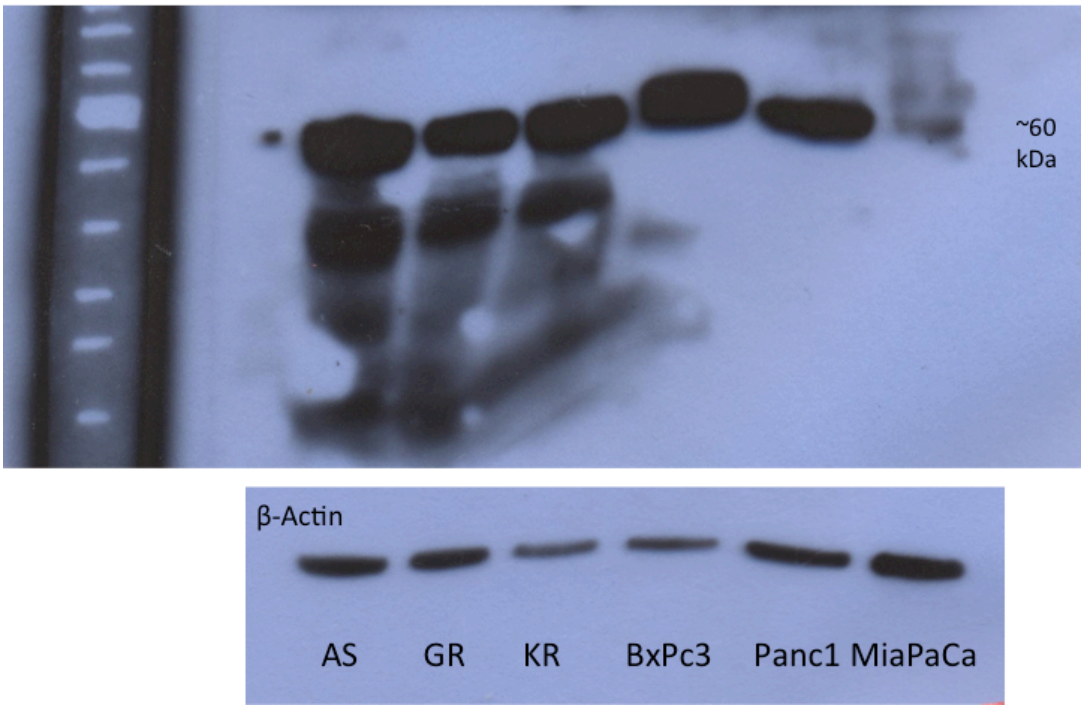

Figure 19: Western blot for CNT-1. Bands demonstrated at approximately 60 kDa and the actin blot shown underneath. The first lane is the control protein ladder and names of cell lines are shown underneath the relevant lanes.

The figure above is an example of a western blot for CNT1, which is represented by the bolder bands above at approximately 60kDa. This was repeated on 3 occasions but this was the 'cleanest' blot obtained. There is some variation in the loading of total protein making it difficult to show any definite difference in the first 5 lanes but there is far less expression of CNT1 in MiaPaCa than the other cell lines.

4.1.3.2 DCK

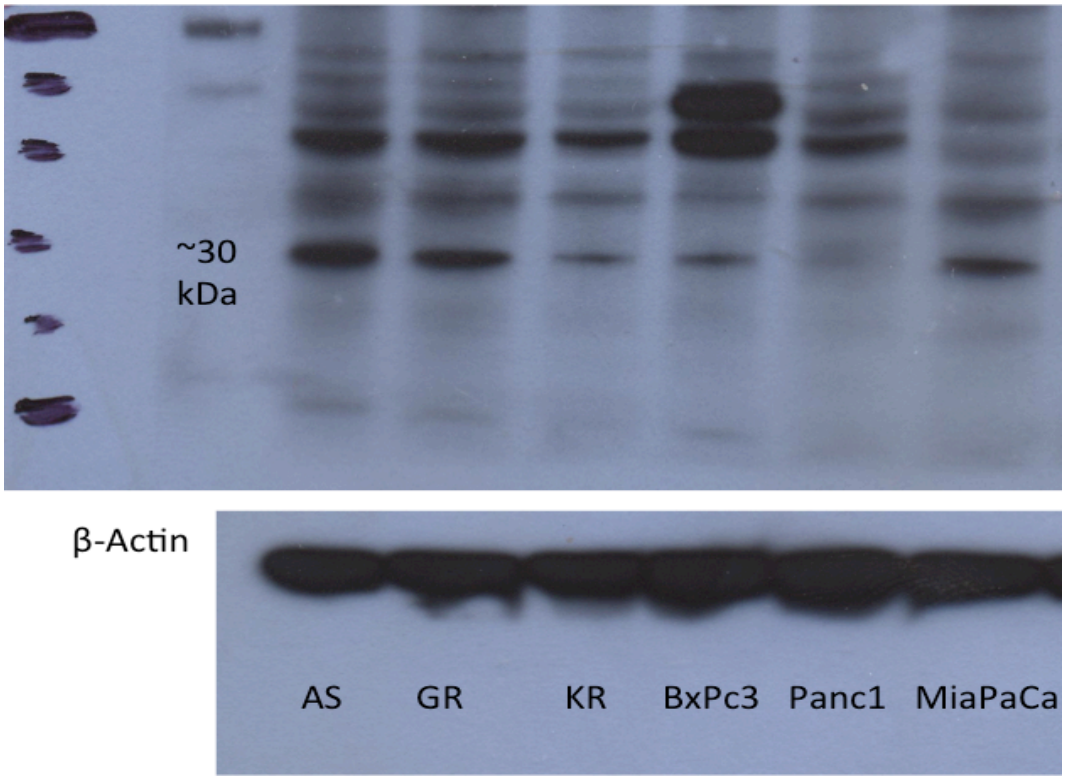

Figure 20: Western blot for DCK. Bands demonstrated at approximately 30 kDa and the actin blot shown underneath. A blocking/dilution agent of 3% BSA/PBS was used with a primary antibody dilution of 1:500 and a secondary rabbit antibody at 1:2000 dilution. No control was required for this blot. The first lane is the protein ladder and names of cell lines are shown underneath the relevant lanes (AS=parenteral Suit2, GR=clonally resistant SUIt2, KR=transiently resistant Suit2).

The figure above is an example of a western blot for DCK. Optimising this commercial antibody was very difficult and it is not a very clean antibody. There are multiple bands in all lanes but the protein DCK should be 30.5kDa which the band marked corresponds to. If this band is taken as being specific to DCK, then KR, BxPc3 and especially Panc1 cell lines show decreased levels

of DCK but it is difficult to draw any meaningful conclusions with this antibody.

4.1.3.3 CDA

Attempts were made to optimise an antibody from Abcam (ab82346) for CDA due to its known role in the metabolism of gemcitabine. However, these were unsuccessful and no further work was performed on this protein.

4.1.3.4 DCTD

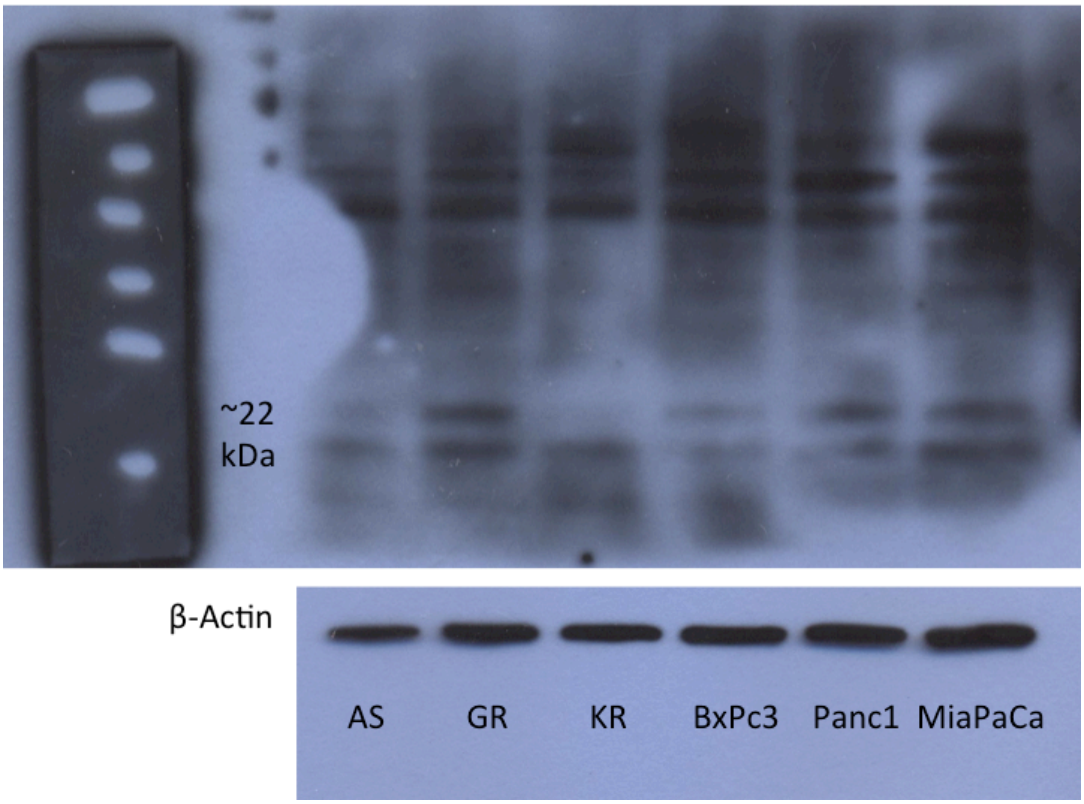

Figure 21: Western blot for DCTD. Bands demonstrated at approximately 20 and 22 kDa and the actin blot shown underneath. A blocking/dilution agent of 5% BSA/PBS was used with a primary antibody dilution of 1:5000 and a secondary rabbit antibody at 1:2000 dilution. A commercial protein control (ab96766) was used for this blot (not shown). The first lane is the protein ladder and names of cell lines are shown underneath the relevant lanes.

The DCTD antibody also proved difficult to optimise. The expected weight of the protein is 20-22kDa but there are 2 bands at these levels and the bands higher up on the blots were always heavier. The blot above is an example of one of the cleanest obtained. Based on this, no meaningful conclusions were possible for the relative expression of DCTD between the cell lines.

4.1.3.5 RRM1

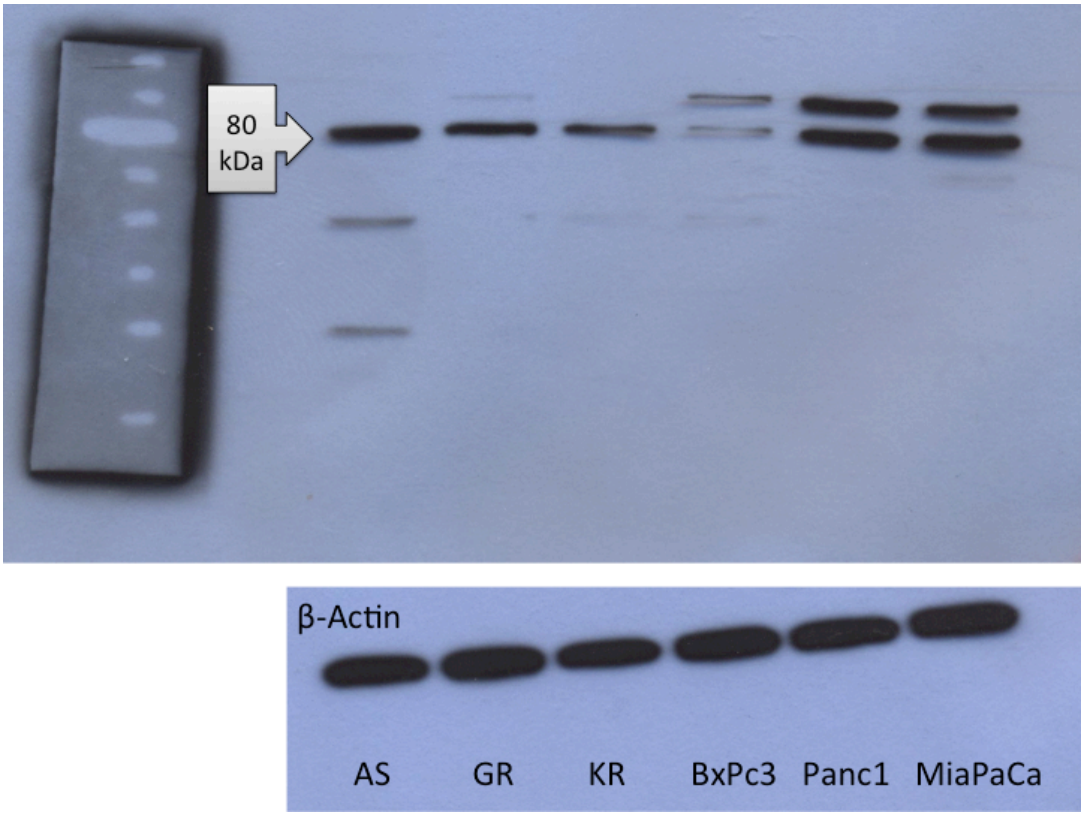

Figure 22: Western blot for RRM1. Bands demonstrated at approximately 80 kDa and the actin blot shown underneath. A blocking/dilution agent of 5% milk/PBS was used with a primary antibody dilution of 1:2000 and a secondary rabbit antibody at 1:2000 dilution. No control was required for this blot. The first lane is the protein ladder and names of cell lines are shown underneath the relevant lanes.

The blot above shows a double band in some of the cell lines (namely BxPc3, Panc1 and MiaPaCa with a very faint second band in GR) which was

consistent throughout all repeats with this antibody. However, the lower band at 80 kDa was felt to represent the protein in question.

The blot shows a possible increase in expression in AS vs KR cell lines but this may be due to slightly uneven loading shown in the actin blot. The only consistent finding in repeated blots was relatively high expression in Panc1 and MiaPaCa and relatively low expression in BxPc3 compared with the 3 Suit two cell lines.

4.1.4 Conclusions

	hENT-1	*CNT-1*	*DcK*	*DCTD*	*RRM1*
AS	↔	↔	↔	-	↑
GR	↔	↔	↔	-	↔
KR	↓	↔	↓	-	↑
BxPC3	↔	↔	↓	-	↓
Panc-1	↑	↔	↓↓	-	↑
MiaPaCa	↔	↓	↔	-	↑

Table 15: Table summarising the findings in this section; relative levels of proteins previously associated with gemcitabine metabolism and resistance in a variety of different immortal pancreatic cancer cell lines.

Looking specifically at the Suit-2 cell lines which form the basis of this thesis (AS, GR, KR), the results above show decreased expression of hENT-1, DCK and possibly RRM1 in the KR cell line compared to the AS and GR cell lines. While these differences could potentially be linked to the differences in

resistance, these differences are not consistent in the 2 resistant cell lines (KR and GR).

Therefore, there seems no reason to discount the results of the microarray and the work proceeded to the validation stage.

Equally, while the levels of the proteins in the other PDAC cell lines did vary, this body of work concentrated on the Suit-2 cell line and continued as such, while also checking levels, where possible, in the other cell lines as a possible source of variations in innate resistance.

4.2 Validation of microarray results

4.2.1 Overview

As described in the previous work section, the bioinformatics analysis comparing the sensitive and resistant Suit2 cell lines showed differential expression in the following genes and proteins:

Genes/RNA	Proteins
BEX4	Glutathione S-transferase P
LOC439949	Zinc finger protein 593
SERPIN A1	Occludin
SNAR-A1	Folate receptor alpha
	Ribonucleotide reductase subunit M2 (RRM2)

Table 5: Differentially expressed genes and proteins

Following a literature search for all these genes and proteins, it was decided to concentrate on the following as potentially affecting resistance: SERPINA1, glutathione S-transferase P (GSTP), occludin, folate receptor alpha (FOLR**)** and ribonucleotide reductase subunit M2 (RRM2).

I therefore went on to validate these findings by quantifying either protein or RNA expression with western blot or PCR respectively.

It was also decided to examine levels of Inerleukin-1β (IL-1β), as this had been implicated in a possible pathway between SERPIN A1 and RRM2 in the pathways shown in the introduction (previous work).

4.2.2 **SERPINA1/α-1-antitrypsin (A1AT)**

4.2.2.1 Western blot with cell lysate

The microarray suggested that the gene SERPIN A1 was under expressed in resistant cells. This gene codes for the protein alpha-1-antitrypsin (A1AT). Therefore, western blots were performed as per section 3.2.4.

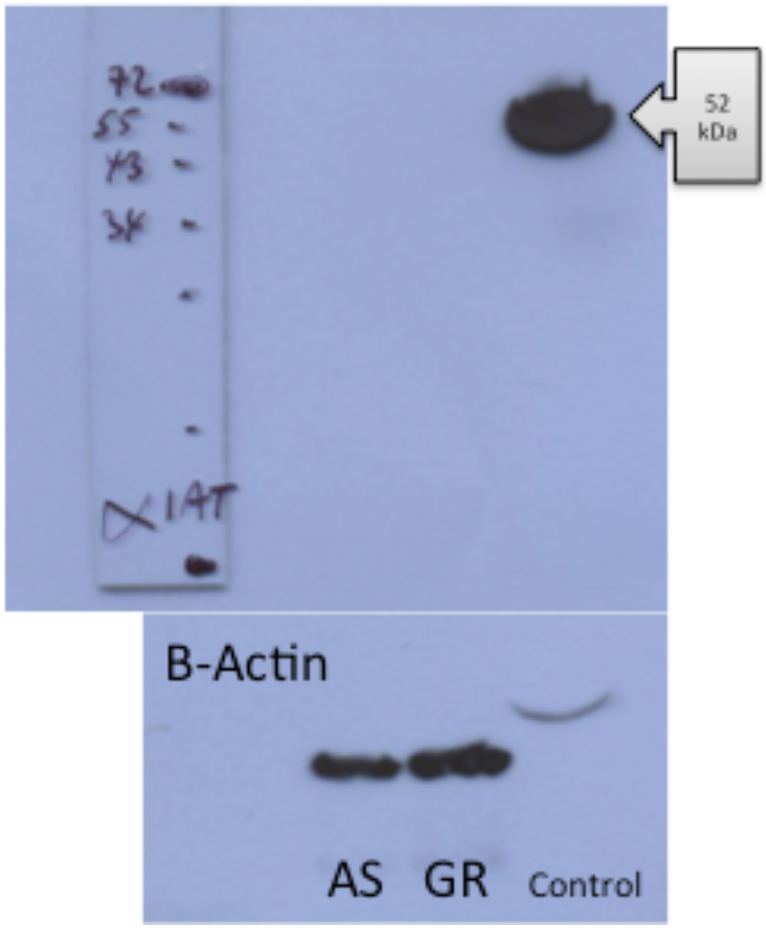

Figure 23: Western blot for A1AT. Original blot shown above on and actin blot shown below. A blocking/dilution agent of 5% milk/TBS, a primary antibody concentration of 1:5000 and a secondary mouse antibody at 1:3000. The control was human serum.

The Western blot above was done with the cell lines AS and GR only but shows no detectable A1AT in either lane. The left-hand film shows a dense band at ~52kDa in the control lane as expected but no other bands. The β-actin film shows adequate loading between the 2 experimental lanes and a small amount of overspill only in the control. The lack of β-actin band is expected in the control as the control was human serum, whereas β-actin is a cellular protein. Note the marks on the left of the films are made by hand to represent the protein ladder visible on the membrane, with their associated weights in kDa.

This experiment was repeated with the AS, GR and KR cell lines to confirm the findings of no protein traceable on western blot:

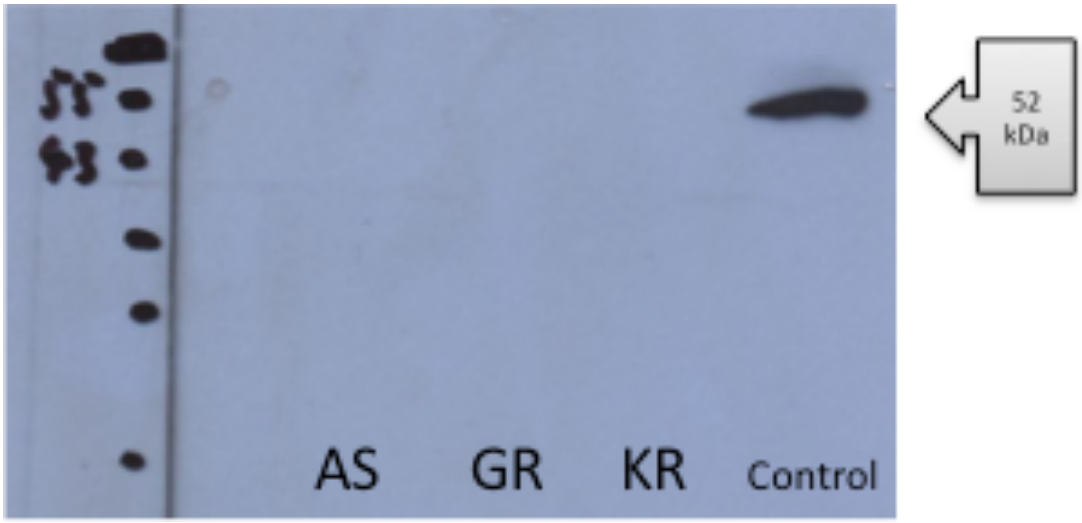

Figure 24: Repeat western blot for A1AT. A blocking/dilution agent of 5% milk/TBS, a primary antibody concentration of 1:5000 and a secondary mouse antibody at 1:3000. The control was human serum. Actin blot not shown.

The repeat once again shows no detectable protein in any of the cell lines but a good clean band at ~52kDa in the control (actin not shown).

4.2.2.2 Western blot with supernatant

Having failed to show any level of A1AT protein within the cells of the various cell lines, I next collected samples of the supernatant in which the cells were cultured as per the methods, looking for a demonstrable secreted level of A1AT.

Figure 25: Western blot for A1AT using supernatant collected from cultured cells. A blocking/dilution agent of 5% milk/TBS, a primary antibody concentration of 1:5000 and a secondary mouse antibody at 1:3000. The control was human serum.

However, this blot again shows no level of A1AT which could be picked up via this method. This suggests that the level of A1AT at the protein level, either within or secreted by the cells was too low for western blot analysis. The reason the control lane is so 'dirty' is that I used relatively long exposures of the film to the membrane in an attempt to show up even very light bands. Because the control provides a very strong band, however, there has been some spill over into the rest of the lane.

As expected there was no β-actin demonstrated in any of the lanes as they were all secreted samples and the control was serum. Standardisation of samples was by volume of supernatant.

4.2.2.3 qRT-PCR for SERPINA1

The decision was therefore made to confirm the microarray data with qRT-PCR for SERPIN A1 RNA as its protein (A1AT) was not detectable in the cells or their supernatant. This required a number of steps. First primers were designed for SERPINA1 using a computer programme as described in the methods. cDNA was then produced for the various cell lines, again as per the methods. The purity of the cDNA was assessed, following which the primers were tested. Finally, qRT-PCR could be performed to quantify levels of SERPINA1 RNA in the cell lines.

4.2.2.3.1 Design of Primers

GAPDH primers (housekeeping gene used as control) were purchased commercially and PCR primers for SERPIN A1 were designed using the Clone MFC application (Scientific and Educational Software). Protocols for PCR were developed using non-quantitative RT-PCR (see below).

GAPDH:

Forward: 5' – GCA TGG ACT GTG GTC – 3'

Reverse: 5' – AGG TGA AGG TCG GAG – 3'

The PCR Protocol for GAPDH was as follows: 95°C for 12 minutes, 40 cycles of (95°C for 30 seconds, 67°C for 30 seconds, 72°C for 1 minute), 72°C for 10 minutes.

SERPIN A1 (expected fragment length=492 base pairs):

Forward: 5' –CACTC AGAAG CCTTC ACTGT- 3'

Reverse: 5' –GGACG CTCTT CAGAT CATAG- 3'

The PCR Protocol for SERPIN A1 was as follows: 95°C for 12 minutes, 40 cycles of (95°C for 30 seconds, 55°C for 30 seconds, 72°C for 1 minute), 72°C for 10 minutes.

4.2.2.3.2 Confirmation of successful RNA extraction and cDNA production for use in PCR

RT-PCR was performed with GAPDH primers (GAPDH is a housekeeping gene, consistently expressed among all animal cells and therefore used as a control) to confirm that RNA had been extracted properly from the cells and cDNA produced.

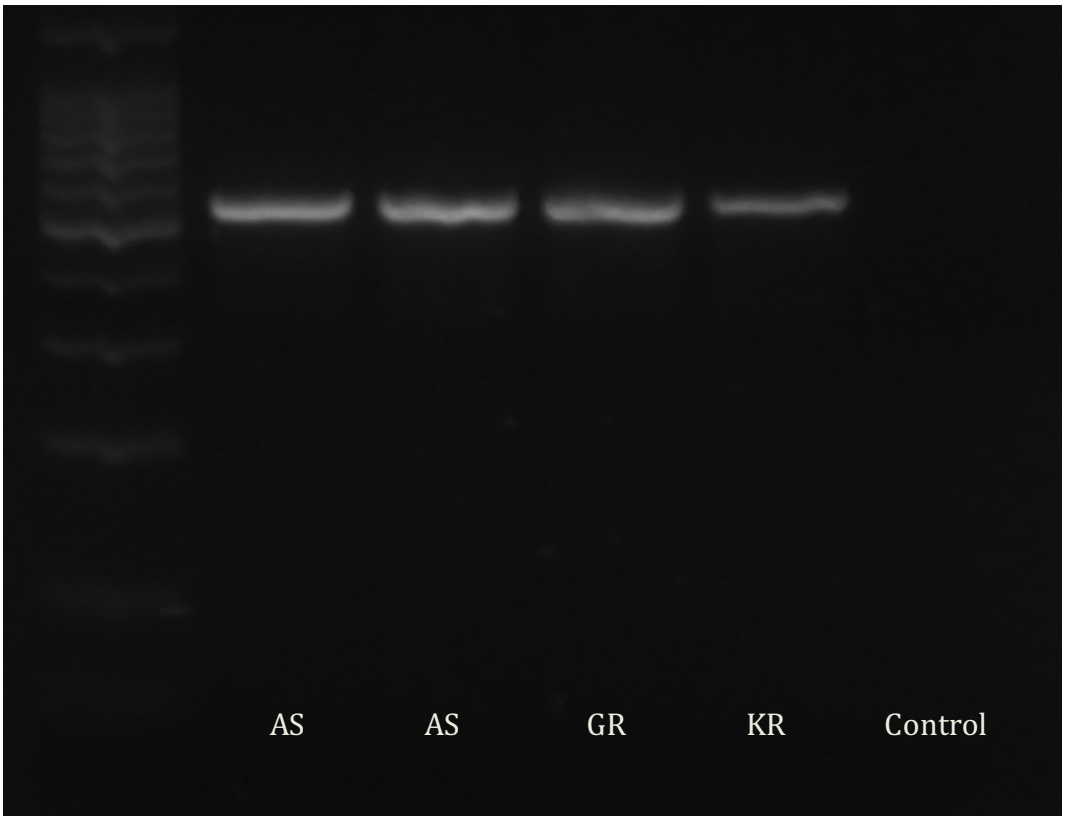

Figure 26: RT-PCR for GAPDH. Performed to assess production of cDNA from the different cell lines. The control was a sample undergoing the same steps of the RT-PCR process but loaded with water rather than RNA. The lanes are left to right: control protein ladder (multiple faint bands), parental Suit2 (AS), parental Suit2 (AS), clonally resistant Suit2 (GR), transiently resistant Suit2 (KR) and control.

The picture of the PCR gel shows 4 bands relating to the cell line lanes and no band in the control lane. The protein ladder can be seen faintly to the left. This confirms the production of cDNA with no contaminant in the control.

4.2.2.3.3 Trial of SERPINA1 primers for use with qRT-PCR

Once the production of cDNA was confirmed, the primers designed against SERPIN A1, which codes for A1AT, were tested. The expected length of the cDNA segments produced was 492 base pairs according to the clone computer programme. 2 lanes of AS cell line cDNA were used for the test.

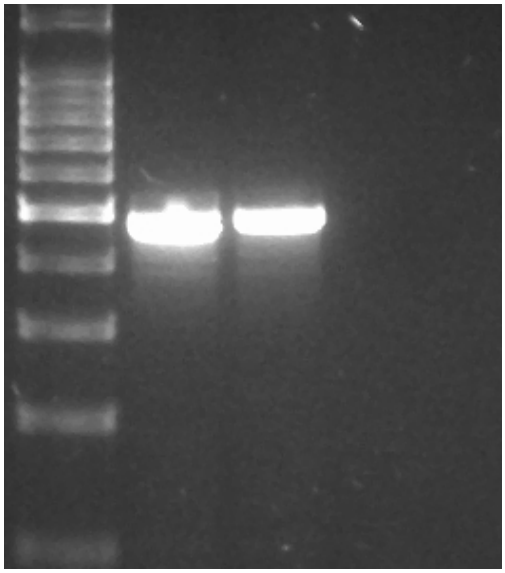

Figure 27: RT-PCR for SERPIN A1. Lanes are left to right: protein ladder with strong band at 500 base pairs, Suit2, Suit2 and control. The control was a sample undergoing the same steps of the RT-PCR process but loaded with water rather than RNA.

The picture of the PCR gel shows 2 bright bands in the 2 cell line cDNA lanes just below the bright lane in the DNA ladder representing DNA of length 500 base pairs. This corresponds to the 492 base pairs expected. Therefore, the primers were suitable to continue using for further experiments.

4.2.2.3.4 qRT-PCR for SERPINA1

The microarray suggested SERPIN A1 was under expressed in the resistant cell lines.

GAPDH is a housekeeping gene, consistently expressed among all animal cells and was therefore used as a control to ensure equal loading. First, GAPDH curves were produced as described in section 3 for the different cell lines to allow quantification of the amount of total cDNA in each sample. The samples were then diluted to what was thought to be equal concentrations of total cDNA. qRT-PCR was then performed in duplicate for the 3 cell lines for GAPDH once more to confirm equal loading:

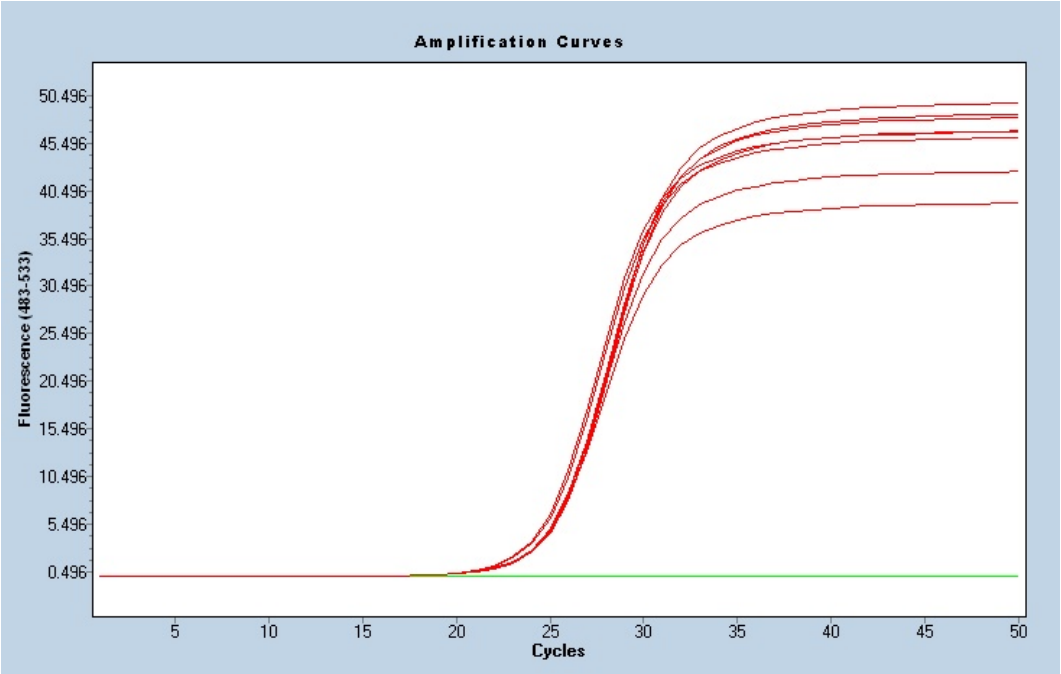

Figure 28: qRT-PCR for GAPDH. Performed in duplicate for AS,GR,KR. The graph shows amplification curves which represent number of cycles plotted against fluorescence.

Cell line	Crossing point
AS	24.68
AS	24.62
GR	24.88
GR	24.85
KR	25.04
KR	25.04

Table 16: Crossing points for qRT-PCR for GAPDH. These provide a number for the curves in the above figure. Which represents the number of cycles at which increase in cDNA is truly exponential.

Overlying curves would represent equal amounts of cDNA within the sample. The Lightcycler machine also provides a crossing point which represents the point at which increase in cDNA fluorescence is truly exponential. These numbers are lower the more cDNA is present as the exponential phase takes

less cycles of PCR to occur. As PCR involves doubling of the DNA per cycle, a number one higher than another represents half as much DNA present, and a number 2 higher represents a quarter as much DNA, etc.

The above figure and table show that there were very similar amounts of cDNA loaded between the samples as expected.

Following confirmation of equal amounts of cDNA in each sample, qRT-PCR was performed looking at the levels of SERPIN A1 using the primers designed above.

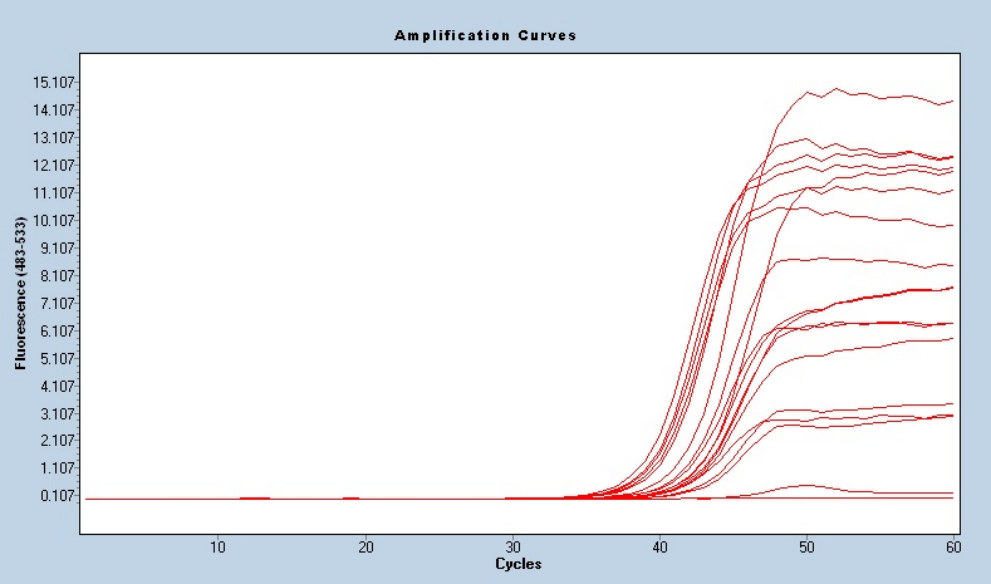

Figure 29: qRT-PCR for SERPIN A1 in AS,GR and KR cell lines. There were 6 wells for each cell line. The graph shows amplification curves which represent number of cycles plotted against fluorescence.

Cell line	Cycles	Mean
AS	38.93	
AS	39.54	
AS	39.56	40.00

AS	41.83	
AS	40.42	
AS	39.73	
GR	42.94	
GR	42.44	
GR	42.44	42.33
GR	41.84	
GR	42.02	
GR	42.28	
KR	42.11	
KR	44.02	
KR	41.63	42.03
KR	41.20	
KR	42.05	
KR	41.15	

Table 17: Crossing points for qRT-PCR for SERPIN A1. The 6 wells of each cell line have been averaged in the right column.

The figure and table above show differing amounts of SERPIN A1 in each of the cell lines. The experiment was performed with 6 wells of each cell line to allow averaging and statistical analysis to be performed to confirm differential expression.

Specifically, comparing levels of SERPIN A1 in the resistant cell lines GR and KR verses the parental cell line AS showed statistically significant differences (GR vs AS, T-test, p=0.002; KR vs AS, T-test, p=0.007). When using the average for each cell line, expression of SERPIN A1 was decreased in the resistant cell lines (AS vs GR = 80.04% decreased expression, AS vs KR = 75.43% decreased expression).

Given the definite decrease in the amount of SERPIN A1 RNA present in both the GR and the KR resistant cell line, it was decided to continue to a knockdown experiment for SERPIN A1 to look for an effect on resistance.

4.2.3 **Glutathione S-transferase P (GSTP)**

Glutathione-S-Transferase-P (GSTP) was investigated by means of western blotting. The experiments were performed in triplicate following optimisation of the antibody conditions as usual. In this case, it was not immediately obvious to the naked eye if there was a significant difference between the sensitive and resistant cell lines (AS vs GR and KR), so the blots were then analysed to measure the density of the bands created and this was adjusted according to the consistency of the loading, as subsequently measured by the actin blots. An example blot is shown below and the density analysis shown below that in both graphical and numerical form.

Figure 30: Example western blot for Glutathione S Transferase P (GSTP). Upper figure shows original blot for GSTP and lower blot is for Actin. Lanes are shown corresponding to the various cell lines.

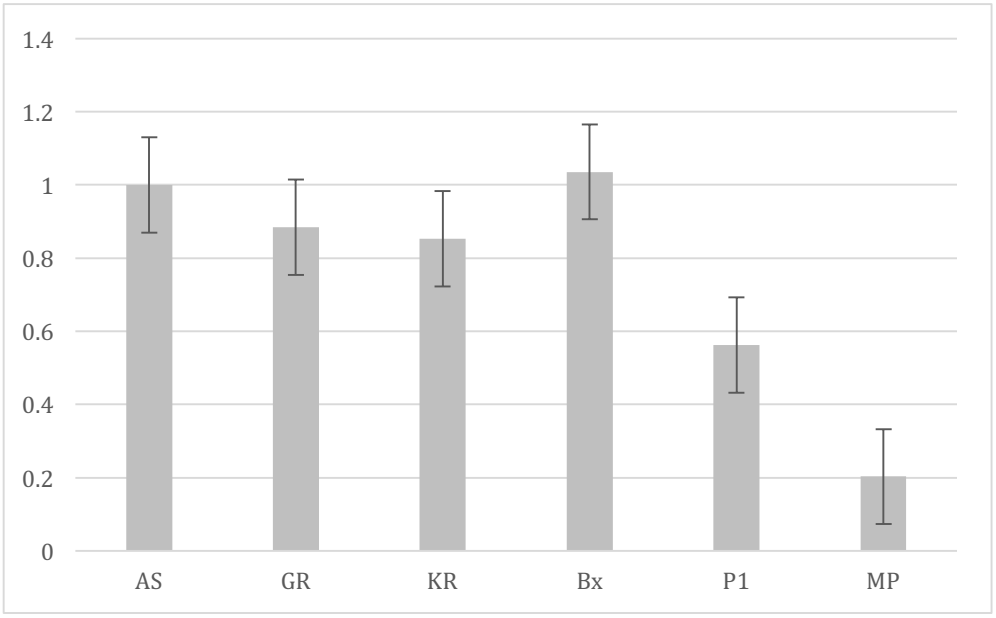

Figure 31: Bar chart representing the results of western blots for GSTP. The blots were repeated in triplicate, the density of the bands measured, with the GSTP bands adjusted for the density of the Actin bands, averaged, then compared with the AS (original Suit-2) cell line which was given an arbitrary value of 1. Error bars represent 95% CI. This allowed variations to be more easily appreciated. The numerical values are shown in the table below.

AS	1
GR	0.88
KR	0.85
Bx	1.04
P1	0.56
MP	0.2

Table 18: Relative density of GSTP western blot bands

The figures and table show a slight reduction in the amount of GSTP present in the resistant cell lines (GR=0.88, KR=0.85) compared with the resistant cell line (AS=1). Although this difference was small and did not reach significance, it was felt that, given the blots were clean and well optimised, it was worth considering GSTP and a potential knockdown candidate in the next stage of experiments.

It was also noted that P1 and MP cell lines produced far lower levels of GSTP than other cell lines.

4.2.4 **Occludin**

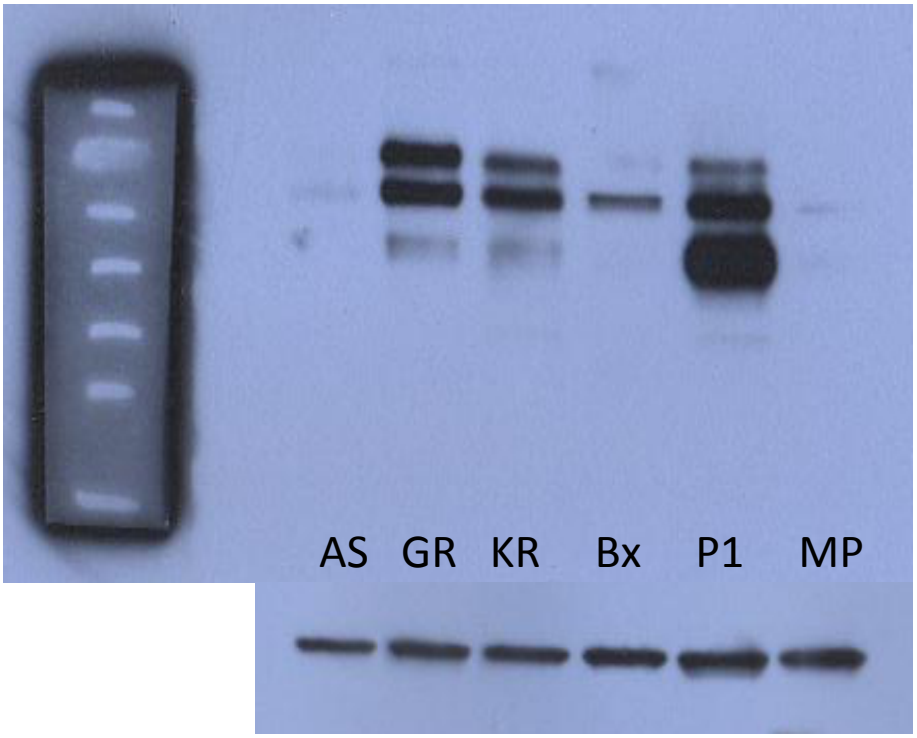

Figure 32: Example western blot for Occludin. Upper figure shows original blot for Occludin and lower blot is for actin. Lanes are shown corresponding to the various cell lines.

Occludin was also investigated by means of western blotting. Despite repeated attempts to optimise the conditions, the best that could be achieved is shown above. This demonstrates a relatively dirty blot with numerous bands at different levels for all the cell lines. There is a potential increase in expression in the resistant cell lines (GR and KR) compared to the parent cell line (AS), however the relative densities of the different bands also varied from cell line to cell line (for instance a large band in P1 at a smaller protein

size (lower on the figure) which is not present in any other cell line). It was therefore felt that meaningful comparisons and conclusions could not be drawn from these westerns, and given more success was had with other proteins, it was decided not to further investigate the protein Occludin.

4.2.5 Folate receptor alpha (FOLR)

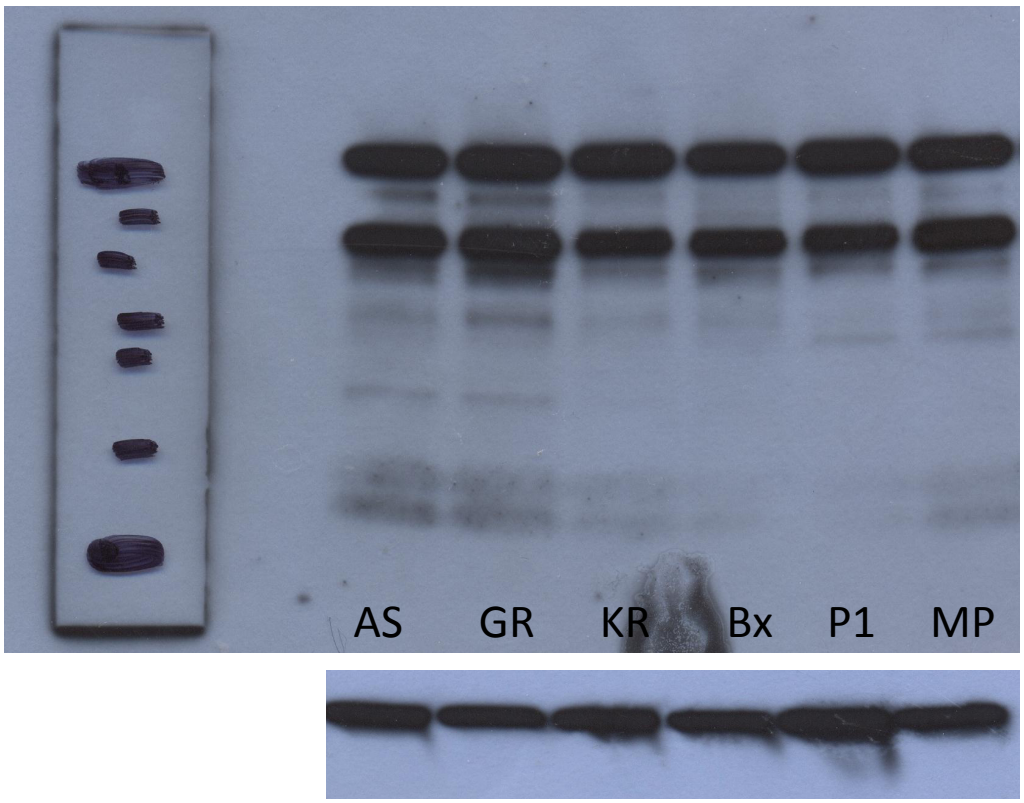

Figure 33: Example western blot for Folate receptor alpha (FOLR). Upper figure shows original blot for FOLR and lower blot is for actin. Lanes are shown corresponding to the various cell lines.

FOLR was similarly investigated by means of western blot. The antibody used provided 2 bands in each cell line but despite this, it can be seen that, despite equal loading of protein as shown by similar densities in the actin blot, there does not appear to be a significant difference in the amount of FOLR present in the different cell lines. In particular, the AS and GR cell lines of most interest are very similar. This finding held true throughout optimisation of the antibody and repeated experiments.

It was therefore decided not to proceed to the next stage if investigation with FOLR.

4.2.6 **Ribonucleotide reductase subunit 2 (RRM2)**

4.2.6.1 Western blot

The microarray suggested that RRM2 was under expressed in the resistant cell line KR compared to the AS cell line.

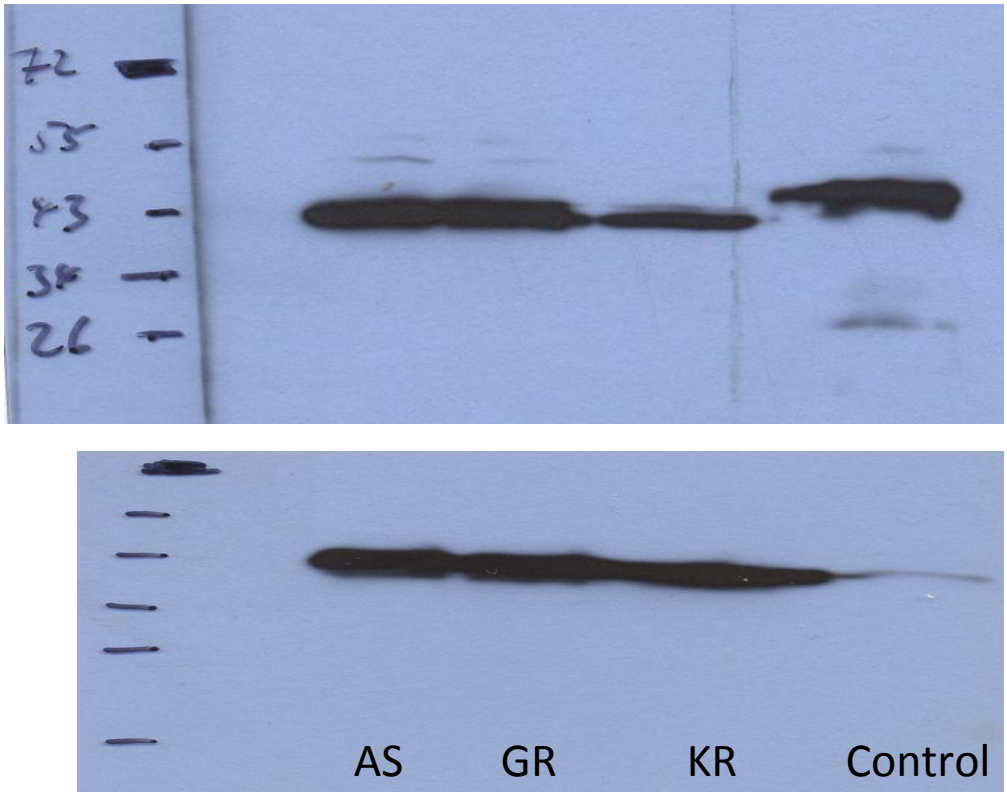

Figure 34: Example western blot for RRM2. Upper figure shows original blot for RRM2 and lower blot is for actin. Lanes are shown corresponding to the various cell lines. In this experiment, a control lane of RRM2 protein is shown the right-hand side of the blot, at the same protein size as those shown in the cell lines (45kDa)

The upper film shows a lower amount of protein in the 3rd lane at ~45 kDa which is the expected weight of RRM2. The control is a commercially available RRM2 protein. The lower film shows relatively consistent loading between the lanes with a small amount of overspill into the control lane.

When these bands were quantified using the Kodak machine and adjusted for the size of the β-actin bands, there was found to be 19.6% less RRM2 in the KR cell line compared to the same amount in the AS and GR cell lines.

A repeat of this experiment was also performed:

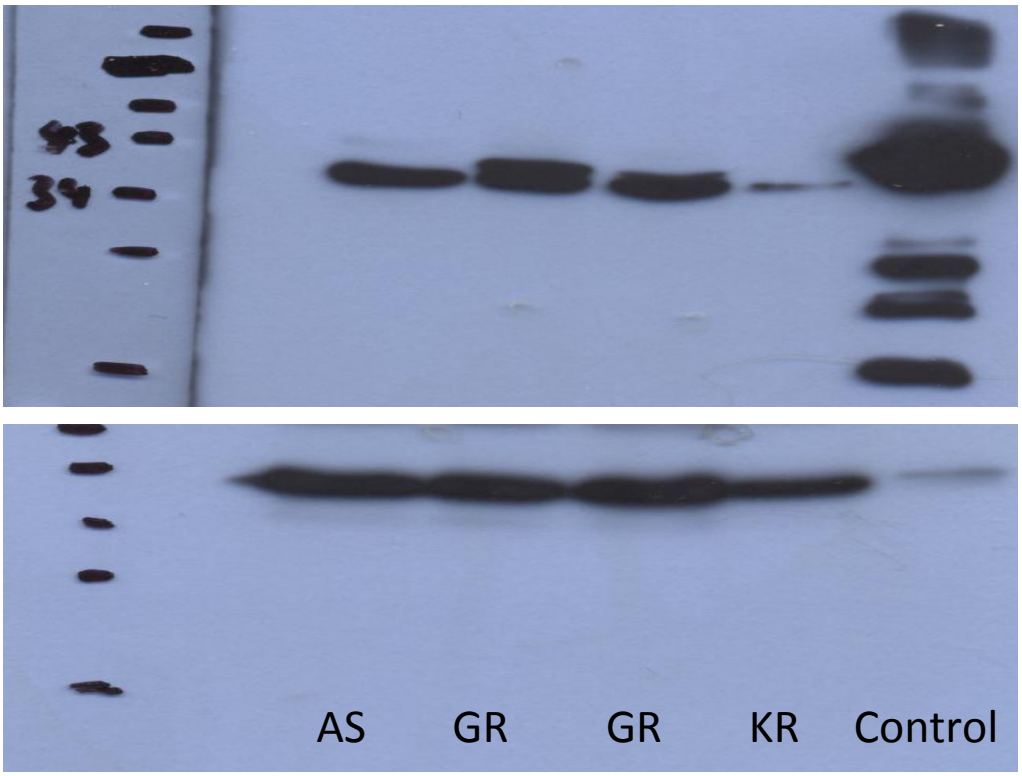

Figure 35: Repeat western blot for RRM2. Upper figure shows original blot for RRM2 and lower blot is for actin. Lanes are shown corresponding to the various cell lines. In this experiment, a control lane of RRM2 protein is shown the right-hand side of the blot. In this experiment, 2 lanes of GR were used in lanes 2 and 3.

The repeat was performed with 2 lanes of GR protein. The film above shows 3 dense bands in the first 3 lanes (with double bands in lanes 2 and 3), and a much lighter band in lane 4 corresponding to the KR cell line. The actin film below does show slightly lighter band representing less loading in lane 4 compared to the others, but not enough to explain the findings above. Due to

the double bands in lanes 2 and 3, quantification was not performed, but in combination with the first western for RRM2, there appears to decreased protein level in the KR cell line.

This film is taken at a longer exposure than the previous experiment which is why the control lane has more bands within it. The far denser band remains present at the 45kDa mark, consistent with above.

Given the definite decrease in the amount of RRM2 present in the KR resistant cell line, it was decided to continue to a knockdown experiment for RRM2 to look for an effect on resistance.

4.2.7 Interleukin-1β

4.2.7.1 Western blot on cell lysate

Interleukin 1-β (Il-1β) was investigated as it was identified on the *Ingenuity* pathway downstream of A1AT and upstream of RRM2. Initially Western blot on whole cell lysate was performed to assess intracellular levels of Il-1β.

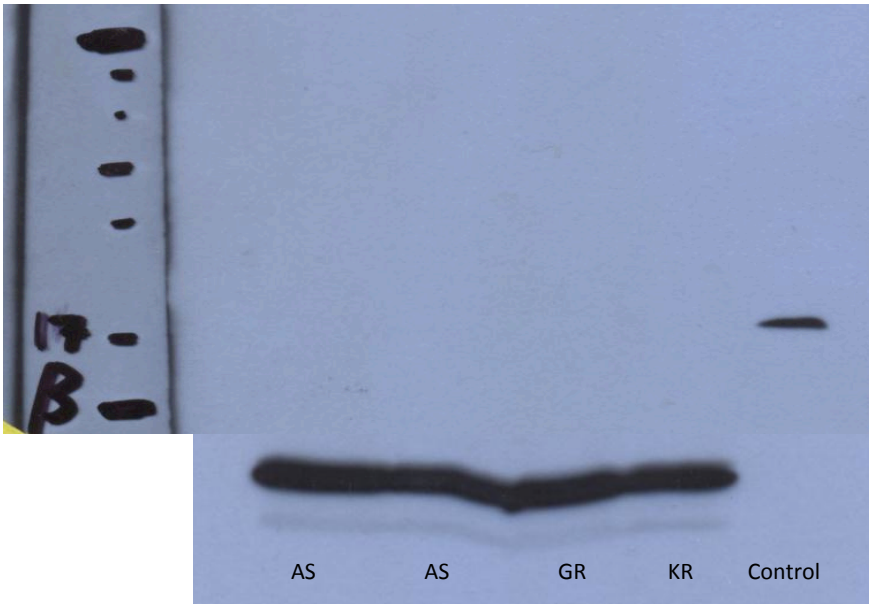

Figure 36: Example western blot for Il-1β. Upper part of figure shows original blot for Il-1β and lower blot is for actin. Lanes are shown corresponding to the various cell lines.

The above films again show no detectable bands, this time for Il-1β. The band seen on the right of the upper film at 17kDa (expected weight of Il-1β) is the control protein. The β-actin film below shows good amounts of total protein were loaded.

4.2.7.2 Western blot on supernatant

Given no Il-1β was identified on Western blots using whole cell lysate, I decided to assess to see of the cells were producing Il-1β into the surrounding media. Therefore, Western blot was performed on supernatant taken from the cell media for the different cell lines.

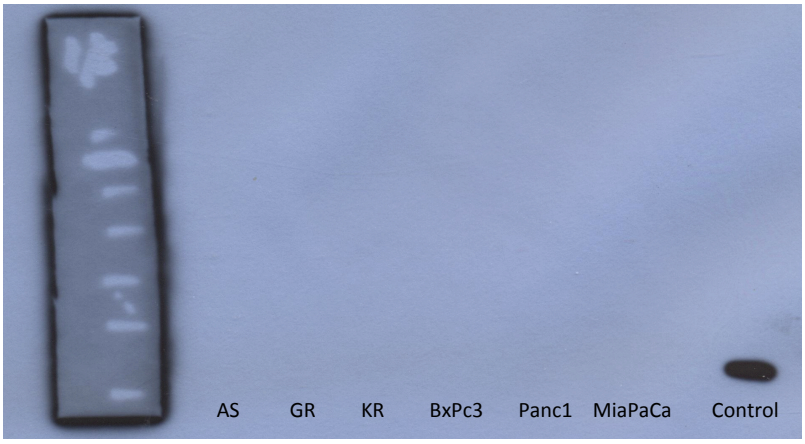

Figure 37: Western blot probing for IL-1β in supernatant. The band seen to the right is the control protein. No actin blot is shown.

However, as can be seen in the Western blot above, there was no measurable level of expression identified for Il-1β.

4.2.8 **Conclusions**

These results have shown the following:

-A decrease in SERPIN A1 RNA in both the GR and KR cell lines compared to the AS cell line.

-A decrease in GSTP protein in both the GR and KR cell lines compared to the AS cell line.

-A decrease in the RRM2 protein in the KR cell line compared to the GR and AS cell lines.

-No difference in the protein levels of FOLR

-Unable to accurately measure levels of Occludin or IL-1β.

	AS	*GR*	*KR*
SERPIN A1	↔	↓	↓
GSTP	↔	↓	↓
Occludin	-	-	-
FOLR	↔	↔	↔
RRM2	↔	↔	↓
IL-1β	-	-	-

Table 19: Table summarising the findings in this section; Relative levels of the proteins and genes of interest in the different suit-2 cell lines

4.3 Knockdown of differentially expressed genes and proteins of interest

4.3.1 Overview

I had confirmed SERPINA1, GSTP and RRM2 as being differentially expressed between the resistant and sensitive Suit2 cell lines. I went on to perform siRNA knockdown of these, confirmed at either RNA or protein level, and performed MTS experiments to assess any potential effect on resistance.

I also performed an experiment involving treating cells with exogenous A1AT to assess for any effect on resistance.

4.3.2 **SERPINA1**

4.3.2.1 Knockdown

The first stage was to confirm consistent loading across the samples with qRT-PCR for GAPDH as previously:

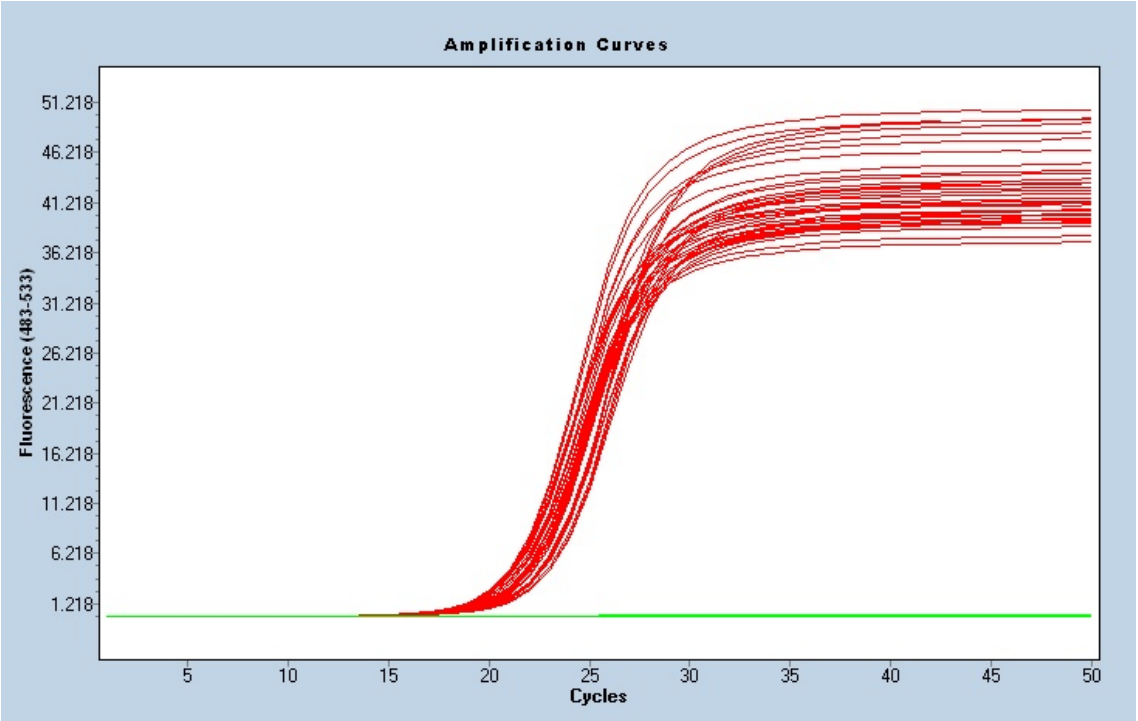

Figure 38: qRT-PCR for GAPDH in SERPINA1 KD. 2 negative controls were used (6 wells used for each).

The above shows qRT-PCR for GAPDH for SERPINA1 knockdown (termed KD), and 2 negative controls used (-1 representing an off-target control and -2 representing a RISC free control). All 3 cell lines were loaded 6 times in separate wells to allow statistical analysis to be performed. However, due to problems with the designed primer (namely primer-dimers, where the

primers bind to each other rather than DNA as intended and therefore create negligible amounts of amplified DNA), some of the samples were unsuitable for analysis and therefore removed from the analysis.

The above figure shows fairly consistent amounts of cDNA loaded throughout the samples.

The experiment therefore continued with qRT-PCR for SERPIN A1.

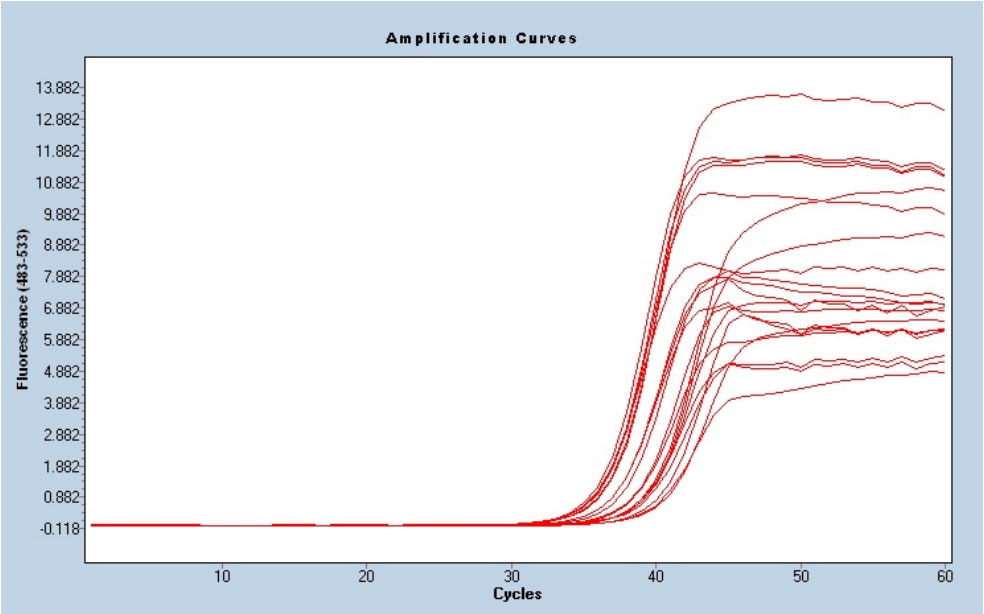

Figure 39: qRT-PCR amplification curves for SERPIN A1 knockdown. These curves represent multiple wells of the attempted knockdown and 2 negative controls named -1, -2. Crossing points are shown in following table.

In the figure above the lines for knockdown cells (KD) are grouped towards the right, which is represented numerically by the crossing point values in the table below. When analysed statistically using the students t-test, the knockdown cells show a significantly different amount of SERPIN A1 cDNA

with p values of <0.001 (KD vs -1), 0.027 (KD vs -2) and <0.001 (KD vs both -1 and -2).

Cell line	Crossing Point	Mean average
KD	39.46	39.55
KD	39.26	
KD	39.31	
KD	40.18	
-1	36.99	36.35
-1	36.43	
-1	36.65	
-1	36.07	
-1	36.22	
-1	35.73	
-2	36.98	37.67
-2	37.91	
-2	39.82	
-2	36.75	
-2	36.89	

Table 20: Crossing points for SERPIN A1 knockdown. Multiple wells of the attempted knockdown (KD) and 2 negative controls (-1,-2) are shown, with averages across the number of wells for each (max=6)

When the 2 negative controls are grouped together the mean is a crossing point of 36.95 versus the mean for the KD cells of 39.55. This represents a successful knockdown of 83.5% of the SERPIN A1 RNA.

4.3.2.2 MTS/IC50

The knockdown of SERPIN A1 was repeated in order to assess the effect on gemcitabine sensitivity/resistance of the cells. This time the knockdown cells (KD) and negative controls (-1 representing an off-target control and -2 representing a RISC free control) were also compared with AS and GR cell lines.

Firstly, the repeat knockdown was confirmed as above, beginning with the GAPDH to confirm consistent loading of the wells:

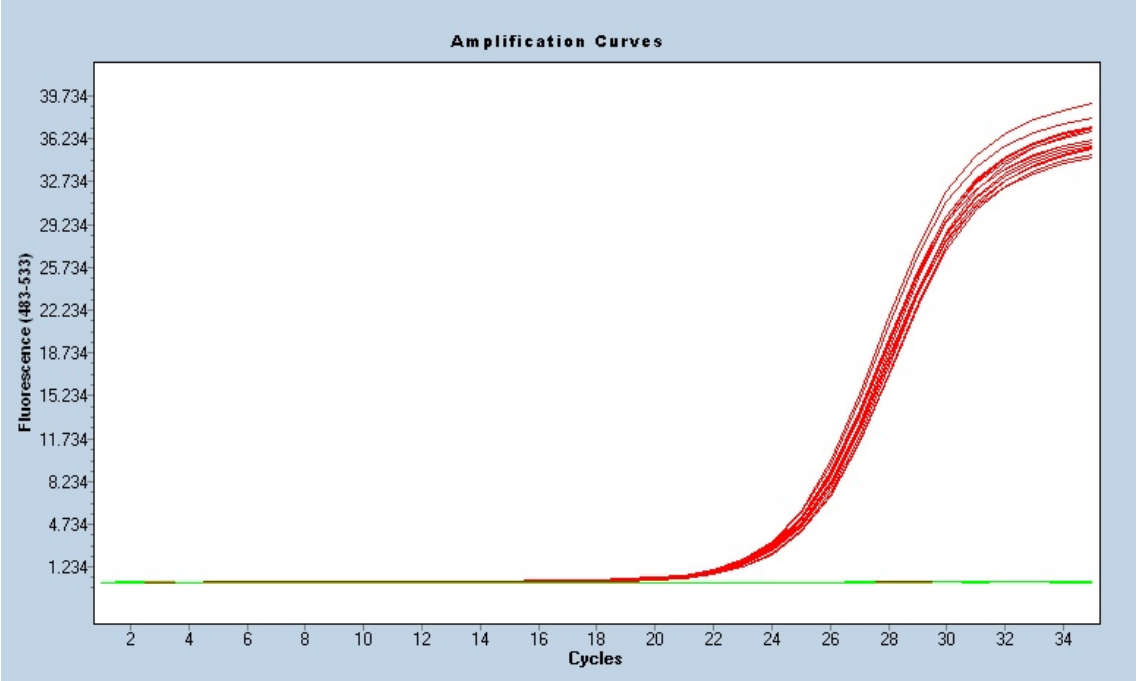

Figure 40: qRT-PCR for GAPDH in repeat SERPIN A1 knockdown. All wells show similar loading amounts of cDNA

The GAPDH curves are again satisfactory.

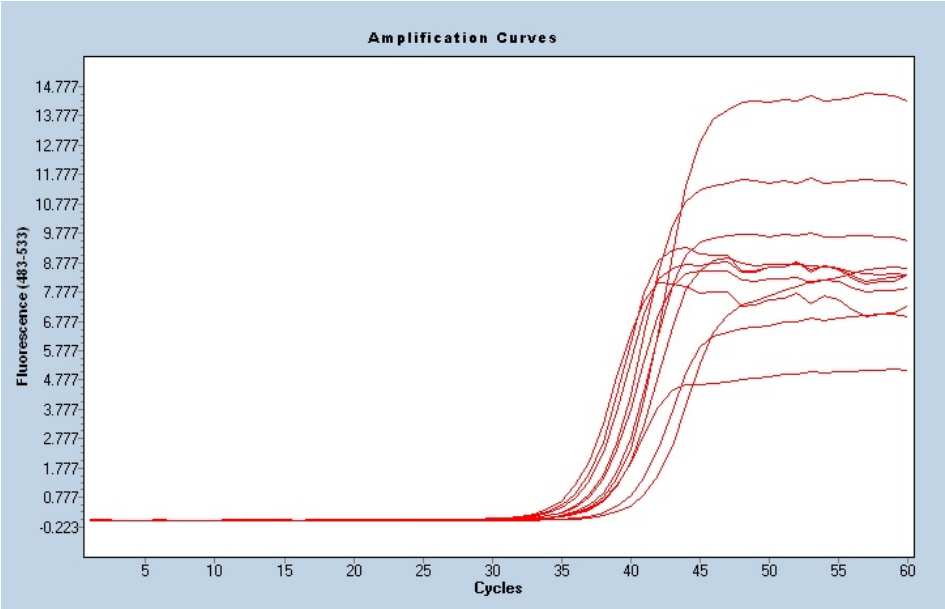

Figure 41: qRT-PCR for SERPIN A1 in repeat SERPIN A1 knockdown. Multiple wells of the attempted knockdown (KD), 2 negative controls (-1,-2), plus the original cell lines AS and GR were used.

Cell line	Crossing point	Mean Average
KD	40.51	
KD	40.82	40.67
-1	36.65	
-1	36.63	36.81
-1	37.16	
-2	37.47	
-2	36.72	37.15
-2	37.26	
AS	36.46	
AS	36.22	36. 08
AS	35.57	
GR	39.53	
GR	39.14	39.34

Table 21: Crossing points for repeat SERPINA1 knockdown. This shows numerical values for the curves shown above.

This time the samples were performed in triplicate (as opposed to 6 times as above). Unfortunately, some of the samples had to be removed from analysis

as insignificant amounts of cDNA were created as in the above experiment. This meant that 2 cell lines (KD and GR) only had two useable results.

The knockdown appears to have decreased the expression in the sensitive cell line used (AS) to less than that produced by the resistant cell line (GR) (Crossing points: AS=36.08 vs GR=39.34 vs Knockdown=40.67, where higher values represent lower amounts of RNA present). This also confirms the result above showing decreased expression of SERPINA1 in the resistant cell line (GR) compared to the sensitive Suit2 (AS). The result was felt successful to continue with the cytotoxicity experiment itself.

The following MTS assay was performed 72 hours after exposure to differing concentrations of gemcitabine but it is similar to that at 24 and 48 hours. The MTS was left for 3 hours before these readings were taken. On this graph C1 represents the knockdown cells (KD), 1 represents the first negative control (-1) and 2 the second negative control (-2).

The curve for the knockdown cell line (C1) is very similar to those of the 3 sensitive cell lines (AS,-1,-2) but dramatically different to that of the resistant cell line GR. The IC50 for KD,-1,-2and AS are all <0.01μM, whereas for the GR cell line has an IC50 of between 10-100μM.

These data are extremely suggestive that the knockdown of SERPIN A1 has no effect on the resistance to gemcitabine of the cells, and was accepted as a result.

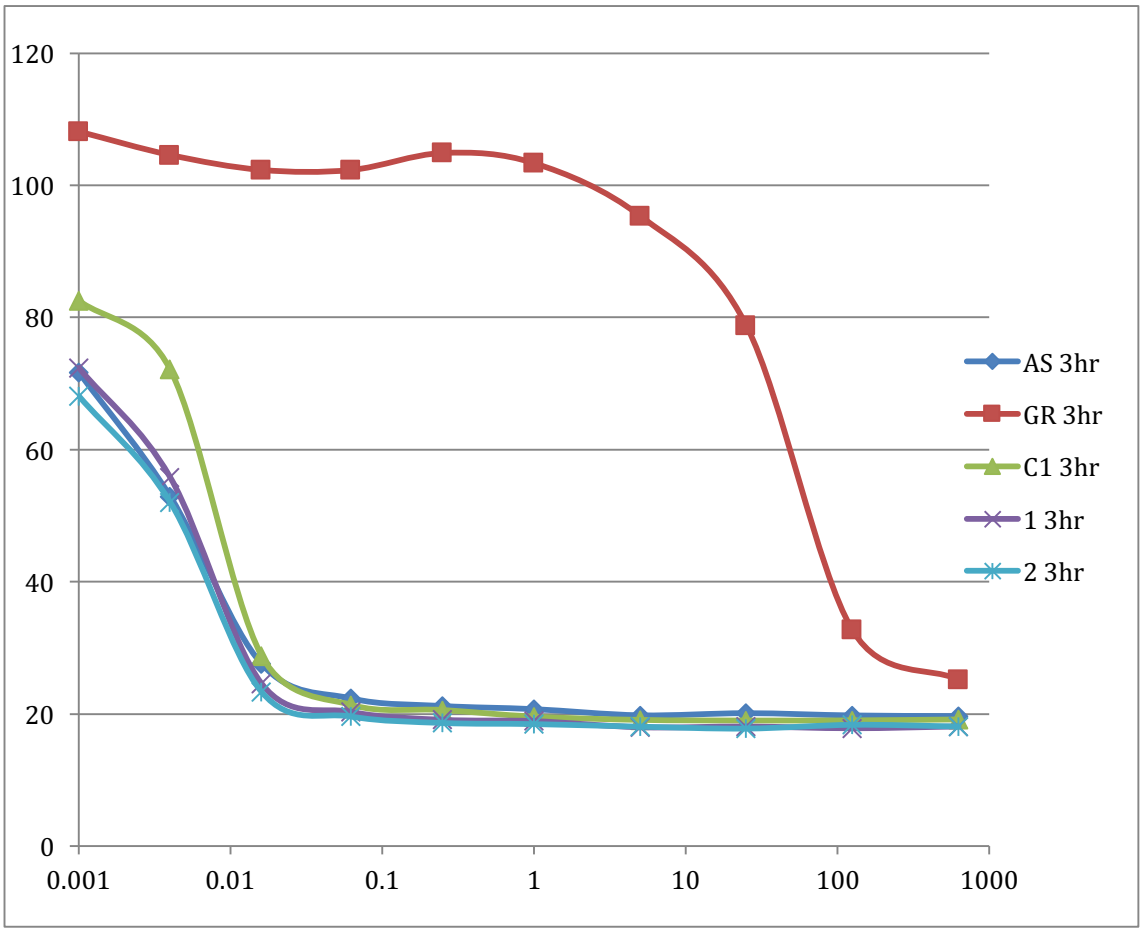

Figure 42: ***MTS assay following SERPIN A1 knockdown. This shows concentration of gemcitabine in µM against % cells alive at 72 hours. The different curves represent the original cell lines AS and GR, the knockdown cells (C1) and 2 negative controls (1 and 2). The curves show no difference in comparing the knockdown to the original cell line AS.***

4.3.3 **GSTP**

4.3.3.1 Knockdown of GSTP

The AS and GR cell lines were manipulated to reduce the amount of GSTP produced by the cells using siRNA knockdown as per the methods. This experiment was performed using 20nM of the siRNA with the cell lysate harvested 72 hours after treatment with the siRNA. In the final experiment shown below, an off target negative control was used (AS-OT or GR-OT) which involved the cells being put through the same procedure except off target siRNA which did not affect expression was used.

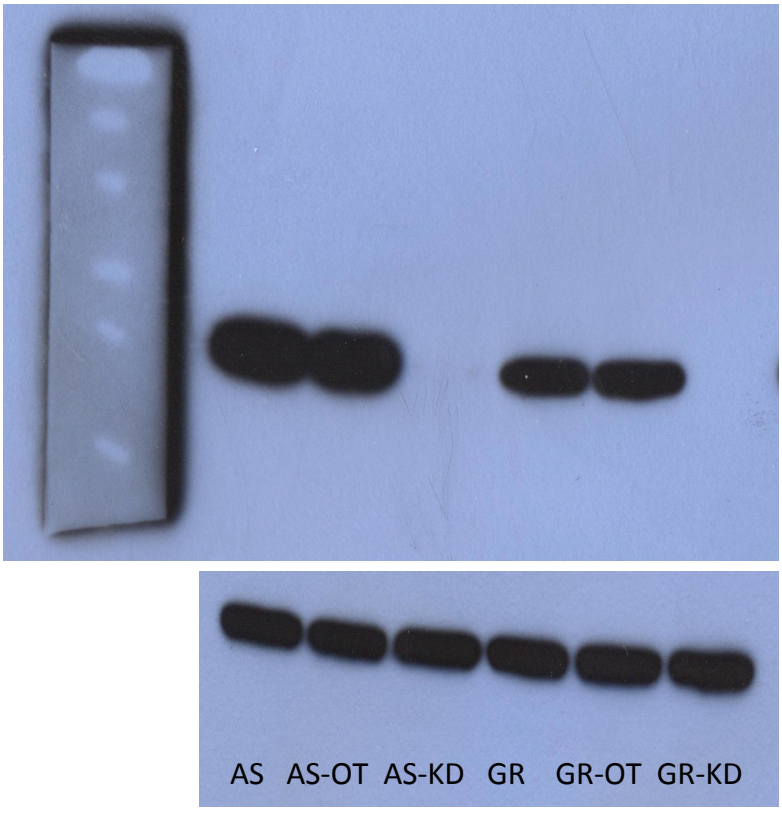

Figure 43: Knockdown of GSTP in AS and GR cell lines. Lanes include off target negative controls (AS-OT and GR-OT) and the knockdown cells (AS-KD and GR-KD). Original blot shown above and actin blot shown below.

The blot above shows a successful knockdown in both AS (AS-KD) and GR (GR-KD) cell lines. There is a very faint band remaining in the AS-KD lane but none seen at all in the GR-KD lane. Both off target controls (AS-OT and GR-OT) show no difference in levels of GSTP compared with the parental cell lane, and the actin blot below shows consistent loading throughout.

Having confirmed the knockdown, it was possible to assess for any effect on resistance.

4.3.3.2 MTS following knockdown of GSTP

The cell lines were subjected to MTS analysis with the cells treated with gemcitabine 48 hours after knockdown to allow the cytotoxicity assessment to be performed 72 hours after knockdown consistent with the western blots above. This meant the curves were produced after treatment with gemcitabine for 24 hours.

The figure below shows cytotoxicity curves for gemcitabine taken after 24 hours and the 6 different curves represent the original cell lines (AS/AS and GR/GR), 2 negative off target controls (AS/OT and GR/OT) and the knockdown cells (AS/KD and GR/KD). There is very little difference seen between the original cell lines, controls and knockdown cells in either parental cell line. This strongly suggests that the impressive knockdown achieved had no effect on resistance to gemcitabine. Therefore, no further experiments were performed on GSTP.

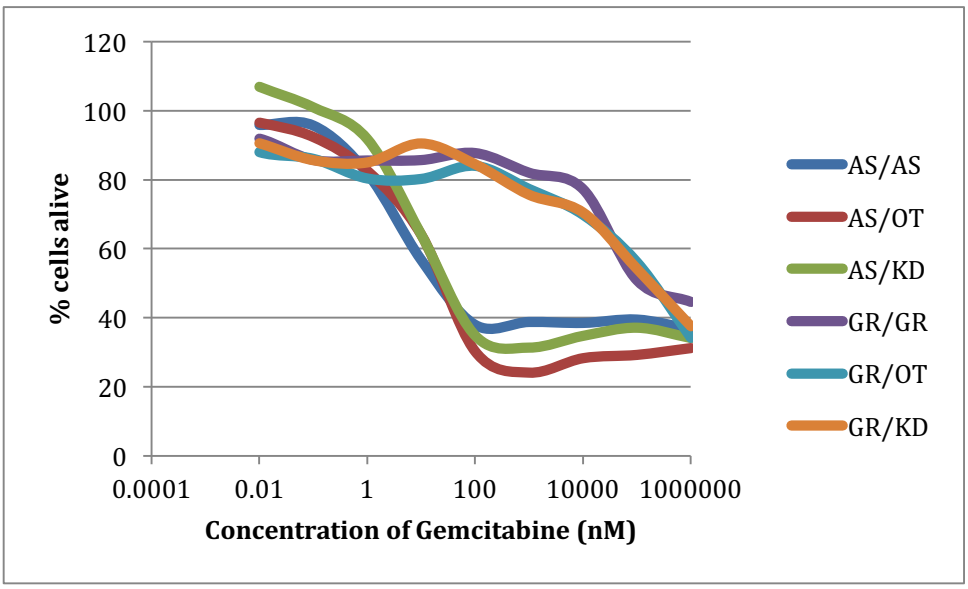

Figure 44: ***IC50 curves following knockdown of GSTP in AS and GR. This plots percentage of cells alive against concentration of gemcitabine and was performed 24 hours after treatment. The 6 different curves represent the original cell lines (AS/AS and GR/GR), 2 negative off target controls (AS/OT and GR/OT) and the knockdown cells (AS/KD and GR/KD).***

4.3.4 **RRM2**

4.3.4.1 Knockdown of RRM2

Both original Suit-2 cell lines (AS and GR) were manipulated to reduce expression of RRM2 by siRNA knockdown as per the methods section. The concentration of siRNA used was 20nM per well in a 6-well plate and the knockdown was optimum at 24 hours after treatment. Once again, an off target negative control (OT) was used by replacing with siRNA which did not code for the RRM2 section of the gene. Following knockdown, western blot was performed on cell lysate to confirm reduced levels of RRM2.

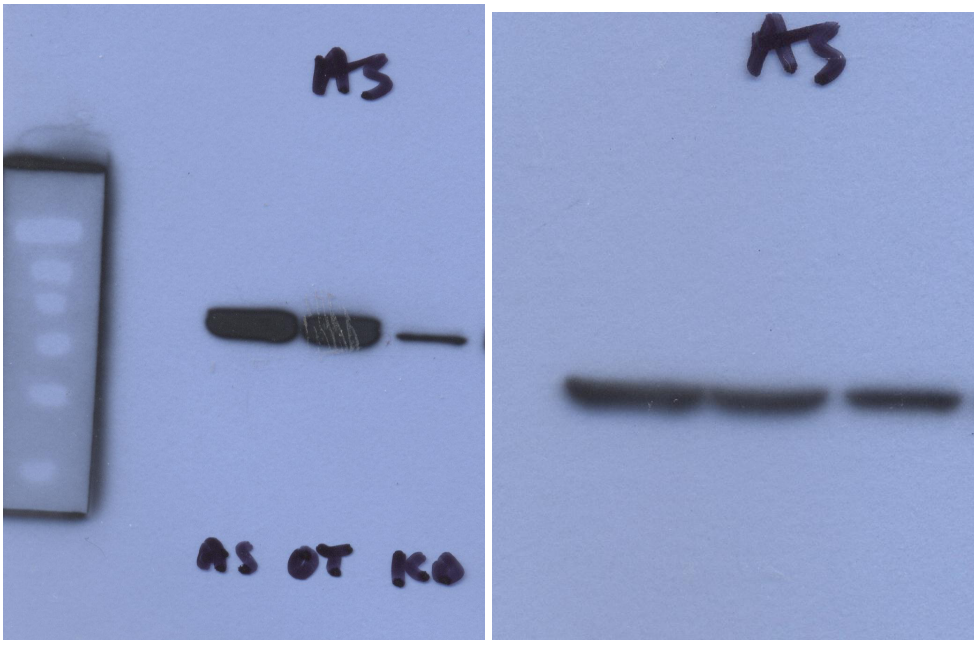

Figure 45: Western blot showing RRM2 knockdown in AS cells. Left side shows western blot for RRM2 following knockdown of RRM2 in AS cell line with lanes representing original cell line (AS), off target negative control (OT) and knockdown cell line (KD). Right side shows the actin for same blot

The figure above shows a western blot for RRM2 (left) and a subsequent actin blot on the same blot (right). The lanes represent original Suit-2 cells (AS), off target siRNA negative control (OT), and the knockdown cells (KD). There has been a significant decrease in the expression of RRM2 in the third lane, despite relatively equally loaded lanes as shown by the actin blot. This is consistent with successful knockdown of RRM2 in the AS cell line.

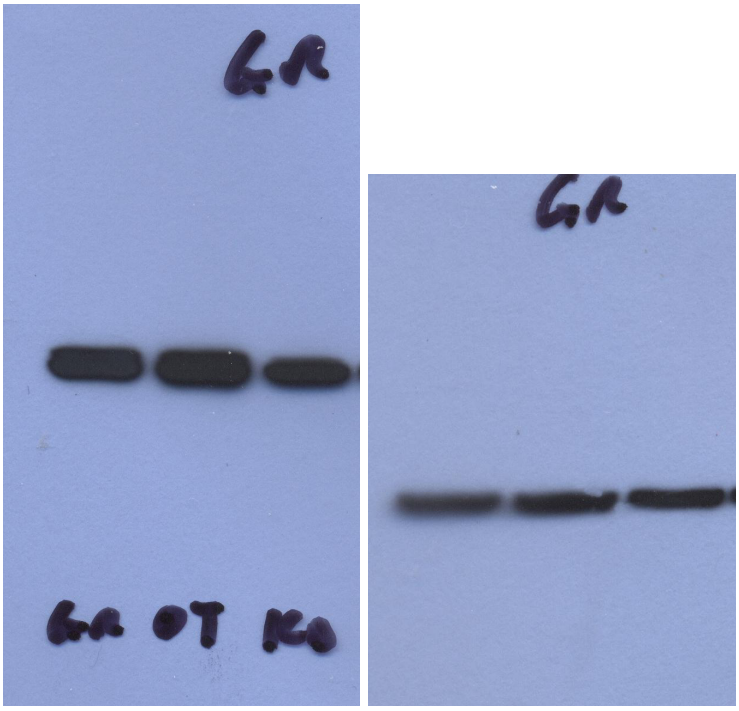

Figure 46: RRM2 knockdown in GR cells. Left shows western blot for RRM2 following knockdown of RRM2 in GR cell line. Lanes represent parent resistant cell line (GR), off target negative control (OT) and knockdown cells (KD). Right shows actin for same blot

The figure above is similar but shows a western blot for RRM2 (left) and a subsequent actin blot on the same blot (right) for the GR cell line. The lanes represent resistant GR Suit-2 cells (AS), off target siRNA negative control (OT), and the knockdown cells (KD). There is a subtle but definite decrease in the density of the band in the third lane corresponding to the knockdown

cells. This is despite consistent loading of lanes shown on the actin blot. This confirms the knockdown was successful in reducing the expression of RRM2 in the GR cell line.

4.3.4.2 MTS following knockdown of RRM2

The cell lines in the knockdown experiment were subjected to MTS analysis to show any effect on resistance to gemcitabine. The knockdown cells were treated with gemcitabine 24 hours after knockdown and the cytotoxicity experiment was performed a further 24 hours later (i.e. 48 hours after knockdown).

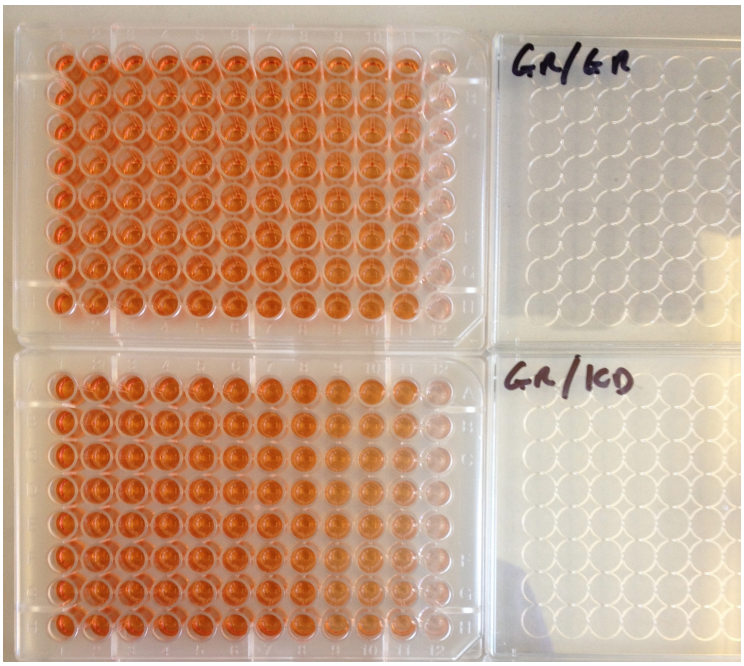

Figure 47: MTS 96-well plates for knockdown of RRM2 in GR cells. An example of an experiment to demonstrate resistance to gemcitabine in the resistant cell line GR with/without knockdown of RRM2 (GR/KD plate below is the knockdown). The depth of colour can be seen to decrease more rapidly in the lower plate from left to right, demonstrating a lower percentage of cells remaining alive. These appearances are quantified below.

The figure above shows an example of the 96-well plates after the cytotoxicity experiment. The upper plate is the original resistant Suit-2 cell ling (GR/GR) whereas the lower plate is the GR cell line after knockdown of RRM2 (GR/KD). This shows a paler colour orange in the 9th, 10th and 11th columns in the knockdown plate as compared to the original cells, which is visible to the naked eye, suggesting less cells have survived.

Gemcitabine concentration (nM)	AS	AS.KD	GR	GR.KD
0.001	97.8	90.0	97.6	99.7
0.01	73.8	34.9	95.9	97.5
0.1	66.7	31.6	94.8	96.8
1	58.7	26.1	92.2	95.1
10	42.4	17.9	91.8	95.3
100	37.2	16.2	90.7	92.7
1000	34.7	15.8	90.9	84.7
10000	32.2	15.0	89.5	45.5
100000	31.4	14.9	77.3	39.1
1000000	29.8	13.8	23.9	27.6

Table 22: Spectrophotometry of MTS 96-well plates for knockdown of RRM2 in GR cells. The results of spectrophotometry of the above figure and a similar experiment for knockdown in the AS cell line showing the measured difference in depth of colour converted to a percentage (compared to a control column of no cells present) for the four cell lines (AS, AS with RRM2 knockdown (AS.KD), GR, GR with RRM2 knockdown(GR.KD)) for the various concentrations of gemcitabine shown in the left-hand column.

The table above shows the results of spectrophotometry of the 96-well plates shown. This allows a numerical value to be attributed to the visually paler colours. This depth of colour been plotted against concentration of gemcitabine used and the table shows the values for both original cell lines (AS and GR) and the 2 knockdown cell lines (AS.KD and GR.KD). This demonstrates a more rapid decrease in depth of colour (i.e. less surviving cells) in both the knockdown cells compared with their parent cell line.

The values in this table re plotted as curves in the figure below.

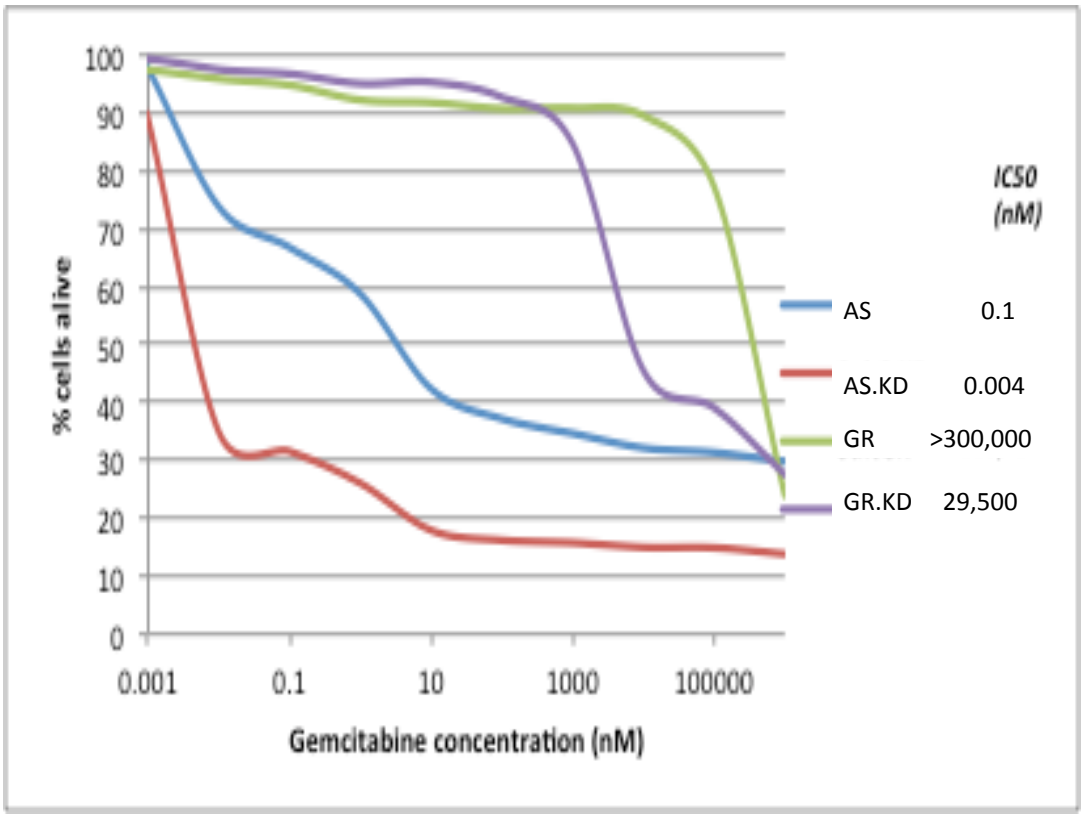

Figure 48: IC50 curves following knockdown of RRM2. This figure plots percentage of cells surviving against concentration of gemcitabine following treatment with gemcitabine for 24 hours. There are 4 curves representing the 2 original cell lines (AS and GR) and the 2 corresponding knockdown cell lines (AS.KD and GR.KD). The IC50 values gained from these curves are also shown.

This figure shows IC50 curves produced from the above table. These curves plot percentage of cells surviving 24 hours after treatment with gemcitabine against concentration of gemcitabine. There are 4 curves corresponding to the 2 original cell lines (AS and GR), and the 2 knockdown cell lines (AS.KD and GR.KD). Both knockdown curves are seen to have shifted to the left

compared to their original cell line, suggesting increased sensitivity to gemcitabine.

This increased sensitivity to gemcitabine is further confirmed when IC50 values are derived from the curves. For the originally resistant cell line GR, the knockdown has taken the IC50 value from greater than 300,000nM to 29,500nM, which is a ten-fold decrease.

For the original Suit-2 cell line AS, the knockdown of RRM2 has reduced the IC50 value from 0.1nM to 0.004nM, which is greater than a ten-fold drop.

These results show a significant effect on resistance by manipulation of the RRM2 expression of the cells.

4.3.5 **Treating with exogenous A1AT**

To further investigate a potential link between A1AT and resistance, cells were treated with exogenous A1AT protein at various concentrations to assess any effect on resistance to gemcitabine.

For this experiment two 96-well plates were seeded with suit-2 AS cells and grown for two days; one plate with A1AT added to the culture media and one plate without. The concentration of A1AT was extrapolated from the dose used clinically: usually 60mg/kg, therefore estimating the cell mass on the base of a 96-well plate to be between 0.1g and 1g, 25μg /plate was used.

The two plates were then subjected to various concentrations of gemcitabine consistent with previous experiments and subjected to MTS assay at 72 hours.

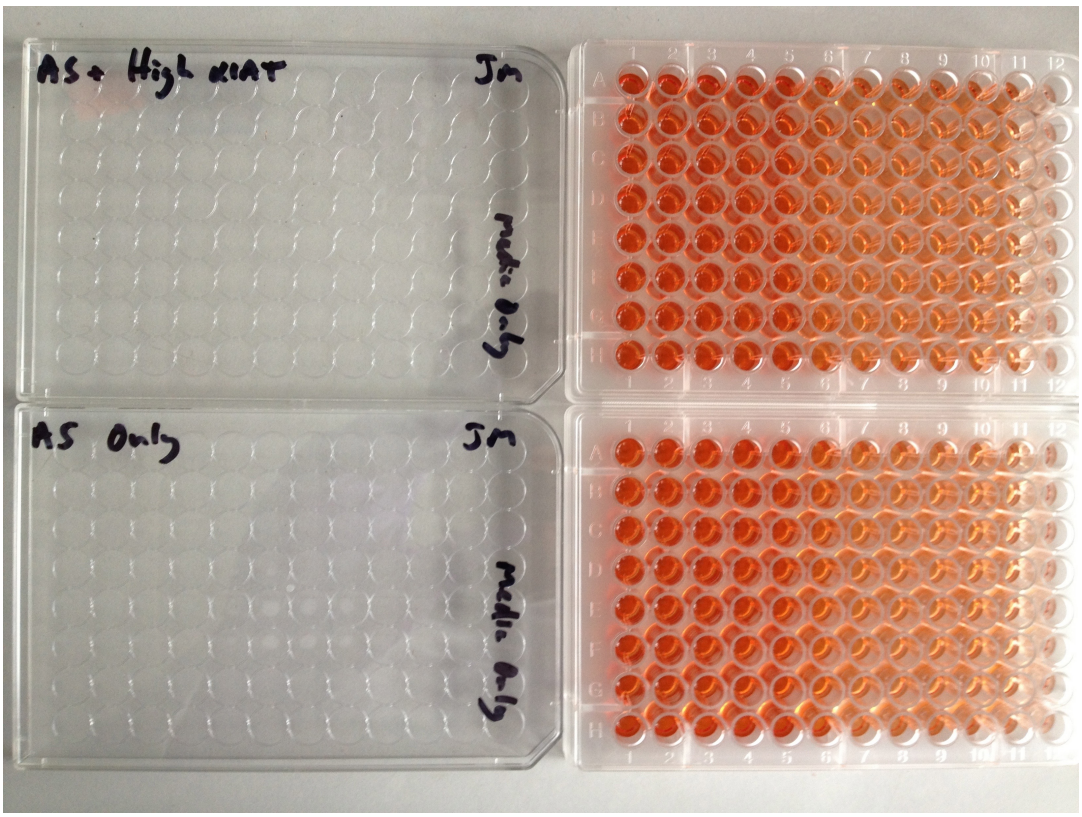

Figure 49: ***MTS assay following exogenous A1AT treatment. A photograph of a 96-well plate from the described experiment, following treatment of AS cells with or without A1AT and varying concentrations of gemcitabine. The above plate has been treated with A1AT, the lower without. The plates are otherwise treated similarly, with increasing concentrations of gemcitabine from left to right, and a control lane on the far right of media only. The colour or the equivalent columns of each plate are very similar.***

The figure above show first the 2 96-well plates (upper plate treated with A1AT and the lower without) following MTS assay, which shows no change in depth of colour between plates visible to the naked eye. The table below then shows the values following spectrophotometry analysis of the same 96-well plates, showing very similar readings between the 2 plates.

Gemcitabine concentration (nM)	% Control	
	With A1AT	No A1AT
0.001	100.9	100.1
0.01	99.1	99.1
0.1	84.7	99.5
1	98.5	98.4
10	51.3	62.0
100	33.0	33.2
1000	30.0	25.7
10000	29.7	24.8
100000	29.6	25.9
1000000	26.8	21.4

Table 23: Spectrophotometry of MTS 96-well plates using AS cells following exogenous A1AT treatment. Values show measured depth of colour adjusted to show percentage of cells alive vs control for 96-well plate treated with or without A1AT for 48 hours prior to and during treatment with varying concentrations of gemcitabine.

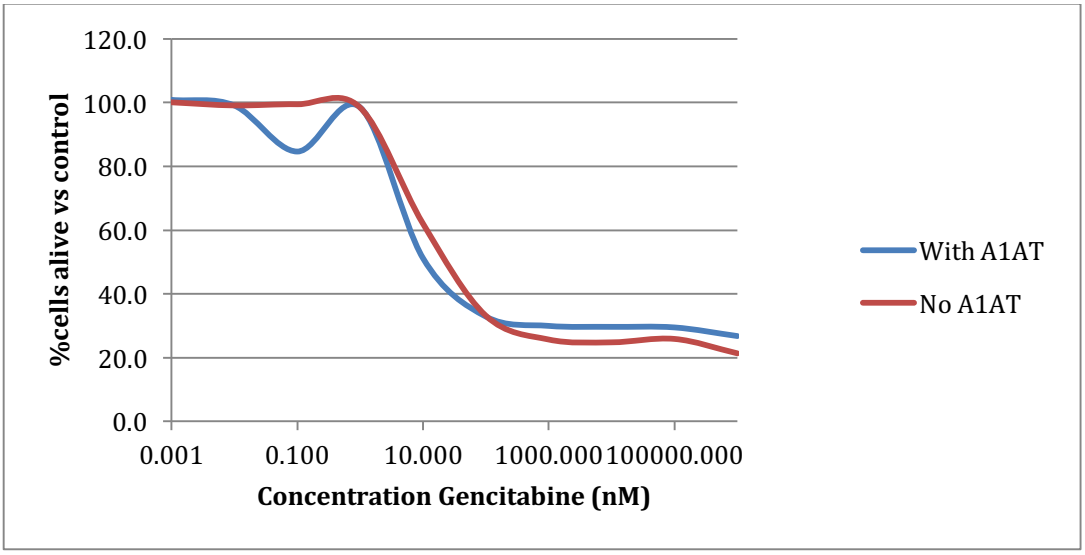

Figure 50: Cytotoxicity curves created from the values in the above table, showing very similar curves for both 96-well plates (i.e. no change in resistance to gemcitabine). These curves are consistent with the naked eye appearances of the plates in the figure above.

These similarities can then be seen quite clearly in graph form. There has been no discernible change in the resistance to gemcitabine of the AS cell line treated with exogenous A1AT compared to that treated without.

4.3.6 **Conclusions**

The knockdown experiments demonstrated successful reduction in the RNA expression of SERPINA1, and also reduction in the protein expression of both GSTP and RRM2.

However, the decrease in SERPINA1 expression had no effect on the response to gemcitabine in either cell line. The decrease in GSTP also failed to have an effect on gemcitabine resistance.

The decrease in RRM2 showed a significant increase in sensitivity (or decreased resistance) to gemcitabine in the region of a ten-fold change for both the parental 'sensitive' Suit-2 cell line (AS) and the clonally resistant Suit-2 cell line (GR).

These results suggest a role for RRM2 in the cellular response to gemcitabine.

4.4 ICC and IHC for RRM2

4.4.1 Overview

A link between RRM2 levels and resistance had now been shown, and had been established as a causative link by manipulating levels via siRNA knockdown. The next step was to optimise the RRM2 antibody for use in ICC and then IHC with a view to the future staining of human tissue microarrays and assessing for a possible link with survival.

4.4.2 Immunocytochemistry (ICC) for RRM2

The RRM2 antibody was optimised and ICC performed on various cells to demonstrate that ICC was successful. ICC was performed as per the methods using an RRM2 antibody concentration of 1:1000. The figure below demonstrates this. Example pictures show the different amount of staining (brown colour) achieved either without or with knockdown of the RRM2 protein. The upper left pane is the original Suit-2 cells and the upper right is one of the negative controls (using off-target siRNA). The lower two panes are pictures of the staining achieved following successful knockdown of RRM2.

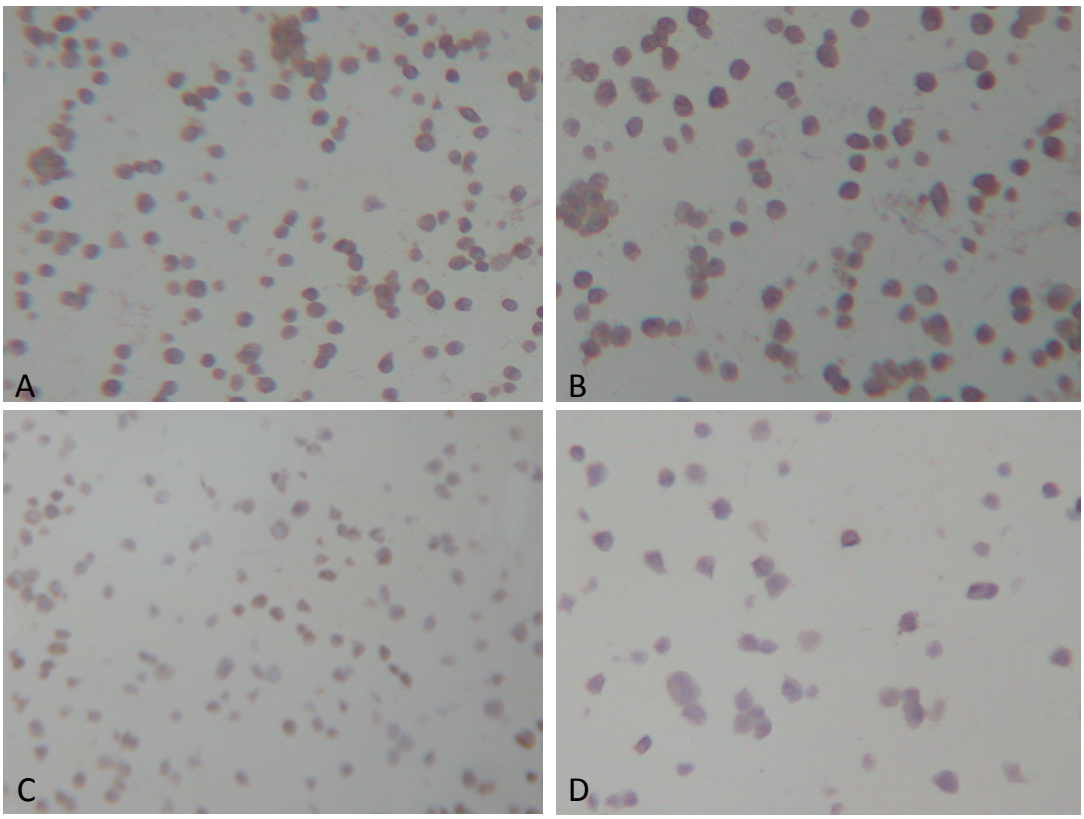

Figure 51: Example ICC for RRM2. The figure shows 4 pictures of plates of parental Suit-2 cells (AS), all stained for the presence of the RRM2 protein, after a knockdown experiment for RRM2. The upper left pane (A) is the original cell, the upper right pane (B) is the cells treated with off-target siRNA (i.e. negative control), the lower left and right panes (C and D) both show cells following knockdown of RRM2.

The pictures show obviously less brown staining of the lower panes compared with the upper (i.e. more blue rather than brown). This shows that there is less RRM2 present in the knockdown cells, and also shows successful staining for RRM2.

Based on the ICC results, I went on to trial the staining conditions and technique on human tissue, in the form of IHC.

4.4.3 **Immunohistochemistry (IHC) for RRM2**

IHC was performed on human tissue again using an RRM2 antibody concentration of 1:1000.

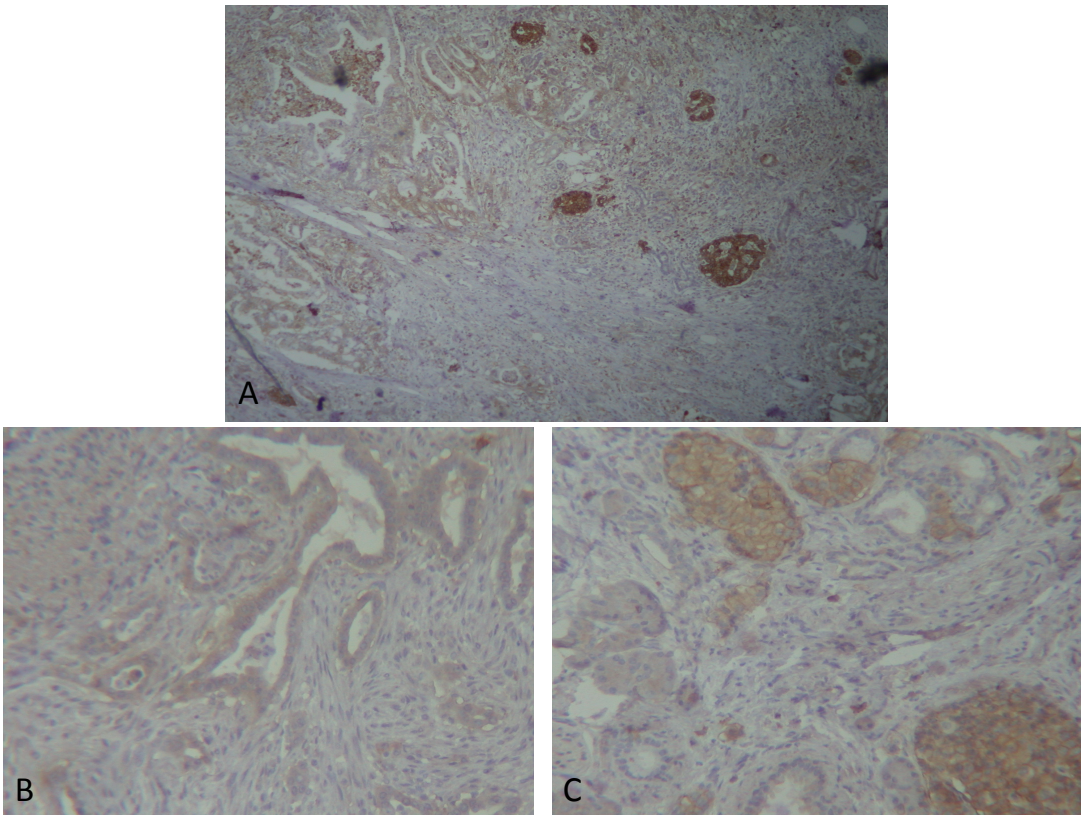

Figure 52: Example of IHC staining for RRM2 using human tissue. The upper pane (A) shows a photograph of human pancreatic tissue, with B and C panes below a showing higher magnification.

The figure above shows examples of human tissue stained for RRM2 using IHC as per the methods section. It shows successful staining as demonstrated by the brown colouring present in various parts of the tissue.

4.4.4 **Conclusion**

Successful staining for RRM2 in human tissue (as shown above) is an important step in taking the work of this thesis forward. It will allow the staining of human tissue microarrays, and comparing the level of staining with the treatment and survival data for those patients, with the hope of demonstrating, or refuting, a link between RRM2 expression and gemcitabine resistance in human PDAC.

5 Discussion

5.1 Summary

The objective of this thesis was to investigate mechanisms of gemcitabine resistance, by building on previous work which had highlighted a number of potential genes and proteins differentially expressed between relatively sensitive and resistant cell lines.

The initial step was to confirm this differential expression. This was successful for the SERPIN A1 gene which codes for A1AT by the use of qRT-PCR which showed 75.4% and 80.0% decreased expression of SERPIN A1 RNA in KR and GR resistant cells respectively compared with native AS Suit-2 cells.

It was also successfully shown that the KR cell line on which the previous work was based showed 19.6% decreased expression compared to the AS cell line. The GR cell line in this case showed similar expression to AS. Differential expression of GSTP was also shown by the results but to a slightly lesser degree (12% decrease for GR and 15% decrease in KR cells compared to AS).

Following this, siRNA knockdown of both SERPIN A1 and the gene coding for GSTP had no effect on resistance to gemcitabine.

Knockdown of RRM2 expression was shown to increase sensitivity to gemcitabine in both AS and GR cell lines. The gemcitabine IC50 for AS cells fell from 0.1nM to 0.004nM and the gemcitabine IC50 for GR cells fell from >300.000nM to 29,500nM. Both of these represent a greater that ten-fold drop in resistance.

Conditions were subsequently optimised to allow IHC probing of human tissue slides for RRM2.

5.2 Clinical relevance and further work

With respect to RRM2, the results are conflicting. The transiently resistant cell line KR had decreased levels of RRM2, whereas knockdown in the AS and GR cell lines caused a reduction in resistance to gemcitabine. The majority of published studies have described low levels of RRM2 being associated with decreased resistance to gemcitabine or vice versa[116,170,172,177–179].

This suggests either the KR cell line had developed another mechanism of resistance and the differing levels of RRM2 are an innocent bystander, or the interaction between gemcitabine and RRM2 is more complex.

Gemcitabine is known to exert its effects in two main ways. Firstly, by competitive incorporation into DNA instead of the natural nucleotide, in which case a lower level of RRM2 producing a smaller pool of natural nucleotide would indeed enhance its effectiveness and reduce resistance.

The outcome of this pathway is DNA damage leading to cell death. This is in agreement with the majority of the literature and the knockdown results from this thesis.

The second pathway is by inhibition of RNR. This again reduces the pool of natural nucleotide, initially leading to the same effect as above, with DNA damage and cell death. However, if the initial amount of RRM2 is so low that the inhibitory effect of gemcitabine on RNR essentially prevents any natural nucleotide production, this would lead to DNA production ceasing and a cytostatic rather than a cytocidal effect. This would allow the cells to weather the storm of a pulse of gemcitabine therapy, ready to start dividing once more when gemcitabine levels fall. This pulsatile level of gemcitabine is what would occur during clinical treatment.

If this theory is true, then gemcitabine resistance could increase when levels of RRM2 are either too high or too low, but sensitivity increase when levels are 'just right', an observation which has been termed the 'Goldilocks effect'. This effect could also explain the seemingly conflicting results mentioned above.

Either way, these results add to a growing evidence base that RRM2 levels can affect resistance to gemcitabine, and need to be investigated in human tissue in the context of randomised trials, to identify if it can be used as a marker for personalised chemotherapy.

Since the experiments described in this thesis, this work on human tissue has been undertaken at the university of Liverpool using IHC probing for RRM2. Tissue microarrays from the ESPAC trials have been examined for both RNA and protein expression of RRM2 and these levels compared with survival data. This has been performed by Karen Aughton and Nils Ellander and the results are yet to be published.

The above results validated the findings of the microarrays for the RNA expression of SERPIN A1, however they fail to show an effect on resistance of manipulating lower expression of SERPIN A1. This could be for a number of reasons including; SERPIN A1 does not have a direct effect on RRM2 levels and is an incidental finding, or perhaps the knockdown of the SERPIN A1 RNA production did not have an effect on protein levels, or SERPIN A1 could be one of a number of changes within the cell which only together produce resistance.

Given the recent increase in interest in A1AT levels and pancreatic cancer[149,150,152], it would seem that the results within this thesis deserve further investigation, particularly in light of the clonally resistant cell line GR displaying decreased levels. This further work is currently being discussed at the university of Liverpool.

5.3 Conclusion

RRM2 levels have been shown to affect gemcitabine resistance in pancreatic cancer in vitro and need to be further investigated in vivo to assess for a potential effect on survival.

SERPIN A1/A1AT levels have been shown to be differentially expressed in resistant pancreatic cancer cell lines in vitro, but further investigation is required to assess the relevance of this decreased expression.

6 References

1. Pancreatic cancer statistics - Cancer Research UK. Available at: http://info.cancerresearchuk.org/cancerstats/types/pancreas/?script=true.
2. GLOBOCAN 2008 Country Fast Stat.
3. Olson, S. H. & Kurtz, R. C. Epidemiology of pancreatic cancer and the role of family history. *J. Surg. Oncol.* **107,** 1–7 (2013).
4. Tersmette, A. C. *et al.* Increased Risk of Incident Pancreatic Cancer Among First-degree Relatives of Patients with Familial Pancreatic Cancer Increased Risk of Incident Pancreatic Cancer Among First-degree Relatives of Patients with Familial Pancreatic Cancer 1. *Clin cancer res* **7,** 738–744 (2001).
5. Landi, S. Genetic predisposition and environmental risk factors to pancreatic cancer: A review of the literature. *Mutat. Res.* **681,** 299–307 (2009).
6. Nitsche, C. *et al.* Environmental risk factors for chronic pancreatitis and pancreatic cancer. *Dig. Dis.* **29,** 235–42 (2011).
7. Bond-Smith, G., Banga, N., Hammond, T. M. & Imber, C. J. Pancreatic adenocarcinoma. *Bmj* **344,** e2476–e2476 (2012).
8. Hidalgo, M. Pancreatic cancer. *N. Engl. J. Med.* **362,** 1605–17 (2010).
9. Zavoral, M., Minarikova, P., Zavada, F., Salek, C. & Minarik, M. Molecular biology of pancreatic cancer. *World J. Gastroenterol.* **17,** 2897–908 (2011).
10. Ghaneh, P., Costello, E. & Neoptolemos, J. P. Biology and management of pancreatic cancer. *Postgrad. Med. J.* **84,** 478–97 (2008).
11. Morris, J. P., Wang, S. C. & Hebrok, M. KRAS, Hedgehog, Wnt and the twisted developmental biology of pancreatic ductal adenocarcinoma. *Nat. Rev. Cancer* **10,** 683–695 (2010).
12. Macgregor-Das, A. M. & Iacobuzio-Donahue, C. a. Molecular pathways in pancreatic carcinogenesis. *J. Surg. Oncol.* **107,** 8–14 (2013).
13. Jones, S. *et al.* Core Signaling Pathways in Human Pancreatic Cancers Revealed by Global Genomic Analyses. **321,** 1801–1806 (2010).
14. Yonezawa, S., Higashi, M., Yamada, N. & Goto, M. Precursor lesions of pancreatic cancer. *Gut Liver* **2,** 137–54 (2008).
15. You, L., Chen, G. & Zhao, Y. Core signaling pathways and new therapeutic targets in pancreatic cancer. *Chinese Med. J. (English Ed.* **123,** 1210–1215 (2010).
16. Wong, H. H. & Lemoine, N. R. Pancreatic cancer: molecular pathogenesis and new therapeutic targets. *Nat. Rev. Gastroenterol. Hepatol.* **6,** 412–22 (2009).
17. Park, J. Y. *et al.* Proteomic analysis of pancreatic juice for the identification of biomarkers of pancreatic cancer. *J. Cancer Res. Clin.*

Oncol. **137,** 1229–1238 (2011).

18. Schutte, M. *et al.* Abrogation of the Rb / p16 Tumor-suppressive Pathway in Virtually All Pancreatic Carcinomas. *Cancer Res.* **57,** 3126–3130 (1997).
19. Kim, W. Y. & Sharpless, N. E. The regulation of INK4/ARF in cancer and aging. *Cell* **127,** 265–75 (2006).
20. Herreros-Villanueva, M., Gironella, M., Castells, A. & Bujanda, L. Molecular markers in pancreatic cancer diagnosis. *Clin. Chim. Acta.* **418,** 22–29 (2013).
21. Schutte, M. *et al.* DPC4 Gene in Various Tumor Types. *Cancer Res.* 2527–2530 (1996).
22. Cano, C. E., Motoo, Y. & Iovanna, J. L. Epithelial-to-mesenchymal transition in pancreatic adenocarcinoma. *ScientificWorldJournal.* **10,** 1947–57 (2010).
23. Karamitopoulou, E. Tumor budding cells, cancer stem cells and epithelial-mesenchymal transition-type cells in pancreatic cancer. *Front. Oncol.* **2,** 209 (2013).
24. Rhim, A. D. *et al.* EMT and dissemination precede pancreatic tumor formation. *Cell* **148,** 349–361 (2013).
25. Haeno, H., Gonen, M. & Davis, M. Computational modeling of pancreatic cancer reveals kinetics of metastasis suggesting optimum treatment strategies. *Cell* **148,** 362–375 (2012).
26. Tuveson, D. a & Neoptolemos, J. P. Understanding metastasis in pancreatic cancer: a call for new clinical approaches. *Cell* **148,** 21–3 (2012).
27. Li, C. *et al.* Identification of pancreatic cancer stem cells. *Cancer Res.* **67,** 1030–7 (2007).
28. Fortini, M. E. Notch signaling: the core pathway and its posttranslational regulation. *Dev. Cell* **16,** 633–47 (2009).
29. Ristorcelli, E. & Lombardo, D. Targeting Notch signaling in pancreatic cancer. *Expert opin ther targets* **14,** 541–52 (2010).
30. Hidalgo, M. & Maitra, A. The hedgehog pathway and pancreatic cancer. *N. Engl. J. Med.* **361,** 2094–2096 (2009).
31. Pasca di Magliano, M. *et al.* Common activation of canonical Wnt signaling in pancreatic adenocarcinoma. *PLoS One* **2,** e1155 (2007).
32. Middleton, G., Ghaneh, P., Costello, E., Greenhalf, W. & Neoptolemos, J. P. New treatment options for advanced pancreatic cancer. *Expert Rev. Gastroenterol. Hepatol.* **2,** 673–96 (2008).
33. Hornsby, P. Cellular aging and cancer. *Crit. Rev. Oncol. Hematol.* **79,** 189–195 (2011).
34. Neesse, A. *et al.* Stromal biology and therapy in pancreatic cancer. *Gut* **60,** 861–8 (2011).
35. Apte, M. V *et al.* Periacinar stellate shaped cells in rat pancreas: identification, isolation, and culture. *Gut* **43,** 128–33 (1998).
36. Feig, C. *et al.* The pancreas cancer microenvironment. *Clin. Cancer Res.* **18,**

4266–76 (2012).

37. Bachem, M. G. *et al.* Pancreatic carcinoma cells induce fibrosis by stimulating proliferation and matrix synthesis of stellate cells. *Gastroenterology* **128,** 907–921 (2005).

38. Vonlaufen, A. *et al.* Pancreatic stellate cells: partners in crime with pancreatic cancer cells. *Cancer Res.* **68,** 2085–93 (2008).

39. Clark, C. E. *et al.* Dynamics of the immune reaction to pancreatic cancer from inception to invasion. *Cancer Res.* **67,** 9518–27 (2007).

40. Provenzano, P. P. & Hingorani, S. R. Hyaluronan, fluid pressure, and stromal resistance in pancreas cancer. *Br. J. Cancer* **108,** 1–8 (2013).

41. Provenzano, P. P. *et al.* Enzymatic targeting of the stroma ablates physical barriers to treatment of pancreatic ductal adenocarcinoma. *Cancer Cell* **21,** 418–29 (2012).

42. Vincent, A., Herman, J., Schulick, R., Hruban, R. H. & Goggins, M. Pancreatic cancer. *Lancet* **378,** 607–20 (2011).

43. Ryan, David; Hong, Theodore; Bardeesy, N. Pancreatic Adenocarcinoma. *N. Engl. J. Med.* **371,** 1039–49 (2014).

44. Pannala, R. *et al.* Prevalence and Clinical Profile of Pancreatic Cancer-Associated Diabetes Mellitus. *Gastroenterology* **134,** 981–987 (2008).

45. Chari, S. T. *et al.* Pancreatic Cancer-Associated Diabetes Mellitus: Prevalence and Temporal Association With Diagnosis of Cancer. *Gastroenterology* **134,** 95–101 (2008).

46. Chari, S. T. *et al.* Probability of pancreatic cancer following diabetes: A population-based study. *Gastroenterology* **129,** 504–511 (2005).

47. Maithel, S. K. *et al.* Preoperative CA 19-9 and the yield of staging laparoscopy in patients with radiographically resectable pancreatic adenocarcinoma. *Ann. Surg. Oncol.* **15,** 3512–20 (2008).

48. Hess, V. *et al.* CA 19-9 tumour-marker response to chemotherapy in patients with advanced pancreatic cancer enrolled in a randomised controlled trial. *Lancet Oncol.* **9,** 132–138 (2008).

49. Denbo, J. W. & Fleming, J. B. Definition and Management of Borderline Resectable Pancreatic Cancer. *Surg. Clin. North Am.* **96,** 1337–1350 (2016).

50. Bockhorn, M., Uzunoglu, F. G., Adham, M. & Imrie, C. Consensus Borderline resectable pancreatic cancer : A consensus statement by the International Study Group of Pancreatic Surgery (ISGPS). *Surgery* **155,** 977–988 (2014).

51. Witt, Benjamin; Hilden, Kristen; Scaife, C. et al. Identification of Factors Predictive of Malignancy in Patients With Atypical Biliary Brushing Results Obtained Via ERCP. *Diagn. Cytopathol.* **35,** 525–528 (2007).

52. Asbun, H. J., Conlon, K. & Fernandez-cruz, L. When to Perform a Pancreaticoduodenectomy in the Absence of Positive Histology ? A consensus statement by the International Study Group of Pancreatic Surgery (ISGPS). *Surgery* **155,** 887–92 (2014).

53. Sobin LH, Gospodarowicz MK, W. C. *International Union Against Cancer*

TNM Classification of Malignant Tumours (7th edn). (Wiley Blackwell, 2009).

54. Neoptolemos, J. P. *et al.* Adjuvant Chemotherapy With Fluorouracil Plus Folinic Acid vs Gemcitabine Following Pancreatic Cancer Resection: A Randomized Controlled Trial. *JAMA J. Am. Med. Assoc.* **304,** 1073–1081 (2010).

55. Oettle, Helmut; Post, Stefan; Neuhaus, P. et al. Adjuvant Chemotherapy With Gemcitabine vs Observation in Patients Undergoing Curative-Intent Resection of Pancreatic Cancer. *JAMA J. Am. Med. Assoc.* **297,** 267–277 (2007).

56. Hartwig, W. *et al.* Pancreatic cancer surgery in the new millennium: better prediction of outcome. *Ann. Surg.* **254,** 311–9 (2011).

57. Kausch, W. Das Carcinom der Papilla duodeni und seine radikale Entfernung. *Beitr Z Klin Chir* **78,** 439–486 (1912).

58. Whipple, A. Observations on radical surgery for lesions of pancreas. *Surg Gynecol Obs.* **82,** 623–631 (1946).

59. Jones, L. *et al.* Standard Kausch-Whipple Pancreatoduodenectomy. *Dig. Surg.* **16,** 297–304 (1999).

60. Artinyan, A. *et al.* The anatomic location of pancreatic cancer is a prognostic factor for survival. *HPB (Oxford).* **10,** 371–6 (2008).

61. Hartwig, W., Werner, J., Jäger, D., Debus, J. & Büchler, M. W. Improvement of surgical results for pancreatic cancer. *Lancet Oncol.* **14,** 476–485 (2013).

62. Correa-Gallego, C. *et al.* Minimally-invasive vs open pancreaticoduodenectomy: Systematic review and meta-analysis. *J. Am. Coll. Surg.* **218,** 129–139 (2014).

63. Zimmerman, Steven; Smith, Frederick; Schein, P. Chemotherapy of pancreatic carcinoma. *Cancer* **47,** 1724–1728 (1981).

64. Bakkevold, KE; Arnesjo, B; Dahl, O. et al. Adjuvant combination chemotherapy (AMF) following radical resection of carcinoma of the pancreas and papilla of Vater--results of a controlled, prospective, randomised multicentre study. *Eu J Cancer* **29A,** 698–703 (1993).

65. Neoptolemos, J. P. *et al.* Adjuvant chemoradiotherapy and chemotherapy in resectable pancreatic cancer: a randomised controlled trial. *Lancet* **358,** 1576–85 (2001).

66. Neoptolemos, J. P. *et al.* A randomized trial of chemoradiotherapy and chemotherapy after resection of pancreatic cancer. *N. Engl. J. Med.* **350,** 1200–10 (2004).

67. Takada, T. *et al.* Is postoperative adjuvant chemotherapy useful for gallbladder carcinoma? A phase III multicenter prospective randomized controlled trial in patients with resected pancreaticobiliary carcinoma. *Cancer* **95,** 1685–95 (2002).

68. Kosuge, T., Kiuchi, T., Mukai, K. & Kakizoe, T. A multicenter randomized controlled trial to evaluate the effect of adjuvant cisplatin and 5-fluorouracil therapy after curative resection in cases of pancreatic cancer.

Jpn. J. Clin. Oncol. **36,** 159–165 (2006).

69. Burris, H. a *et al.* Improvements in survival and clinical benefit with gemcitabine as first-line therapy for patients with advanced pancreas cancer: a randomized trial. *J. Clin. Oncol.* **15,** 2403–13 (1997).

70. Neuhaus, P; Riess, H; Post, S; Gellert, K; Ridwelski, K; Schramm, H; Zuelke, C; Fahlke, J; Langrehr, J; Oettle, H. CONKO-001: Final results of the randomized, prospective, multicenter phase III trial of adjuvant chemotherapy with gemcitabine versus observation in patients with resected pancreatic cancer. *J Clin Oncol* **26,** (2008).

71. Ueno, H. *et al.* A randomised phase III trial comparing gemcitabine with surgery-only in patients with resected pancreatic cancer: Japanese Study Group of Adjuvant Therapy for Pancreatic Cancer. *Br. J. Cancer* **101,** 908–15 (2009).

72. Neoptolemos, J. P. *et al.* Adjuvant 5-fluorouracil and folinic acid vs observation for pancreatic cancer: composite data from the ESPAC-1 and -3(v1) trials. *Br. J. Cancer* **100,** 246–50 (2009).

73. Maeda, A. *et al.* Randomized phase III trial of adjuvant chemotherapy with gemcitabine versus S-1 in patients with resected pancreatic cancer: Japan Adjuvant Study Group of Pancreatic Cancer (JASPAC-01). *Jpn. J. Clin. Oncol.* **38,** 227–229 (2008).

74. Antoniou, G., Kountourakis, P., Papadimitriou, K., Vassiliou, V. & Papamichael, D. Adjuvant therapy for resectable pancreatic adenocarcinoma: Review of the current treatment approaches and future directions. *Cancer Treat Rev* **40,** 78–85 (2014).

75. Neoptolemos, J. P. *et al.* Comparison of adjuvant gemcitabine and capecitabine with gemcitabine monotherapy in patients with resected pancreatic cancer (ESPAC-4): a multicentre, open-label, randomised, phase 3 trial. *Lancet* **6736,** 1–14 (2017).

76. Liao, W. *et al.* Adjuvant treatments for resected pancreatic adenocarcinoma : a systematic review and network meta-analysis. *Lancet Oncol.* **14,** 1095–1103 (2013).

77. Jones, O. P., Melling, J. D. & Ghaneh, P. Adjuvant therapy in pancreatic cancer. *World J. Gastroenterol.* **20,** 14733–14746 (2014).

78. Jones, O., Melling, J. & Ghaneh, P. Adjuvant therapy in pancreatic cancer. *World J. Gastroenterol.* **20,** 14733–14746 (2014).

79. Van Rijswijk, R. E. N. *et al.* Weekly high-dose 5-fluorouracil and folinic acid in metastatic pancreatic carcinoma: a phase II study of the EORTC GastroIntestinal Tract Cancer Cooperative Group. *Eur. J. Cancer* **40,** 2077–81 (2004).

80. Moore, M. J. *et al.* Erlotinib plus gemcitabine compared with gemcitabine alone in patients with advanced pancreatic cancer: A phase III trial of the National Cancer Institute of Canada Clinical Trials Group. *J. Clin. Oncol.* **25,** 1960–1966 (2007).

81. Cunningham, D. *et al.* Phase III randomized comparison of gemcitabine versus gemcitabine plus capecitabine in patients with advanced pancreatic cancer. *J. Clin. Oncol.* **27,** 5513–5518 (2009).

82. Cid-Arregui, A. & Juarez, V. Perspectives in the treatment of pancreatic adenocarcinoma. *World J. Gastroenterol.* **21,** 9297–316 (2015).

83. Buanes, T. A. Updated therapeutic outcome for patients with periampullary and pancreatic cancer related to recent translational research. *World J. Gastroenterol.* **22,** 10502–10511 (2016).

84. Conroy, T. *et al.* FOLFIRINOX versus gemcitabine for metastatic pancreatic cancer. *N Engl J Med* **364,** 1817–1825 (2011).

85. Von Hoff, D. D. *et al.* Increased survival in pancreatic cancer with nab-paclitaxel plus gemcitabine. *N. Engl. J. Med.* **369,** 1691–703 (2013).

86. Lee, H. S. & Park, S. W. Systemic Chemotherapy in Advanced Pancreatic Cancer. *Gut Liver* **10,** 340–347 (2016).

87. Wong, A., Soo, R. a, Yong, W.-P. & Innocenti, F. Clinical pharmacology and pharmacogenetics of gemcitabine. *Drug Metab. Rev.* **41,** 77–88 (2009).

88. Cheema, A. R. & Reilly, E. M. O. Management of Metastatic Pancreatic Adenocarcinoma. *Surg Clin N Am* **96,** 1391–1414 (2016).

89. Toschi, L., Finocchiaro, G., Bartolini, S., Gioia, V. & Cappuzzo, F. Role of gemcitabine in cancer therapy. *Future Oncol.* **1,** 7–17 (2005).

90. Castellanos, E., Berlin, J. & Cardin, D. B. Current treatment options for pancreatic carcinoma. *Curr. Oncol. Rep.* **13,** 195–205 (2011).

91. Binenbaum, Y., Na'Ara, S. & Gil, Z. Gemcitabine resistance in pancreatic ductal adenocarcinoma. *Drug Resist. Updat.* **23,** 55–68 (2015).

92. Pourquier, P; Gioffre, C, Kohlhagen, G. et al. Gemcitabine (2',2'-difluoro-2'-deoxycytidine), an antimetabolite that poisons topoisomerase 1. *Clin cancer res* **8,** 2499–2504 (2002).

93. Nakano, Y. *et al.* Gemcitabine chemoresistance and molecular markers associated with gemcitabine transport and metabolism in human pancreatic cancer cells. *Br. J. Cancer* **96,** 457–63 (2007).

94. Chen, Y.-W. *et al.* Proteomic analysis of gemcitabine-induced drug resistance in pancreatic cancer cells. *Mol. Biosyst.* **7,** 3065–3074 (2011).

95. De Sousa Cavalcante, L. & Monteiro, G. Gemcitabine: Metabolism and molecular mechanisms of action, sensitivity and chemoresistance in pancreatic cancer. *Eur. J. Pharmacol.* **741,** 8–16 (2014).

96. Mackey, J. R. *et al.* Functional Nucleoside Transporters Are Required for Gemcitabine Influx and Manifestation of Toxicity in Cancer Cell Lines Functional Nucleoside Transporters Are Required for Gemcitabine Influx and Manifestation of Toxicity in Cancer Cell Lines1. *Cancer Res.* **58,** 4349–4357 (1998).

97. Damaraju, V. L. *et al.* Nucleoside anticancer drugs: the role of nucleoside transporters in resistance to cancer chemotherapy. *Oncogene* **22,** 7524–36 (2003).

98. Giovannetti, E. *et al.* Transcription analysis of human equilibrative nucleoside transporter-1 predicts survival in pancreas cancer patients treated with gemcitabine. *Cancer Res.* **66,** 3928–35 (2006).

99. Kim, R. *et al.* Prognostic roles of human equilibrative transporter 1 (hENT-

1) and ribonucleoside reductase subunit M1 (RRM1) in resected pancreatic cancer. *Cancer* **117,** 3126–34 (2011).

100. Spratlin, J. *et al.* The absence of human equilibrative nucleoside transporter 1 is associated with reduced survival in patients with gemcitabine-treated pancreas adenocarcinoma. *Clin. Cancer Res.* **10,** 6956–61 (2004).

101. Maréchal, R. *et al.* Human equilibrative nucleoside transporter 1 and human concentrative nucleoside transporter 3 predict survival after adjuvant gemcitabine therapy in resected pancreatic adenocarcinoma. *Clin. Cancer Res.* **15,** 2913–9 (2009).

102. Farrell, J. J. *et al.* Human equilibrative nucleoside transporter 1 levels predict response to gemcitabine in patients with pancreatic cancer. *Gastroenterology* **136,** 187–95 (2009).

103. Morinaga, S. *et al.* Immunohistochemical Analysis of Human Equilibrative Nucleoside Transporter-1 (hENT1) Predicts Survival in Resected Pancreatic Cancer Patients Treated with Adjuvant Gemcitabine Monotherapy. *Ann. Surg. Oncol.* **19,** S558-564 (2012).

104. Greenhalf, W. *et al.* Pancreatic Cancer hENT1 Expression and Survival From Gemcitabine in Patients From the ESPAC-3 Trial. *J. Natl. Cancer Inst.* **106,** 20–25 (2013).

105. Bird, N. T. E. *et al.* Immunohistochemical hENT1 expression as a prognostic biomarker in patients with resected pancreatic ductal adenocarcinoma undergoing adjuvant gemcitabine-based chemotherapy. *Br. J. Surg.* **104,** 328–336 (2017).

106. Bergman, A. M., Pinedo, H. M. & Peters, G. J. Determinants of resistance to 2',2'-difluorodeoxycytidine (gemcitabine). *Drug Resist. Updat.* **5,** 19–33 (2002).

107. Bouffard, D. Y., Laliberté, J. & Momparler, R. L. Kinetic studies on 2',2'-difluorodeoxycytidine (Gemcitabine) with purified human deoxycytidine kinase and cytidine deaminase. *Biochem. Pharmacol.* **45,** 1857–61 (1993).

108. Wang, L. *et al.* Human thymidine kinase 2: molecular cloning and characterisation of the enzyme activity with antiviral and cytostatic nucleoside substrates. *FEBS Lett.* **443,** 170–4 (1999).

109. Ruiz van Haperen, V. W. *et al.* Development and molecular characterization of a 2',2'-difluorodeoxycytidine-resistant variant of the human ovarian carcinoma cell line A2780. *Cancer Res.* **54,** 4138–43 (1994).

110. van Haperen, V. W., Veerman, G., Vermorken, J. B., Pinedo, H. M. & Peters, G. Regulation of phosphorylation of deoxycytidine and 2',2'-difluorodeoxycytidine (gemcitabine); effects of cytidine 5'-triphosphate and uridine 5'-triphosphate in relation to chemosensitivity for 2',2'-difluorodeoxycytidine. *Biochem. Pharmacol.* **51,** 911–8 (1996).

111. van der Wilt, C. L. *et al.* The role of deoxycytidine kinase in gemcitabine cytotoxicity. *Adv. Exp. Med. Biol.* **486,** 287–90 (2000).

112. Blackstock, A. W. *et al.* Tumor uptake and elimination of 2',2'-difluoro-2'-deoxycytidine (gemcitabine) after deoxycytidine kinase gene transfer: correlation with in vivo tumor response. *Clin. Cancer Res.* **7,** 3263–8 (2001).

113. Ohhashi, S. *et al.* Down-regulation of deoxycytidine kinase enhances acquired resistance to gemcitabine in pancreatic cancer. *Anticancer Res.* **28,** 2205–12 (2008).

114. Tang, K. *et al.* Enhancement of gemcitabine sensitivity in pancreatic cancer by co-regulation of dCK and p8 expression. *Oncol. Rep.* **25,** 963–70 (2011).

115. Fujita, H., Ohuchida, K. & Mizumoto, K. Gene expression levels as predictive markers of outcome in pancreatic cancer after gemcitabine-based adjuvant chemotherapy. *Neoplasia* **12,** 807–817 (2010).

116. Goan, Y. G., Zhou, B., Hu, E., Mi, S. & Yen, Y. Overexpression of ribonucleotide reductase as a mechanism of resistance to 2,2-difluorodeoxycytidine in the human KB cancer cell line. *Cancer Res.* **59,** 4204–7 (1999).

117. Bergman, A. M. *et al.* Collateral sensitivity to gemcitabine (2',2'-difluorodeoxycytidine) and cytosine arabinoside of daunorubicin- and VM-26-resistant variants of human small cell lung cancer cell lines. *Biochem. Pharmacol.* **61,** 1401–8 (2001).

118. Eda, H; Ura, M; F-Ouchi, K. et al. The antiproliferative activity of DMDC is modulated by inhibition of cytidine deaminase. *Cancer Res.* **58,** 1165–1169 (1998).

119. Funamizu, N. *et al.* Is the resistance of gemcitabine for pancreatic cancer settled only by overexpression of deoxycytidine kinase ? *Oncol. Rep.* **23,** 471–475 (2010).

120. Nakahira, S. *et al.* Involvement of ribonucleotide reductase M1 subunit overexpression in gemcitabine resistance of human pancreatic cancer. *Int. J. Cancer* **120,** 1355–1363 (2007).

121. Ohtaka, kazuma; Kohya, Naohiko; Sato, K. et al. Ribonucleotide reductase subunit M1 is a possible chemoresistance marker to gemcitabine in biliary tract carcinoma. *Oncol. Rep.* **20,** 279–286 (2008).

122. Bergman, A. M. *et al.* In vivo induction of resistance to gemcitabine results in increased expression of ribonucleotide reductase subunit M1 as the major determinant. *Cancer Res.* **65,** 9510–9516 (2005).

123. Davidson, J. D. *et al.* An increase in the expression of ribonucleotide reductase large subunit 1 is associated with gemcitabine resistance in non-small cell lung cancer cell lines. *Cancer Res* **64,** 3761–3766 (2004).

124. Duxbury, M. S., Ito, H., Zinner, M. J., Ashley, S. W. & Whang, E. E. RNA interference targeting the M2 subunit of ribonucleotide reductase enhances pancreatic adenocarcinoma chemosensitivity to gemcitabine. *Oncogene* **23,** 1539–48 (2004).

125. Gandhi, V; Chen, F; Hertel, L; Plunkett, W. Excision of 2',2'-difluorodeoxycytidine (gemcitabine0 monophosphate residues from DNA. *Cancer Res* **56,** 4453–4459 (1996).

126. Ceppi, P. *et al.* ERCC1 and RRM1 gene expressions but not EGFR are predictive of shorter survival in advanced non-small-cell lung cancer treated with cisplatin and gemcitabine. *Ann. Oncol.* **17,** 1818–1825 (2006).

127. Akita, H. *et al.* Significance of RRM1 and ERCC1 expression in resectable

pancreatic adenocarcinoma. *Oncogene* **28,** 2903–9 (2009).

128. Jimeno, A. *et al.* A fine-needle aspirate-based vulnerability assay identifies polo-like kinase 1 as a mediator of gemcitabine resistance in pancreatic cancer. *Mol. Cancer Ther.* **9,** 311–8 (2010).

129. Habiro, A. *et al.* Involvement of p38 mitogen-activated protein kinase in gemcitabine-induced apoptosis in human pancreatic cancer cells. *Biochem. Biophys. Res. Commun.* **316,** 71–77 (2004).

130. Yoon, H., Min, J. K., Lee, J. W., Kim, D. G. & Hong, H. J. Acquisition of chemoresistance in intrahepatic cholangiocarcinoma cells by activation of AKT and extracellular signal-regulated kinase (ERK)1/2. *Biochem. Biophys. Res. Commun.* **405,** 333–337 (2011).

131. Neesse, A., Algül, H., Tuveson, D. a & Gress, T. M. Stromal biology and therapy in pancreatic cancer: a changing paradigm. *Gut* **64,** 1476–84 (2015).

132. Bailey, J. M. *et al.* Sonic hedgehog promotes desmoplasia in pancreatic cancer. *Clin. Cancer Res.* **14,** 5995–6004 (2008).

133. Olive, K. P. *et al.* Inhibition of Hedgehog Signaling a Mouse Model of Pancreatic Cancer. *Science (80-.).* **324,** 1457–1461 (2009).

134. Bahra, M. *et al.* Combination of Hedgehog Signaling Blockage and Chemotherapy Leads to Tumor Reduction in Pancreatic Adenocarcinomas. *Pancreas* **41,** 222–229 (2012).

135. Huang, F. T. *et al.* Inhibition of hedgehog signaling depresses self-renewal of pancreatic cancer stem cells and reverses chemoresistance. *Int. J. Oncol.* **41,** 1707–1714 (2012).

136. Xu, M. *et al.* ABCB2 (TAP1) as the downstream target of SHH signaling enhances pancreatic ductal adenocarcinoma drug resistance. *Cancer Lett.* **333,** 152–158 (2013).

137. Rajabpour, A., Rajaei, F. & Teimoori-toolabi, L. Molecular alterations contributing to pancreatic cancer chemoresistance. *Pancreatology* **xx,** 1–11 (2016).

138. Arumugam, T. *et al.* Epithelial to mesenchymal transition contributes to drug resistance in pancreatic cancer. *Cancer Res.* **69,** 5820–8 (2009).

139. Meidhof, S. *et al.* ZEB1-associated drug resistance in cancer cells is reversed by the class I HDAC inhibitor mocetinostat. *EMBO Mol. Med.* **7,** 831–47 (2015).

140. Elaskalani, O., Razak, N. B. A., Falasca, M. & Metharom, P. Epithelial-mesenchymal transition as a therapeutic target for overcoming chemoresistance in pancreatic cancer. *World J. Gastrointest. Oncol.* **9,** 37–41 (2017).

141. Iwamura T, Katsuki T, I. K. Establishment and characterization of a human pancreatic cancer cell line (SUIT-2) producing carcinoembryonic antigen and carbohydrate antigen 19-9. *Japanese J. cancer Res.* **78,** 54–62 (1987).

142. Schröder, C. *et al.* Dual-color proteomic profiling of complex samples with a microarray of 810 cancer-related antibodies. *Mol. Cell. Proteomics* **9,** 1271–80 (2010).

143. Gettins, P. G. W. Serpin structure, mechanism, and function. *Chem. Rev.*

102, 4751–804 (2002).

144. Travis, J; Salvesen, G. Human plasma proteinase inhibitors. *Ann Rev Biochem* **52,** 655–709 (1983).

145. Bosco, D. *et al.* Expression and secretion of alpha1-proteinase inhibitor are regulated by proinflammatory cytokines in human pancreatic islet cells. *Diabetologia* **48,** 1523–33 (2005).

146. Trachte, A. L. *et al.* Increased expression of alpha-1-antitrypsin, glutathione S-transferase pi and vascular endothelial growth factor in human pancreatic adenocarcinoma. *Am J Surg* **184,** 642–648 (2002).

147. Koomen, J. M. *et al.* Plasma protein profiling for diagnosis of pancreatic cancer reveals the presence of host response proteins. *Clin. Cancer Res.* **11,** 1110–8 (2005).

148. Huang, H. *et al.* Alpha1-antitrypsin inhibits angiogenesis and tumor growth. *Int. J. Cancer* **112,** 1042–8 (2004).

149. Matsubara, J. *et al.* Survival prediction for pancreatic cancer patients receiving gemcitabine treatment. *Mol. Cell. Proteomics* **9,** 695–704 (2010).

150. Ina, S., Hirono, S., Noda, T. & Yamaue, H. Identifying molecular markers for chemosensitivity to gemcitabine in pancreatic cancer: increased expression of interferon-stimulated gene 15 kd is associated with intrinsic chemoresistance. *Pancreas* **39,** 473–85 (2010).

151. Wu, W. *et al.* Solid Serous Cystadenoma of the Pancreas: A Case Report of 2 Patients Revealing Vimentin, b-Catenin, a-1 Antitrypsin, and a-1 Antichymotrypsin as New Immunohistochemistry Staining Markers. *Medicine (Baltimore)*. **94,** e644 (2015).

152. Yi, Q. *et al.* PRSS1 mutations and the proteinase/antiproteinase imbalance in the pathogenesis of pancreatic cancer. *Tumor Biol.* **37,** 5805–5810 (2016).

153. Gao, W. *et al.* Decreased brain-expressed X-linked 4 (BEX4) expression promotes growth of oral squamous cell carcinoma. *J. Exp. Clin. Cancer Res.* **35,** 92 (2016).

154. Sidhar, H. & Giri, R. K. Induction of Bex genes by curcumin is associated with apoptosis and activation of p53 in N2a neuroblastoma cells. *Sci. Rep.* **7,** 41420 (2017).

155. Hayes, J. D., Flanagan, J. U. & Jowsey, I. R. Glutathione Transferases. *Annu. Rev. Phamacol. Toxicol.* **45,** 51–88 (2005).

156. Jiao, L. *et al.* Glutathione S-transferase gene polymorphisms and risk and survival of pancreatic cancer. *Cancer* **109,** 840–848 (2007).

157. Yamada, I. *et al.* Lack of associations between genetic polymorphisms in GSTM1, GSTT1 and GSTP1 and pancreatic cancer risk: A multi-institutional case-control study in Japan. *Asian Pacific J. Cancer Prev.* **15,** 391–395 (2014).

158. Tan, X. *et al.* Analysis of invasion-metastasis mechanism in pancreatic cancer: Involvement of tight junction transmembrane protein occludin and MEK/ERK signal transduction pathway in cancer cell dissociation. *Oncol. Rep.* **11,** 993–998 (2004).

159. Kojima, T. *et al.* Downregulation of tight junction-associated MARVEL protein marvelD3 during epithelial-mesenchymal transition in human pancreatic cancer cells. *Exp. Cell Res.* **317,** 2288–2298 (2011).

160. Kojima, T. & Sawada, N. Regulation of tight junctions in human normal pancreatic duct epithelial cells and cancer cells. *Ann. N. Y. Acad. Sci.* **1257,** 85–92 (2012).

161. Işeri, O. D. *et al.* Drug resistant MCF-7 cells exhibit epithelial-mesenchymal transition gene expression pattern. *Biomed. Pharmacother.* **65,** 40–5 (2011).

162. Kyuno, D. *et al.* Protein kinase Cα inhibitor protects against downregulation of claudin-1 during epithelial-mesenchymal transition of pancreatic cancer. *Carcinogenesis* **34,** 1232–43 (2013).

163. Assaraf, Y; Leamon, C; Reddy, J. The folate receptor as a rational therapeutic target for personalised cancer treatment. *Drug Resist. Updat.* **17,** 89–95 (2014).

164. Bergamini, A. *et al.* Folate receptor alpha antagonists in preclinical and early stage clinical development for the treatment of epithelial ovarian cancer. *Expert Opin. Investig. Drugs* **25,** 1405–1412 (2016).

165. Sato, S; Itamochi, H. Profile of farletuzumab and its potential in the treatment of solid tumors. *Onco targets ther* **7,** 1181–1188 (2016).

166. Zhou, J. *et al.* Folate-chitosan-gemcitabine core-shell nanoparticles targeted to pancreatic cancer. *Chin J Cancer Res* **25,** 527–535 (2013).

167. Duxbury, M. S. *et al.* Retrovirally mediated RNA interference targeting the M2 subunit of ribonucleotide reductase: A novel therapeutic strategy in pancreatic cancer. *Surgery* **136,** 261–9 (2004).

168. Itoi, T. *et al.* Ribonucleotide reductase subunit M2 mRNA expression in pretreatment biopsies obtained from unresectable pancreatic carcinomas. *J. Gastroenterol.* **42,** 389–94 (2007).

169. Fisher, S. B. *et al.* An analysis of human equilibrative nucleoside transporter-1, ribonucleoside reductase subunit M1, ribonucleoside reductase subunit M2, and excision repair cross-complementing gene-1 expression in patients with resected pancreas adenocarcinoma: Implication. *Cancer* **119,** 445–453 (2013).

170. Wei, C. H. *et al.* A Meta-Analysis of Gemcitabine Biomarkers in Patients With Pancreaticobiliary Cancers. *Pancreas* **42,** 1303–1310 (2013).

171. Xie, H., Lin, J., Thomas, D. & Jiang, W. Ribonucleotide reductase M2 does not predict survival in patients with resectable pancreatic adenocarcinoma. *Int. J.* **5,** 347–355 (2012).

172. Farrell, J. J., Moughan, J., Wong, J. L., Schaefer, P. & Benson, A. B. Precision Medicine and Pancreatic Cancer A Gemcitabine Pathway Approach. **45,** 1485–1493 (2016).

173. Dinarello, C. a. Why not treat human cancer with interleukin-1 blockade? *Cancer Metastasis Rev.* **29,** 317–29 (2010).

174. Poch, B. *et al.* Systemic immune dysfunction in pancreatic cancer patients. *Langenbecks. Arch. Surg.* **392,** 353–8 (2007).

175. Ebrahimi, B., Tucker, S. L., Li, D., Abbruzzese, J. L. & Kurzrock, R. Cytokines in pancreatic carcinoma: Correlation with phenotypic characteristics and prognosis. *Cancer* **101,** 2727–2736 (2004).

176. Wang, Y. *et al.* Hedgehog Signaling Non-Canonical Activated by Pro-Inflammatory Cytokines in Pancreatic Ductal Adenocarcinoma. *J. Cancer* **7,** 2067–2076 (2016).

177. Taylor, P. *et al.* miR-211 Modulates Gemcitabine Activity Through Downregulation of Ribonucleotide Reductase and Inhibits the Invasive Behavior of Pancreatic Cancer Cells. *Nucleosides , Nucleotides Nucleic Acids* **33,** 384–393 (2014).

178. Wang, C. *et al.* Establishment of human pancreatic cancer gemcitabine-resistant cell line with ribonucleotide reductase overexpression. *Oncol. re* **33,** 383–390 (2015).

179. Lewis, C. S., Voelkel-johnson, C. & Smith, C. D. Suppression of c-Myc and RRM2 expression in pancreatic cancer cells by the sphingosine kinase-2 inhibitor ABC294640. *Oncotarget* **7,** 60181–60192 (2016).